

Experimental and Numerical Investigation on The Elastic Properties of Natural Fiber Composites

Mohamad Alhijazi

Submitted to the
Institute of Graduate Studies and Research
in partial fulfilment of the requirements for the degree of

Doctor of Philosophy
in
Mechanical Engineering

Eastern Mediterranean University
August 2021
Gazimağusa, North Cyprus

Approval of the Institute of Graduate Studies and Research

Prof. Dr. Ali Hakan Ulusoy
Director

I certify that this thesis satisfies all the requirements as a thesis for the degree of Doctor of Philosophy in Mechanical Engineering.

Prof. Dr. Hasan Hacısevki
Chair, Department of Mechanical
Engineering

We certify that we have read this thesis and that in our opinion it is fully adequate in scope and quality as a thesis for the degree of Doctor of Philosophy in Mechanical Engineering.

Assoc. Prof. Dr. Qasim Zeeshan
Co-Supervisor

Asst. Prof. Dr. Babak Safaei
Supervisor

Examining Committee

1. Prof. Dr. Fuat Egelioglu

2. Prof. Dr. Tien-Chien Jen

3. Prof. Dr. Alireza Setoodeh

4. Assoc. Prof. Dr. Qasim Zeeshan

5. Asst. Prof. Dr. Mohammed Asmael

6. Asst. Prof. Dr. Babak Safaei

7. Asst. Prof. Dr. Davut Solyalı

ABSTRACT

In recent years, the application of natural fibers as reinforcement in composite structures has received increasing attention due to their advantages of low cost, environmental friendliness and favorable biocompatibility over synthetic fiber composite materials. The present work is an investigation on the tensile properties of palm as well as luffa natural fiber composites (NFC) in high density polyethylene (HDPE), polypropylene (PP), epoxy, and ecopoxy (BioPox 36) matrices, taking into consideration the effect of fibers volume fraction (V_f) variation. Finite element analysis i.e. representative volume element (RVE) models with unidirectional and chopped random fiber orientations, as well as analytical simulation i.e. Rule of Mixture (ROM), Halpin-Tsai, Chamis, and Nielsen approaches were utilized for predicting the elastic properties. Tensile test following ASTM D3039 standard was conducted. Artificial Neural Network (ANN), Multiple Linear Regression (MLR), Adaptive Neuro-Fuzzy Inference System (ANFIS), and Support Vector Machine were implemented for defining the design space upon the considered parameters and evaluating the reliability of these machine learning approaches in predicting the tensile strength of natural fibers composites. Furthermore, biopox 36 with 0.3 luffa fibers exhibited the highest tensile strength. Finite element analysis findings profusely agreed with the experimental results. ANFIS machine learning (ML) tool showed least prediction error in predicting tensile strength of natural fibers composites.

Keywords: Natural Fibers Composites, Palm Fibers, Luffa Fibers, Thermoplastics and Thermosets Matrices, Numerical and Analytical Simulation, Machine Learning.

ÖZ

Son yıllarda, doğal liflerin kompozit yapılarda takviye olarak uygulanması, sentetik lifli kompozit malzemelere göre düşük maliyet, çevre dostu olma ve uygun biyouyumluluk avantajları nedeniyle artan bir ilgi görmüştür. Bu çalışma, yüksek yoğunluklu polietilen (HDPE), polipropilen (PP), Epoksi ve Ecopoxy (BioPox 36) matrislerinde palmye'nin yanı sıra lif kabağı doğal elyaf kompozitlerinin (NFC) çekme özellikleri üzerinde, etkiyi dikkate alarak bir araştırmadır. liflerin hacim oranı (V_f) varyasyonu. Elastik özellikleri tahmin etmek için sonlu eleman analizi, yani tek yönlü ve doğranmış rastgele fiber yönelimli temsili hacim elemanı (RVE) modelleri ve analitik simülasyon, yani karışım kuralı (ROM), Halpin-Tsai, Chamis ve Nielsen yaklaşımları kullanılmıştır. ASTM D3039 standardına göre çekme testi yapılmıştır. Tasarım uzayını göz önüne alınan parametreler üzerinden tanımlamak ve bu makine öğrenmesi yaklaşımlarının doğal elyaf kompozitlerinin çekme mukavemetini tahmin etmedeki güvenilirliğini değerlendirmek için Yapay Sinir Ağı, Çoklu Doğrusal Regresyon, Uyarlamalı Nöro-Bulanık Çıkarım Sistemi ve Destek Vektör Makinesi uygulandı. Ayrıca, 0,3 lifli BioPox 36 en yüksek gerilme mukavemetini sergiledi. Sonlu Elemanlar Analizi (finite element analysis) bulguları deneysel sonuçlarla büyük ölçüde uyumluydu. ANFIS ML aracı, doğal lifli kompozitlerin gerilme mukavemetini tahmin etmede en az tahmin hatası gösterdi.

Anahtar Kelimeler: Doğal Elyaf Kompozitleri, Palmye Elyafı, lif kabağı Elyafı, Termoset ve Termosetler Matrisleri, Sayısal ve Analitik Simülasyon, Makine Öğrenimi.

DEDICATION

To My Family

ACKNOWLEDGMENT

I would like to express my deepest gratitude to my co-supervisor Assoc. Prof. Dr. Qasim Zeeshan for his continuous advice and encouragement throughout my PhD Studies. Also, I would like to express my very sincere sense to my supervisor Assist. Prof. Dr. Babak Safaei and also, Assist. Prof. Dr. Mohammed Bsher A. Asmael for their guidance, and motivation. I would like to express my appreciation to Prof. Dr. Fuat Egelioglu, Assoc. Prof. Dr. Tülin Akçaoğlu, and Assist. Prof. Dr. Davut Solyalı for being my committee members as well as providing me their invaluable support and guidance. I would like to express my special appreciation and thanks to the chair of mechanical engineering department Prof. Dr. Hasan Hacışevki for his unwavering support. Moreover, I would like to thank my friend Mr. Zeki Murat Çınar for being next to me on the same journey through all ups and downs. I also would like to offer my thanks to my supportive colleagues and academic staff at the Mechanical Engineering Department.

I would like to express my sincerest gratitude to my wife and parents for their constant support throughout my post-graduate studies, their effective motivation in tough moments, and their perpetual love and patience.

I would like to express my deep appreciation to Assoc. Prof. Dr. Zhaoye Qin from Tsinghua University China, Assist. Prof. Dr. Mohamad Harb from the American University of Beirut, and the CEO of EcoPoxy Canada, Mr. Jack Maendel for providing their facilities for this research.

TABLE OF CONTENTS

ABSTRACT.....	iii
ÖZ	iv
DEDICATION	v
ACKNOWLEDGMENT.....	vi
LIST OF TABLES	x
LIST OF FIGURES	xii
LIST OF ABBREVIATIONS	xv
1 INTRODUCTION	1
1.1 Natural Fibers	4
1.2 Palm Fibers.....	6
1.2.1 Classification of Palm Fibers	6
1.3 Luffa Sponge	10
1.4 Research Significance	12
1.4.1 Aerospace Industry	12
1.4.2 Automotive Industry.....	13
1.4.3 Civil Engineering Industry	14
1.5 Research Objective and Novelty	15
1.6 Research Organization	16
2 LITERATURE REVIEW	17
2.1 Palm Natural Fibers Composites.....	17
2.1.1 Fiber Treatments.....	17
2.1.2 Coupling Agents and Hardeners.....	19
2.1.3 Matrix	20

2.1.4 Fiber Size and Fibers Volume Fraction.....	21
2.1.5 Tensile Properties of PFCs	23
2.2 Luffa and Its Composite Materials	28
2.2.1 Fiber Treatment	29
2.2.2 Matrices Selected for LNFCs	30
2.2.3 Tensile Properties of LFCs.....	31
2.3 Modeling and Simulation	35
2.4 Machine Learning Application for Composite Materials	43
3 METHODOLOGY	45
3.1 Modeling and Simulation	47
3.1.1 Finite Element Analysis	47
3.1.2 FEA of Natural Fibers Composites	48
3.1.3 Representative Volume Element (RVE)	50
3.1.4 Numerical and Analytical Simulation of Palm and Luffa NFC	51
3.1.4.1 Analytical Models.....	52
3.1.4.1.1 Rule of Mixture.....	53
3.1.4.1.2 Halpin Tsai.....	54
3.1.4.1.3 Nielsen	54
3.1.4.1.4 Chamis	55
3.1.4.2 Finite Element Analysis.....	56
3.2 Composite Materials Preparation	56
3.2.1 Composites' Components.....	57
3.2.2 Molds Development	57
3.2.3 Samples Preparation	58
3.3 Tensile Test	62

3.4 Design of Experiment.....	63
3.5 Machine Learning Models	64
3.5.1 Artificial Neural Network	66
3.5.2 Multiple Linear Regression	67
3.5.3 Adaptive Neuro-Fuzzy Inference System	68
3.5.4 Support Vector Machine	69
4 RESULTS AND DISCUSSION	71
4.1 FEA and Analytical Simulation Model Validation	71
4.1.1 Longitudinal Modulus	71
4.1.2 Transverse Modulus	76
4.1.3 Shear Modulus.....	80
4.1.4 Poisson’s Ratio	84
4.2 Tensile Test Results	87
4.3 FEA and Experimental Results	93
4.4 Machine Learning Findings	97
5 CONCLUSION.....	103
5.1 Research Limitations and Future Recommendations	106
REFERENCES	108

LIST OF TABLES

Table 1: Advantages and Disadvantages of NFCs [38-42].....	5
Table 2: Palm Fibers Chemical Composition	10
Table 3: Physical Properties and Chemical Composition of Luffa Fibers [66-68]....	11
Table 4: Natural Fiber Composite Applications In Industry [70-74].....	12
Table 5: Application of NFC in Automotive Industry [70, 75-78].....	14
Table 6: Fiber Treatments Used for PNFCs.....	18
Table 7: Hardeners and Coupling Agents Used in PNFCs	19
Table 8: Matrices Used for PNFC.....	20
Table 9: Classification of Researches According to Fibers Size	22
Table 10: Classification of Researches According to Fiber Content	22
Table 11: Mechanical Properties	24
Table 12: Luffa Fiber Treatments	29
Table 13: Thermoplastics and Thermosets Used in Luffa Natural Fiber Composite (LNFC) Development	31
Table 14: Mechanical Properties of Luffa Natural Fiber Composites	32
Table 15: Numerical M&S of Tensile and elastic behavior of NFCs.....	39
Table 16: Input Properties of The Selected Materials for Model Validation.....	51
Table 17: Input Properties of The Selected Materials for Simulation	52
Table 18: Fibers Volume Fraction and Weights Calculations	59
Table 19: Design of Experiment Approaches [328]	64
Table 20: E1 of Palm/HDPE Obtained from RVE Chopped Model and Literature ..	71
Table 21: Poisson's Ratio of Palm and Luffa Reinforced Thermosets	86
Table 22: Tensile Test Outcome	90

Table 23: Predicted Tensile Strength Using ANN, MLR, ANFIS, and SVM	101
---	-----

LIST OF FIGURES

Figure 1: Growing Trend of Research on NFCs	2
Figure 2: General Classification of Natural Fibers [37]	4
Figure 3: NFC Manufacturing Process Flowchart	6
Figure 4: Flowchart of Palm Categories and Extracts	7
Figure 5: Sugar Palm Tree	7
Figure 6: Oil Palm Fruit Bunch	9
Figure 7: Peach Palm Tree	9
Figure 8: Luffa and Its Internal Structure [62, 63]	11
Figure 9: Effect of Palm Type and Matrix on Tensile Strength.....	26
Figure 10: Tensile Strength of Luffa Natural Fiber Composites	34
Figure 11: Displacement profile of double hat profile after impact [265]	42
Figure 12: Research Methodology	46
Figure 13: Overview of Finite Element Analysis (FEA) Adapted from [294]	48
Figure 14: Elements Type [314]	50
Figure 15: a) RVE with Unidirectional Fibers, B) RVE with Chopped Fibers	56
Figure 16: Silicone and Wood Molds Preparation	58
Figure 17: Palm and Luffa NFCs Specimens Preparation	61
Figure 18: Tensile Testing Machine	63
Figure 19: Classification of Machine Learning Algorithms	65
Figure 20: Artificial Neural Network Model Structure	67
Figure 21: ANFIS Model Structure	69
Figure 22: Predict versus Real SVM Data	70

Figure 23: Longitudinal Modulus of a) Palm/Epoxy and b) Luffa/Epoxy Natural Fibers Composites.....	72
Figure 24: Longitudinal Modulus of a) Palm/EcoPoxy and b) Luffa/EcoPoxy Natural Fibers Composites.....	73
Figure 25: Longitudinal Moduli of a) Palm/PP and b) Luffa/PP NFCs	74
Figure 26: Longitudinal Moduli of a) Palm/HDPE and b) Luffa/HDPE Reinforced Composites.....	75
Figure 27: Transverse Modulus of a) Palm/Epoxy and b) Luffa/Epoxy Natural Fibers Composites.....	76
Figure 28: Transverse Modulus of a) Palm/EcoPoxy and b) Luffa/EcoPoxy Natural Fibers Composites.....	77
Figure 29: Transverse Moduli of a) Palm/PP and b) Luffa/PP Reinforced Composites	78
Figure 30: Transverse Moduli of a) Palm/HDPE and b) Luffa/HDPE Reinforced Composites.....	79
Figure 31: Shear Modulus of a) Palm/Epoxy and b) Luffa/Epoxy Natural Fibers Composites.....	80
Figure 32: Shear Modulus of a) Palm/EcoPoxy and b) Luffa/EcoPoxy Natural Fibers Composites.....	81
Figure 33: Shear Moduli of a) Palm/PP and b) Luffa/PP Reinforced Composites....	82
Figure 34: Shear Moduli of a) Palm/HDPE and b) Luffa/HDPE Reinforced Composites.....	83
Figure 35: Stress and Strain Curve of Luffa/BioPoxy "0.1"	87
Figure 36: Stress and Strain Curve of Palm/Epoxy "0.3"	88
Figure 37: Stress and Strain Curve of Palm/PP "0.1"	88

Figure 38: Stress and Strain Curve of Luffa/HDPE "0.1"	89
Figure 39: Tensile Strength Variation of BioPoxy/Palm and BioPoxy/Luffa	91
Figure 40: Tensile Strength Variation of Epoxy/Palm and Epoxy/Luffa	91
Figure 41: Tensile Strength Variation of PP/Palm and PP/Luffa	92
Figure 42: Tensile Strength Variation of HDPE/Palm and HDPE/Luffa	93
Figure 43: FEA Beam Model Following ASTM D3039	94
Figure 44: Experimental versus FEA Tensile Strength of BioPoxy/Palm and BioPoxy/Luffa.....	94
Figure 45: Experimental versus FEA Tensile Strength of Epoxy/Palm and Epoxy/Luffa	95
Figure 46: Experimental versus FEA Tensile Strength of PP/Palm and PP/Luffa	96
Figure 47: Experimental versus FEA Tensile Strength of HDPE/Palm and HDPE/Luffa	96
Figure 48: Regression Plot of ANN Model	98
Figure 49: Response Surface Fitting of Palm NFCs	98
Figure 50: Response Surface Fitting of Luffa NFCs	99
Figure 51: Adaptive Neuro-Fuzzy Inference System Plot.....	100

LIST OF ABBREVIATIONS

ANFIS	Artificial Neuro-Fuzzy inference System
ANN	Artificial Neural Network
DOE	Design of Experiments
DP	Date Palm
DPF	Date Palm Fibers
FEA	Finite Element Analysis
HDPE	High-Density Polyethylene
LNFC	Luffa Natural Fibers Composite
ML	Machine Learning
MLR	Multiple Linear Regression
M&S	Modeling and Simulation
NFC	Natural Fibers Composites
OP	Oil Palm
OPF	Oil Palm Fibers
Pe-P	Peach Palm
PF	Palm Fibers
PNFC	Palm Natural Fibers Composites
PP	Polypropylene
ROM	Rule of Mixture
RVE	Representative Volume Element
SEM	Scanning Electron Microscopy
SP	Sugar Palm
SPB	Sugar Palm Bunch
SPF	Sugar Palm Fronds
SPS	Sugar Palm Starch
SPT	Sugar Palm Trunk
SVM	Support Vector Machine
TS	Tensile Strength

Chapter 1

INTRODUCTION

Fiber-reinforced composites are becoming significantly popular in various engineering fields due to their low density as well as their remarkable mechanical characteristics. Composite materials' properties are based on their selected components, viz., matrix and fibers [1-3]. Previously, the utilized matrices and fibers were mostly obtained from petroleum origins. Although they possess attractive properties, the aforementioned composite materials are restricted from being used for long periods, yet can endure regular environmental conditions for tens of years [4-9]. Moreover, composite recycling and reprocessing methods are unavailable. The manufacturing of most synthetic fibers has several environmental effects, as it requires high electric power, is toxic for humans, may deplete the ozone layer, as well as cause global warming and eutrophication [10-13]. The increased attentiveness to environmental matters has augmented the search for an alternative natural source in order to increase the utilization of renewable materials, reduce waste production, boost recycling, and so on [14, 15].

Hence, numerous scientists and engineers tend toward green materials that can enhance the products' environmental aspects [13, 16-19]. Thus, materials extracted from natural resources gained more attention as an alternative to synthetic fibers in composite materials. Natural fibers (NFs) can be extracted from many parts of a plant, i.e., fruit, leaves, trunk, roots, and etc. Throughout the decades, natural fibers have

been widely utilized in countless applications due to their advantages, as they are strong, lightweight, tough, recyclable, biodegradable, abundant in nature, and have negligible cost and low density [20-27]. Additionally, their environmental advantages include decreased respiratory and dermal irritation, improved energy consumption, less wear and abrasion on tools, and minimal health hazards. Natural fiber composites have been significantly involved in various engineering fields such as automotive, marine, sports gear, construction, and aerospace [17, 28-34]. While their disadvantages (i.e., high moisture absorption, short service life, and degradation) limited their application in other fields [15, 16]. Published data regarding NFC, PNFCs and M&S of NFCs have been gathered from the Scopus database (Fig. 1), which shows a drastic increase in papers on this topic.

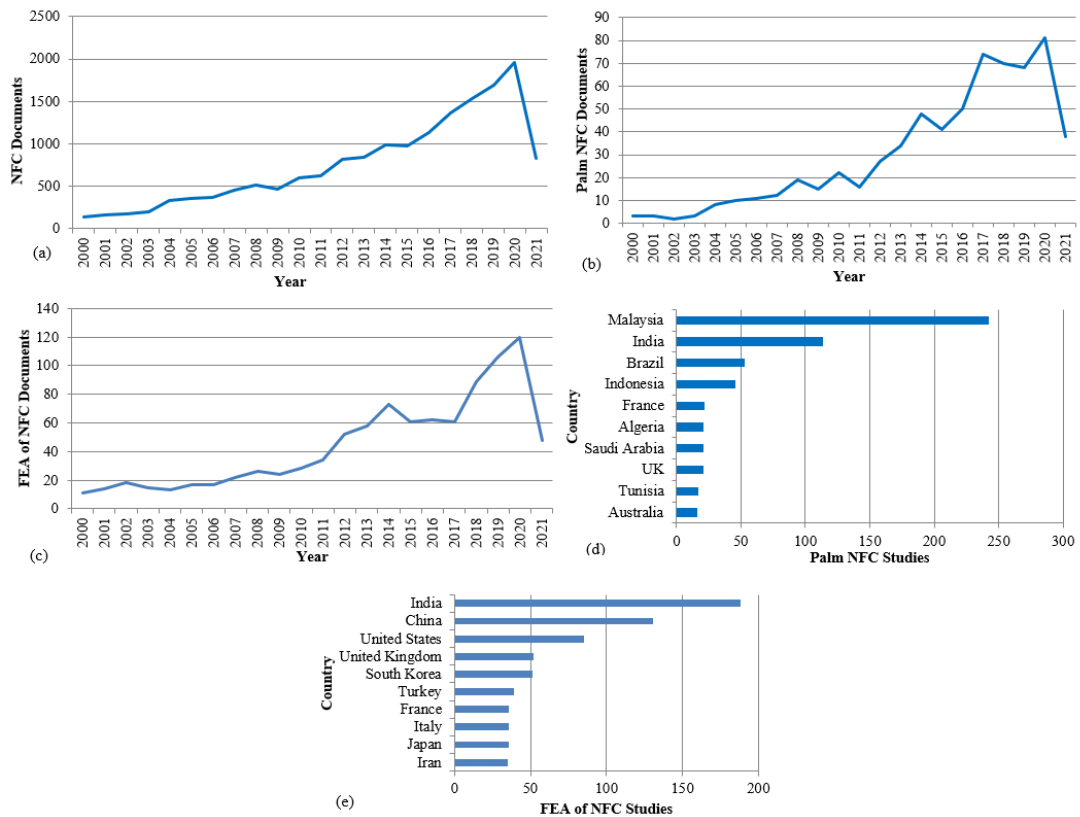


Figure 1: Growing Trend of Research on NFCs

Figure 1a shows the year wise trend of the published documents on NFC from 2000 to 2021. Figure 1b shows the published documents per year on palm NFC from 2000 to 2021. In 2015, 41 papers in the area of palm NFC were published, followed by 74 in 2017 to hit a peak of 81 in 2020, although only three were published a decade ago. Studies on Palm fibers were mostly carried out in Malaysia and India because of its high availability in those countries, Fig. 1d. While Figure 1c shows a building momentum in the trend of research interest of NFC specifically to FEA. In Figure 1c, modeling and simulation of natural fibers composites began in 2000 with 11 publications and remained below 30 researches per year until 2011, where studies in this area profusely increased and reached a total of 120 published article in 2020. While, Fig. 1e shows that India is the country with most active research in the field of FEA of NFC. Results published from various research activities illustrates that NFCs can successfully be adapted for various applications. However, before applying these fiber-reinforced composites into real-life applications, particularly for massive production, the characteristics of the materials have to be studied in-depth to ensure obtaining repeatable and reliable results. These include the fiber/matrix interaction, mechanical performance, manufacturing process and dispersion properties of the resultant composites. Several issues such as the moisture absorbability and change in microstructure of these fibers subjected to loading may also substantially affect the final properties of these composites. On the other hand, their biodegradability with different fiber compositions may also play a key role to produce fully biodegradable composites. Natural fiber is indeed a renewable resource that can be grown and made within a short period of time, in which the supply can be unlimited as compared with traditional glass and carbon fibers for making advanced composites. The deficiencies in the natural fibers can be reduced by subjecting them to morphological changes by

various physical or chemical treatment methods [35]. Some researchers have proposed hybridization of NFC with synthetic fiber like hemp fabric/kevlar fabric/epoxy and jute fabric/kevlar fabric/epoxy to improve the overall mechanical properties of the material [36].

1.1 Natural Fibers

Fibers are a hair-like material's category that are separate outstretched parts or continuous filaments, they may be turned into ropes, threads or filaments [28, 30, 31]. Fibers can be involved in composite materials development. Fibers have two main categories: synthetic and natural fibers [14, 32]. The classification of natural fibers is shown in Fig. 2 and Table 1 respectively.

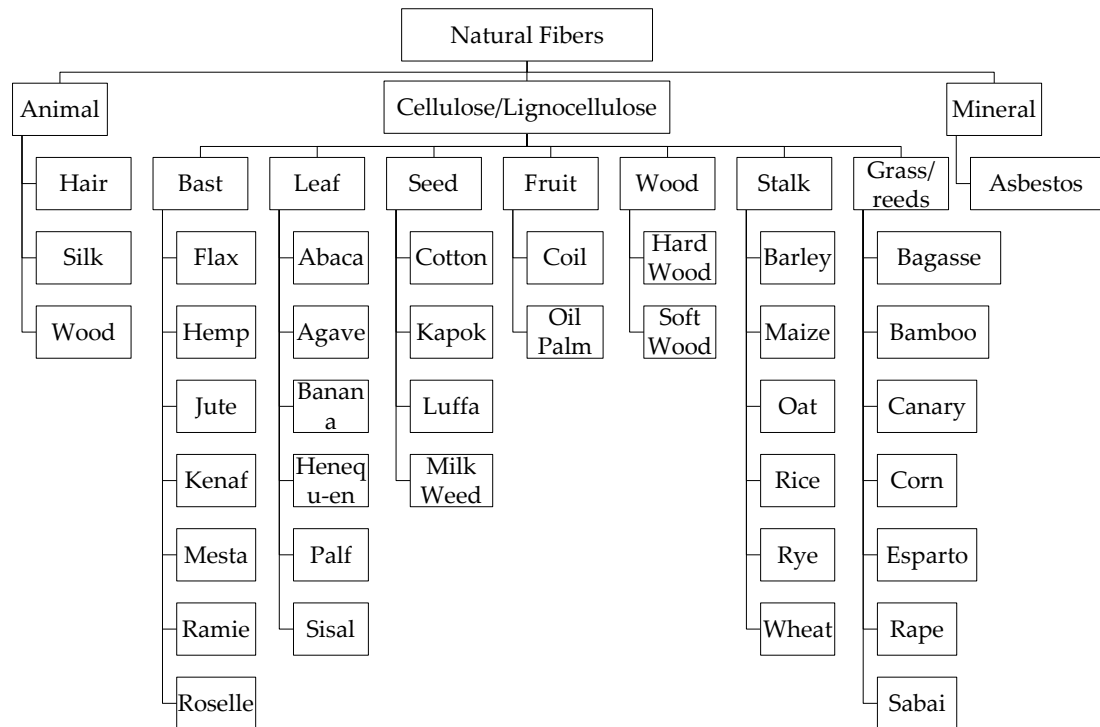


Figure 2: General Classification of Natural Fibers [37]

Natural fibers comprise those obtained from minerals, animals and plants. Hence, their classification is related to their source of extraction. Several natural fibers can be selected as a reinforcement with various polymeric matrices i.e. sisal, jute, kenaf,

bamboo, kenaf, jowar, sugar palm, date palm, coir, pineapple leaf, hemp, flax, rice husk, cotton, etc. [35-37].

Table 1: Advantages and Disadvantages of NFCs [38-42]

Advantages	Disadvantages
<ul style="list-style-type: none"> • Low density with high stiffness and strength. 	<ul style="list-style-type: none"> • Shorter life time compared to synthetic fibers composite materials, yet it can be improved through fiber' treatment.
<ul style="list-style-type: none"> • Fibers are from renewable resources; therefore, they do not lead to any toxic gases emission throughout the development. 	<ul style="list-style-type: none"> • Notable moisture absorption, which leads to thickness swelling.
<ul style="list-style-type: none"> • Cheaper than synthetic fibers. 	<ul style="list-style-type: none"> • Lower mechanical properties than synthetic fibers composite materials.
<ul style="list-style-type: none"> • Low tool wear while machining compared to synthetic fibers. 	<ul style="list-style-type: none"> • Wider properties variability.

Traditional manufacturing techniques used for composite materials with thermosetting and thermoplastics can be implemented in natural fibers composites development [34], for example, injection molding, vacuum infusion, hand layup, resin transfer molding, compression molding and direct extrusion [43-45]. First, the extracted fibers are washed and dried under sunlight or in an oven for a few days. Then, to improve the microstructure of fibers, they can be treated by a variety of methods such as seawater wash, microwave and chemical treatments [46, 47]. Hence, a suitable matrix must be chosen taking into account the fiber/matrix bonding which plays a key role in the performance of the end NFC. Finally, the volume fraction and size of fibers are selected. In the following section, fiber treatments, selected resins, fiber sizes and fibers volume fraction considered in palm and luffa NFCs throughout the last ten years are discussed. Figure 3 shows NFC development steps.

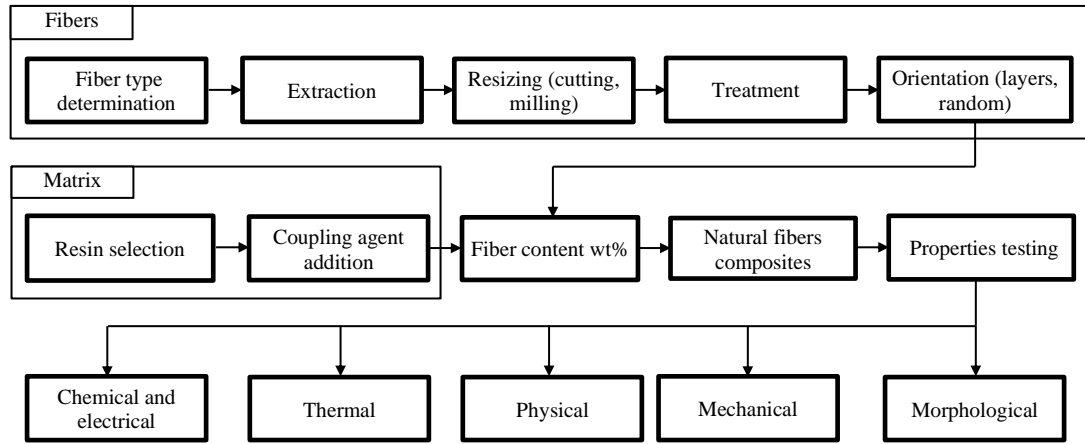


Figure 3: NFC Manufacturing Process Flowchart

1.2 Palm Fibers

Several researchers have applied palm tree extracts in different matrices. However, leaf fibers, meshes, ijuk, and empty fruit bunches have shown dissimilar characteristics. Every year, palm harvest produces tons of biomass fibrous wastes worldwide; thus, these fibers can be recycled and used for the development of palm NFCs [1-6].

1.2.1 Classification of Palm Fibers

Arecaceae “Palm” is a huge botanical family and its subfamilies are similar in having fronds and long trunks. Lately, extracts from sugar palm (SP) “*Borassus* or *Arenga pinnata*” [38], oil palm (OP) “*Elaeis*” [39], date palm (DP) “*Phoenix*” [40], and peach palm (Pe-P) “*Bactris gasipaes*” [41] have been utilized in NFC development. The main categories of palm and their extracts are showed in Fig. 4. The aforementioned species are briefly introduced in the following section, highlighting their differences and fiber sources.

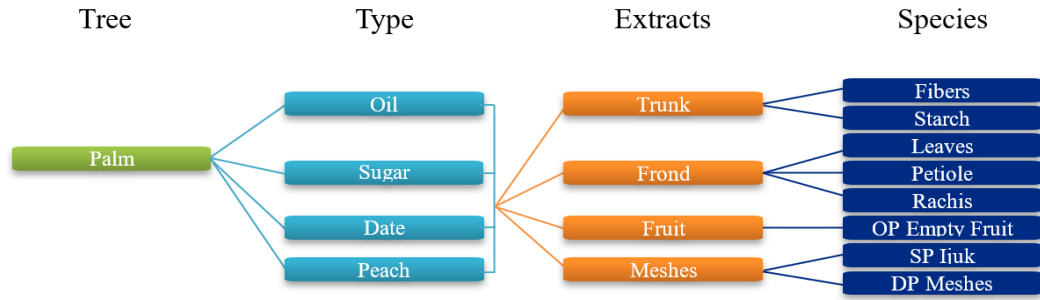


Figure 4: Flowchart of Palm Categories and Extracts

Sugar Palm Fibers “Borassus”

All parts of SP tree, such as leaves trunk, fruits and palm sap, can be utilized, therefore this tree is titled as a multipurpose tree. It is made of a single trunk with diameter of 30-40 cm and height 15-20 m with no branch [48]. SP tree leaves are in pinnate shape with a width of 1.5 m and length 6-12 m [49]. This tree is ordinarily wrapped with a black fibrous material, called ijuk. This tree is grown for more than thirty years before it becomes ready to extract its sago from the trunk [50]. For NFC applications, fibers can be obtained from several parts of a SP tree, such as trunk (SPT), frond (SPF), bunch (SPB) and black SP fibers (Ijuk). Furthermore, the conducted researches on SP fibers have proved that these fibers are convenient in composites as reinforcements and have good mechanical properties [50, 51]. Sugar palm tree is illustrated in Fig. 5.



Figure 5: Sugar Palm Tree

Date Palm Fibers “Phoenix”

DP trees (*Phoenix dactylifera* L.) are the largest Phoenix class, with heights reaching beyond 30 m and date fruit bunch sizes of up to 1 m x 0.4 m. DP tree has many branches formed at its trunk base. Persistent grayish leaf bases cover DP tree trunk. Its leaves are long and have pinnate shape with a good arrangement and its fronds are needle sharp. Every year, 10 to 20 new leaves are grown. The bases of DP leaves are surrounded by a strong fibrous sheath [52]. These trees have special characteristics that allow them to grow under various conditions, such as deserts and hot environments [53]. For NFC applications, DPF can be extracted from different parts of the tree such as trunk, leaves, fruit bunch, and mesh that surrounds the stem [54].

Oil Palm Fibers “Elaeis”

Like the majority of “Arecaceae” subfamilies, OP tree has single trunk and several fronds. Its height is up to 20 m and its leaves are in pinnate shape with a length that ranges between 3 and 5 m. Each year, up to 30 new leaves are produced by young OP trees, while mature trees grow around 20 new leaves annually [55]. OP fruit takes between 5 and 6 months to completely grow and has reddish color with sizes similar to peach fruits, and matures in big bunches. The external layer of OP fruit is called pericarp and is puffy and oily, it also has a single seed called kernel. Depending on the age of OP tree, the weight of each fruit bunch ranges from 5 to 30 Kg. Several researchers and companies are aiming to find new applications for OP and planning to turn kernel shells, empty fruit bunches and fronds into biomass energy. For NFC applications, OP fibers can be obtained from empty fruit bunch, fruit mesocarp, frond and trunk. Figure 6 shows an OP fruit bunch.



Figure 6: Oil Palm Fruit Bunch

Peach Palm “*Bactris Gasipaes*”

PE-P tree has a single trunk. At the age of 3 years, its trunk reaches its maximum diameter and thereby it grows only in height. It has pinnate shaped leaves and fruits grow as bunches. PE-P have two fruit harvesting seasons, where in the primary harvesting season it produces around 7 bunches, while in the secondary only 3 bunches are produced [56]. Three years after planting this tree, it starts to produce fruits for about 72 years. Fibers can be extracted from stem, leaves, fronds, etc. Figure 7 shows a PE-P tree and fruit bunches.



Figure 7: Peach Palm Tree

All palm types discussed previously have similar chemical components with comparable compositions. SP trees have the highest cellulose and holocellulose quantities in their bunch, Ijuk and frond fibers, while OP trunk contains 7% more cellulose and 11% more holocellulose than sugar palm trunks. Maximum lignin percentage is found in the trunks of SP trees with 46.4%. Comparing with other types, DP fibers (DPF) hold the lowest chemical compositions. Table 2 lists the proportion of chemical components in palm extracts.

Table 2: Palm Fibers Chemical Composition

Fibers	Cellulose (%)	Holocellulose (%)	Lignin (%)	Reference
Ijuk	52.3	65.6	31.5	[57]
Sugar Palm Bunch	61.8	71.8	23.5	[57]
Sugar Palm Fibers	66.5	81.2	18.9	[57]
Sugar Palm Trunk	40.6	61.1	46.4	[57]
Oil Palm Fibers	49.8	83.5	20.5	[58]
Oil Palm Trunk	46.58	72.1	23.0	[59]
Date Palm Fibers	46	18	20	[60]

1.3 Luffa Sponge

Luffa is a category of the Cucurbitaceae family (cucumber), its ripe fruits are utilized as natural cleaning sponges, while its immature fruits are consumed as vegetables. It is spread from South Asia to East and Central Asia. Luffa vegetables are widespread in Vietnam and China. Figure 8 shows mature luffa fruit and its fiber structure. Luffa fibers comprise significant toughness, strength, and stiffness, similar to the ones observed in various metals with same density ranges [61].

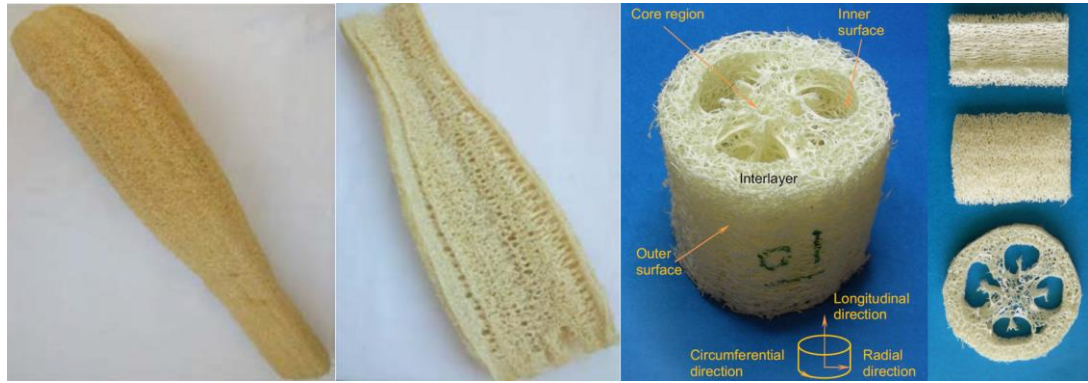


Figure 8: Luffa and Its Internal Structure [62, 63]

Luffa chemical composition mostly consists of lignin and hemicellulose/cellulose, as well as includes some inorganic elements like glycosides, polypeptides, amino acids, proteins, and so on [64]. However, the hemicellulose content ranges between 8% and 22%, lignin content is between 10% and 23%, and cellulose content is between 55% and 90%. Table 3 shows the physical and chemical properties of luffa. At the early stage of luffa growth, its cellular structure begins with numerous single fibers and turn into fibrous mat at the end [65].

Table 3: Physical Properties and Chemical Composition of Luffa Fibers [66-68]

Physical Properties				Chemical Composition			
Density (gm/cm ³)	Diameter (μm)	Aspect ratio	Micro fibrillar angle (°)	Cellulose (%)	Lignin (%)	Hemi cellulose (%)	Ash (%)
0.56–0.92	270 ± 20	340 ± 5	12 ± 2	63.0 ± 2.5	11.69 ± 1.2	20.88 ± 1.4	0.4 ± 0.10

As Table 3 shows, luffa density varies from 0.56 to 0.92 g/cm³, it has an average fibers' diameter of ~270 μm, and its microfibrillar angle is around 12°. The chemical composition of luffa consists of 63% cellulose, 20.88% hemicellulose, 11.69% lignin, and 0.4% ash. It is worth mentioning that in addition to its use as a vegetable and cleaning sponge, luffa is also utilized in Chinese medication, military filters, and shock absorbers [69].

1.4 Research Significance

Throughout the last two decades, natural fibers composites were significantly considered in automotive applications, circuit boards, aerospace industry building materials, and domestic sector, yet it is still limited in further sectors. However, following a suitable development process, NFC have a solid potential to emerge in new markets.

Table 4: Natural Fiber Composite Applications In Industry [70-74]

Fiber Type	Application
Jute	Chip boards, geotextiles, transport, packaging, door shutters, door frames, roofing sheets, and building panels.
Ramie	Paper manufacture, clothing, household furnishings, filter cloths, fishing nets, packing industrial sewing thread.
Cotton	Cordage, goods, yarn, textile, furniture
Coir	Seat cushions, mattresses padding mats, bags, net yarns, ropes, brooms, brushes, seat filling, voltage stabilizer cover, projector cover, paper weights, mirror casing helmets, packing, storage tank, roofing sheets, flush door shutters, and building panels.
Kenaf	Material that absorbs oil and liquid, animal bedding soilless potting mixes, clothing-grade cloth, insulations, bags, mobile cases, and packing.
Stalk	Constructing drains and pipelines, bricks, furniture, and building panels.
Sisal	Manufacturing of paper and pulp, roofing sheets, shutting plate, and doors.
Bagasse	Fences, railing systems, decking, panels, and window frame.
Rice husk	Fences, railing systems, decking, panels, bricks and window frame.
Flax	Laptop cases, snowboarding, seat post, fork, bicycle frame, tennis racket, fencing, railing systems, decking, panels, and window frame.
Wood	Fences, railing systems, decking, panels, and window frame.
Oil Palm	Building materials, decking, roofing, fencing, siding, insulations, doors and window frames.
Hemp	Pipes, bank notes, electrical products, furniture, packaging and papers, geotextile, cordage, textiles, and construction products.

1.4.1 Aerospace Industry

Main concern in considering new materials for structural components in the aerospace field is the reliability. Natural fibers composites may face serious degradation upon high stress environments, UV exposure, low pressure, and low temperature. Hence, in aerospace structural design the main aim is to have “Defect-free” components.

Therefore, it is a difficult access to replace synthetic fiber composites by NFCs. Moisture presence inside a composite material harms the matrix/fibers bonding, thus degrading the mechanical characteristics. Similarly, ultra-violet radiations can detach the molecule bonds inside the polymeric matrix, thereby degrading the overall properties. Moreover, in aerospace field, majority of structural components have the capability to withstand external object effects, such as birds' strikes, hail damage, and thunders, thus the airplane body has to be electrically conductive. To date, comprehensive researches that focus on developing a highly conductive NFC is still limited. However, addition of carbon-based particles into the matrix contributes in improving the electrical conductivity of a natural fibers composite.

1.4.2 Automotive Industry

natural fibers composites are applicable in automotive industry for the manufacturing of front and side panels of a vehicle as they are not primary structural components. Replacing traditional aluminum and glass fibers' composite materials by natural fibers composite can partially reduce the weight and cost of a vehicle. The diverse application of natural fiber composites in automotive industry are listed in Table 5 [70, 75-78].

Table 5: Application of NFC in Automotive Industry [70, 75-78]

Manufacturer	Model	Application
Audi	A2, A3, A4, A4 Avant, A6, A8, Roadstar, Coupe	Boot-liner, spare tire- lining, side and back door panel, seat back, and hat rack
BMW	3, 5 and 7 series	Seat back, headliner, panel, boot-lining, door panels, noise insulation panels, and moulded foot well linings
Citroen	C5	Interior door panelling
Daimler/ Chrysler	A, C, E, and S class, EvoBus (exterior)	Pillar cover panel, door, panels, car windshield/ car dashboard, and business table
Fiat	Punto, Brava, Marea, Alfa Romeo 146,156,159	Door panel
Ford	Mondeo CD 162, Focus	Floor trays, door inserts, door panels, B- pillar, and boot-liner
General Motors	Cadillac De Ville, Chevrolet Trail Blazer	Seat backs, cargo area, floor mat
Opel	Vectra, Astra, Zafira	Door panels, pillar cover, panel, head-liner panel, and instrumental panel
Lotus	Eco Elise (July 2008)	Body panels, spoiler, seats, and interior carpets
Peugeot	406	Front and rear door panels, seat backs, and parcel shelf
Renault	Clio, Twingo	Rear parcel shelf
Rover	2000 and others	Rear storage shelf/panel, and insulations
Saab	9S	Door panels
Saturn	L300	Package trays and door panel
Toyota	ES3	Pillar garnish and other interior parts
	Raum, Brevis, Harrier, Celsior,	Floor mats, spare tire cover, door panels, and seat backs
Mercedes Benz	C, S, E, and A classes	Door panels (flax/sisal/wood fibers with epoxy resin/UP matrix), glove box (cotton fibers/wood molded, flax/sisal), instrument panel support, insulation (cotton fiber), molding rod/ apertures, seat backrest panel (cotton fiber), trunk panel (cotton with PP/PET fibers), and seat surface/backrest (coconut fiber/natural rubber)
Mercedes Benz	Trucks	Internal engine cover, engine insulation, sun visor, interior insulation, bumper, wheel box, and roof cover
Mitsubishi		Cargo area floor, door panels, and instrumental panel
VAUXHALL	Corsa, Astra, Vectra, Zafira	Headliner panel, interior door panels, pillar cover panel, and instrument panel
Volkswagen	Passat Variant, Golf, A4, Bora	Seat back, door panel, boot-lid finish panel, and boot-liner
Volvo	V70, C70	Seat padding, natural foams, and cargo floor tray

1.4.3 Civil Engineering Industry

Generally cementitious materials exhibit low tensile behavior, though tensile loads can be absorbed by embedded steel bars. After the hydration process, micro-cracks form on the interface between aggregate and cement as well as on the surface due to shrinkage and water content reduction. Addition of large amount of fibers into the cement will result in a degradation of compressive strength. Recently, many researchers studied the effect of natural fibers' addition on tensile strength

improvement, insulation and so on, taking into account its side effects on the compressive properties.

1.5 Research Objective and Novelty

The present research objective is to develop a new natural fibers composite material through the following stages:

A. Model and simulate the micro-mechanical properties (longitudinal elastic modulus, transverse elastic modulus, in-plane poisson's ratio, and in-plane shear modulus) of NFC using analytical approaches and FEA RVE unidirectional as well as chopped fibers' orientation.

B. Conduct simulation based design of experiments (DOE) and analyze the effect of various parameters (Resin type, natural fiber type, and fibers' volume fraction).

C. Validate the optimal configuration by experimentally testing it and validating its mechanical properties (Tensile ASTM D3039).

D. Develop an ANN, MLR, ANFIS, and SVM based Metamodel.

The novelty of this research is:

1. Evaluating tensile properties of palm NFC in bio-based epoxy resin "BioPoxy 36".
2. Evaluating tensile properties of luffa NFC in bio-based epoxy resin "BioPoxy 36".
3. Identifying a convenient matrix luffa NFC through selecting 4 different matrices.
4. Comparing the behavior of luffa NFC with date palm NFC under same testing conditions and testing procedure.

5. Comparing the behavior agreement of 2 different representative volume elements (RVE) models of date palm NFC.
6. Comparing the behavior agreement of 2 different representative volume elements (RVE) models of luffa NFC.
7. Comparing the behavior agreement of 4 different analytical approaches in analyzing date palm NFC.
8. Comparing the behavior agreement of 4 different analytical approaches in analyzing luffa NFC.
9. Determining a convenient machine learning tool for predicting tensile strength of palm NFCs by comparing ANN, MLR, ANFIS, and SVM.
10. Determining a convenient machine learning tool for predicting tensile strength of luffa NFCs by comparing ANN, MLR, ANFIS, and SVM.
11. Investigating optimal tensile characteristics through comparing 8 different NFCs under same testing conditions taking into account fibers volume fraction variation.

1.6 Research Organization

The first chapter provides an explanation on natural fibers composites, their types, applications, advantages and disadvantages, types of palm trees and their extracts, luffa cylindrica, finite element analysis, research objectives and novelty. Chapter 2 lists a literature review of palm fibers and their composites, luffa NFCs, modeling and simulation of NFCs, and Machine learning of NFCs. Chapter 3 describes the research methodology, design of experiment, metamodeling, etc. The results of this research are introduced and discussed in Chapter 4, which includes the findings of analytical analysis, FEA simulation, experimental, and machine learning findings. Chapter 5 summarizes the major facts, steps, theories and methods implemented in this research.

Chapter 2

LITERATURE REVIEW

2.1 Palm Natural Fibers Composites

Recently many researches have reviewed date palm [79], sugar palm [50] and oil palm fibers [80, 81], the aim of this section is to summarize and classify the research on all types of Palm Natural Fibers Composites, while considering matrix types, fibers treatment, fibers size and fibers volume fraction, and tensile properties. However many researches have paid attention to extend the application of PNFC by aerospace, automotive, furniture [82-84], marine [85], construction [86] and sports industries, and other engineering fields.

2.1.1 Fiber Treatments

Usually, raw fibers have amorphous surfaces with weak nanoparticles, creating an invisible thin layer around each fiber. Treatments reduce fibers weight, enhance its surface, remove impurities and improve fiber properties by affecting their chemical contents.

As clearly shown in Table 6, sodium hydroxide (alkaline) has been most commonly utilized as a chemical treatment for all palm types with different soaking times and percentages, few experiments have considered more than a single soaking time (1, 4 and 8 h) with multiple NaOH concentrations. Alkaline treatment at different concentrations (up to 6%) improved PF performance, however, in terms of mechanical characteristics, the highest tensile strength (1246.7 MPa) and young's modulus (160

GPa) were obtained in PNFC with 1% NaOH treated palm fibers [87, 88]. The effect of hydrochloric acid treatment was compared with NaOH on DP meshes and the latter showed superior effect. While chemical treatments with sodium chlorite (NaClO_2) and ethanoic acid (CH_3COOH) were used by Ilyas et al. [89] on SP fibers. Agberi et al. and Leman et al. [90, 91] soaked SP fibers in seawater to remove its impurities, while Mohammed et al. [92] treated SPF by heating in microwave at three different temperatures. Sodium hydroxide treatment consists of mixing NaOH with water or other chemicals at the concentration range of 0.25% to 15% at a specific temperature, soaking the fibers for a certain duration, and then washing them with water.

Table 6: Fiber Treatments Used for PNFCs

Treatment	Oil Palm Fiber	Sugar Palm Fiber	Date Palm Fiber	Peach Palm
Alkaline (NaOH)	[93-101]	[51, 89, 90, 92, 102-109]	[87, 88, 110-122]	[123]
Sodium Chlorite (NaClO_2)	-	[89]	-	-
Ethanoic acid (CH_3COOH)	-	[89]	[119]	-
Hydrochloric acid	-	-	[88]	-
Acrylonitrile	-	-	-	[123]
Sea Water	-	[90, 91]	-	-
Hydrogen peroxide	-	-	-	[123]
Ethanol and Acetone	-	-	[124]	-
Sodium Bicarbonate (NaHCO_3)	-	[108]		
Xylanase	-	-	[122]	-
Pectinase	-	-	[122]	-
Acetyl Chloride	-	-	[125]	-
Microwave (70 to 90 C)	-	[92]	-	-

Alawar et al. [88] utilized hydrochloric acid for treating DP meshes. Their technique involved soaking fibers in HCl solutions with three different concentrations (0.3, 0.9, 1.6 N) at 100 °C for one hour. Then, fibers were washed with fresh water after cooling to room temperature and were finally dried at 60 °C in an oven for 24 h. Santos et al. [123] treated Pe-P fibers with acrylonitrile and hydrogen peroxide; a chemical solution of 99.5% ethanol and 3% $\text{C}_3\text{H}_3\text{N}$, it was considered for fiber soaking throughout 24

and 48 h. Then, fibers were dried at room temperature. Moreover, H₂O₂ treated PE-P fibers were soaked in the chemical solution for 144 h. Agrebi et al. and Leman et al. [90, 91] used sea water for treating SP fibers by immersing these fibers in sea water for a period of up to 30 days, washing them with distilled/tap water, and finally keeping them at certain temperature to dry out. Mohammed et al. [92] treated SP fibers in microwave at 70, 80, to 90 °C before treating them with NaOH. Comparing with other chemical treatments, sodium hydroxide proved its efficiency on palm fibers by improving their properties, decreasing their weight and removing their surface impurities.

2.1.2 Coupling Agents and Hardeners

When higher properties are desired, coupling agents can be added to polymer mixtures to reach higher levels of strength and better matrix/fiber adhesions. Researchers who selected epoxy or other thermosetting materials as matrix, had to utilize hardeners for resin cross-linking and solidification.

Table 7: Hardeners and Coupling Agents Used in PNFCs

Coupling Agents/ Hardeners	Oil Palm Fiber	Sugar Palm Fiber	Date Palm Fiber	Peach Palm Fiber
Epoxy Hardener (A062)	[96, 126, 127]	[91, 105, 106, 128, 129]	[115]	-
Epoxy Hardener (D-230)	-	-	[118]	-
Silane	[130]	[129]	-	-
Acetone	[130]	-	-	
Methyl ethyl ketone peroxide	-	[85, 131]	[132]	[123]
Maleic anhydride grafted	[95, 97, 130, 133, 134]	-	[113, 116, 124]	-

As shown in Table 7, epoxy hardener (A062) has most commonly been added to the matrix of OP fibers (OPF), SPF and DPF, while D230 grade was added to DPF by Abdal-hay et al. [118]. Silane and acetone coupling agents have been used to coat OPF

[130]. Methyl ethyl ketone peroxide was added to polyester matrices of SP composite by Misri et al. [85], DP composites by Al-Kaabi [132] and PE-PF by Santos et al. [123].

2.1.3 Matrix

Besides fiber properties, the performance of the chosen matrix and its interaction with fibers determines the final characteristics of the composite. In a few studies palm fibers alone without matrix have been investigated. Meanwhile, palm fibers have been examined in various polymeric matrices such as epoxy, polyester, high density polyethylene (HDPE), polypropylene (PP), etc. Table 8 lists the utilized matrices in palm natural fibers composites.

Table 8: Matrices Used for PNFC

Matrix	Oil Palm Fiber	Sugar Palm Fiber	Date Palm Fiber	Peach Palm
Polyester	[93, 99, 100]	[85, 103, 107, 135, 136]	[110, 132]	[123, 137]
Epoxy	[96, 126, 127, 138, 139]	[51, 91, 105, 106, 109, 128, 135]	[114, 115, 117, 118, 120, 140-142]	-
Expanded Polystyrene Waste	-	-	[143]	-
Recycled Polypropylene (RPP)	-	-	[144, 145]	-
Polypropylene	[81, 95, 97, 134]	-	[116, 124, 145]	-
Polyethylene Terephthalate (PET)	[146]	-	-	-
Vinyl ester	-	[131, 135]	[125]	-
Cement	[101, 147]	-	[86, 148-150]	-
HDPE	[133, 151]	-	[111, 113]	-
Polyethylene –Low Density	-	-	[124, 152]	-
Polyhydroxyalkanoate (PHA)	[130]	-	-	-
Reinforced-phenolic (PF)	-	[90]	[153]	-
Polyurethane (PU)	-	[92, 104, 129, 154, 155]	-	-
Cornstrach resin	-	[156]	[157]	-
Wheat Gluten	[94]	-	-	-

Table 8: Matrices Used for PNFC (Continued)

Matrix	Oil Palm Fiber	Sugar Palm Fiber	Date Palm Fiber	Peach Palm
Glycerol (Glycerine)	-	[89, 158]	[112]	-
Polyvinylidene Fluoride	-	[159]	[152]	-
Polyvinyl Alcohol (PVA)	-	-	[160, 161]	-
Polylactic Acid (PLA)	-	-	[162]	-
Homopolymer (HPP)	-	-	[145]	-
Impact Copolymer (ICP)	-	-	[145]	-
Sorbitol	-	[89]	-	-
Butylene Succinate “Bio-polyester” (PBE)	-	-	[122]	-
Araldite	-	-	[121]	-
UHU plus end fest 300	-	-	[121]	-
ADEKIT H 9951T	-	-	[121]	-
Eponate	-	-	[121]	-
Bitumen	-	-	[163]	-

As exhibited in Table 8, compared with polyester that was used for the same PF types, epoxy was commonly selected as matrix for OPF, SPF, DPF and Pe-PF and its good performance resulted in high properties. Various thermoplastic, thermosetting, ceramic and natural matrices have been evaluated and diverse properties have been obtained.

2.1.4 Fiber Size and Fibers Volume Fraction

In properties related to matrix-to-fiber stress transmission, the most important factors in the design of a composite material are fiber size and orientation. Fibers are extracted from trees with random sizes. Hence, a variety of fiber lengths and diameters can be obtained following diverse resizing methods, such as milling and scissors. In recent studies, fiber lengths ranged from 75 μm to 6 cm with diameters of 200 μm to 6 mm. As clearly shown in Table 9, the most common fiber length range was 180 to 500 μm for OPF and SPF [92, 97, 98, 133, 155]. However, only few researchers have studied multiple fiber dimensions, such as DPF lengths of 20 mm and 30 mm [112], OPF lengths of 2 mm to 10 mm and DPF diameters of 200 μm to 800 μm .

Table 9: Classification of Researches According to Fibers Size

Fiber Size	OPF	SPF	DPF	PE-P
Powder	-	-	[144]	[137]
75 μm	-	-	[116]	-
100-500 μm	[94, 97, 98, 133]	[92, 131, 154, 155]	-	-
0.5 mm	-	[91, 128]	[113, 120, 121, 132]	[137]
0.1-1 mm	-	-	[120, 140, 141, 143, 163]	-
2-5 mm	[99]	[89, 158]	[86, 120, 145]	-
8-10 mm	[99]	-	[121, 145, 164]	-
20 mm	-	-	[88, 112, 121]	-
25 mm	-	-	-	[123, 137]
30 mm	-	-	[112, 120]	-
1-1.5 cm	[93]	-	[124]	-
2-15 cm	[130, 147]	[135]	-	-
30 cm	-	-	[119]	-
Diameter				
200-400 μm	[93]	-	[118, 160]	-
400-600 μm	-	-	[118, 160, 165]	-
600-800 μm	-	-	[118, 160]	-

However, fibers volume fraction is defined as the volume ratio of fibers and matrix in a composite material. This property can be controlled during specimen preparation by knowing the volume of the mold. Thus, the required quantity of fibers can be calculated based on the considered composition.

Table 10: Classification of Researches According to Fiber Content

Weight Ratio	OPF	SPF	DPF	PE-P
1-8 wt%	[134, 146]	[156]	[111, 120-122, 125, 145, 162, 163]	-
10 wt%	[95, 101, 134, 146]	[131, 136, 154, 155, 158]	[86, 111, 120, 122, 125, 145, 152]	[123, 137]
15 wt%	[94, 134]	[91, 128]	[86, 111, 145, 148]	-
18 wt%	-	[85]	-	-
20 wt%	[95, 100, 101]	[136, 154, 155, 158]	[86, 111, 113, 122, 143, 152]	-
25 wt%	[146]	-	[86, 166]	-
30 wt%	[95, 133]	[90, 103, 107, 136, 154, 155, 158]	[86, 113, 122, 143, 152]	-

Table 10: Classification of Researches According to Fiber Content (Continued)

Weight Ratio	OPF	SPF	DPF	PE-P
40 wt%	[95, 99, 133]	[103, 107, 136, 154]	[113, 140, 141, 153]	-
50% up to 80 wt%	[95, 99, 139]	[107, 136]	[140, 141, 153, 161, 164, 166]	-

In previous studies on palm fiber NFCs, fiber content ranged between 5 and 80 %. Meanwhile, several researchers considered multiple weight ratios in order to prove the impact of palm fibers on the overall properties. As a result, the addition of superfluous amounts of palm fiber led to strength degradation. As listed in Table 10, researchers who focused on SPF added up to 30 wt% fibers in the specimens. Atiqah et al. [155] and Sahari et al. [158] investigated SP composites with four different fiber content compositions. Similarly, Mulinari et al. [111] considered 5, 10, 15 and 20 wt% date palm fibers in NFC specimens. While Karina et al. [99] evaluated the effects of adding 40% to 80 wt% OPF. It is worth mentioning that, there was a significant tendency toward 10 wt% composition for all PF types. Nevertheless, 20 wt% seemed to be the most common selection for DPF composites. Fiber size, content (V_f and wt%) and orientation were found to have significant impacts on the overall characteristics of natural fibers composite materials.

2.1.5 Tensile Properties of PFCs

The capability of a material to resist high stresses relies on its mechanical properties. It means that, obtaining the highest strength of this material can endure by measuring its tensile strength. Young's modulus can be calculated to determine the beginning of its plastic deformation. In this section, a compilation of the aforementioned characteristics including the results reported in recent studies is provided (Table 11).

Table 11: Mechanical Properties

Palm Fiber Type	Mechanical Properties	Resin	Result	Testing Standard	Reference
Oil Palm Fiber	Tensile	Epoxy	37.9 MPa	ASTM D3039	[126]
		Epoxy	27.4 MPa	ASTM D3039	[96]
		Epoxy	64.7 MPa	ASTM D3039	[139]
		Polyester	21.88 MPa	ASTM D638	[100]
		PET	167 MPa	ASTM D638	[146]
		PHA	24 MPa		[130]
		HDPE	15 MPa	ISO 527-1	[133]
		PP	35 MPa	ASTM 1882L	[81]
		PP	42 MPa	ASTM D638	[97]
	Single Fiber-Pull out		64 MPa	ASTM D3379	[98]
	Young's Modulus	Epoxy	3.31 GPa		[126]
		Epoxy	2.59 GPa		[96]
		Epoxy	3640 MPa		[139]
		Polyester	3.95 GPa		[100]
		Polyhydroxy-alkanoate	425 MPa		[130]
		HDPE	1.04 GPa		[133]
		PP	2.3 GPa		[97]
			2.763 GPa		[98]
			78 MPa		[93]
Sugar Palm Fiber	Tensile	Epoxy	50 MPa		[105]
		Epoxy	92 MPa		[109]
		Epoxy	23 MPa	ASTM D638	[91]
		Polyester	43 MPa	ASTM D5083-10	[85]
		Polyester	40 MPa	ASTM 3039	[136]
		Glycerol/Sorbitol	11.47 MPa	ASTM D882-02 (2002)	[89]
		Corn Starch	19 MPa	ASTM D882-02	[156]
		Polyurethane	18.42MPa	ASTM D638	[92]
	Single Fiber-Pull out		292 MPa		[102]
	Young's Modulus	Epoxy	3.89 GPa		[105]
		Polyester	1.841 GPa		[85]
		Polyester	4.43 GPa		[136]
		Glycerol/Sorbitol	178.83 MPa		[89]
		Corn Starch	1.17 GPa		[156]
		Polyurethane	1.3 GPa		[92]
			3.37 GPa		[102]
Date Palm meshes surrounding the steams	Tensile	Epoxy	67 MPa	ASTM D638	[115]
	Single Fiber-Pull out		800 MPa	ASTM D3379	[88]
	Young's Modulus	Epoxy	1.38 GPa		[115]
			160 GPa		[88]
Date Palm Leaf Fiber	Tensile	PP	30 MPa	ASTM D638	[116]
		PE-LD / PP	31 MPa		[124]
	Young's Modulus	PP	2.2 GPa		[116]
		PE-LD / PP	1.35 GPa		[124]

Table 11: Mechanical Properties (Continued)

Palm Fiber Type	Mechanical Properties	Resin	Result	Testing Standard	Reference
Date Palm Fiber	Tensile	Epoxy	41 MPa		[118]
		Polyester	14.34 MPa		[110]
		Glycerol	31 MPa	ASTM D5083-10	[112]
		HDPE	26 MPa	ASTM D638	[111]
		HDPE	20 MPa	ASTM D638	[113]
		RPP	24 MPa	ASTM STP452	[144]
		UHU	41 MPa		[121]
		PBE	32 MPa		[122]
		Phenolic	15 MPa	ASTM D3039	[153]
		Vinyl ester	35 MPa	ASTM D638	[125]
	Single Fiber- Pull out		1246.7 MPa		[87]
			400 MPa		[117]
			366 MPa		[118]
			453 MPa	ASTM D3822	[119]
	Young's Modulus	Epoxy	2.5 GPa		[118]
		Glycerol	2.8 GPa		[112]
		HDPE	1.22 GPa		[111]
		HDPE	1.5 GPa		[113]
		RPP	1.48 GPa		[144]
		Phenolic	4.35 GPa		[153]
			26.1 GPa		[87]
			7.15GPa		[118]
			16.1 GPa		[119]
Date Palm Sheath	Tensile	Epoxy	72 MPa	ASTM D638	[114]
Peach Palm Fiber	Tensile	Polyester	28 MPa		[137]
		Polyester	44.8 MPa		[123]
	Young's Modulus	Polyester	4.18 GPa		[137]
		Polyester	500 MPa		[123]

Tensile testing has extensively been conducted in PNFC studies aiming to compare the effect of different treatment percentages as well as fibers volume fraction variation on the tensile strength and young's modulus. As displayed in Table 11, tensile testing was significantly conducted on DPF composites with different matrices, fibers treatments and fiber contents, however, tensile strengths results ranged from 24 MPa to 67 MPa. However, less studies tested the tensile strength of OPF composites, thus, HDPE/OPF composites showed the lowest strength values (15 MPa), while polyethylene terephthalate matrix/ijuk/OPF hybrid material showed the highest value (167 MPa). However, for SPF composites, peak strength was revealed with NaOH chemical treatment and epoxy matrix (50 MPa). Polyester resin was considered in PE-P

composites and the observed tensile strengths ranged between 28 and 44.88 MPa. Figure 9 shows the highest tensile strength obtained for PNFCs with various matrices.

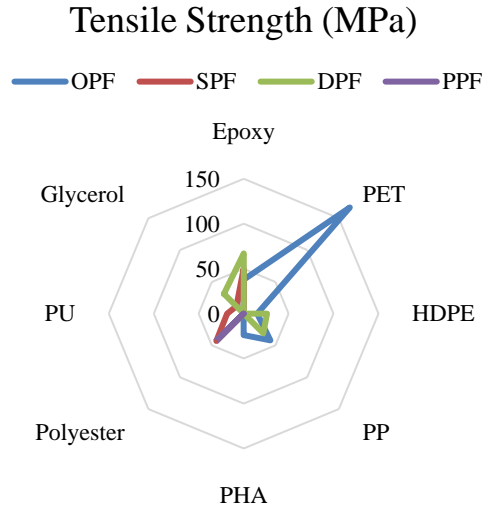


Figure 9: Effect of Palm Type and Matrix on Tensile Strength

Furthermore, sodium hydroxide treatment improved palm sheath properties, and highest tensile strength of 72 MPa was recorded with epoxy matrix. As shown in Fig. 9, OPF was drastically compatible with PET matrix, SPF and DPF were compatible with epoxy, and PE-PF were suitable with polyester matrix. By comparing the aforementioned results, OPF/ijuk/PET hybrid composites exhibited the highest tensile strength among all PFCs regardless of their matrices. Ilyas et al. [89] observed that elastic modulus and tensile strength were simultaneously improved by the addition of up to 0.5 wt% SP nanocrystalline cellulose. The obtained results showed that tensile strength increased from 4.8 MPa to a peak value of 11.47 MPa, and elastic modulus increased from 53.97 MPa to a maximum value of 178.83 MPa.

Moreover, treatment with 0.5 wt% SPS/SP nanocrystalline cellulose showed higher young's modulus and tensile strength than 0.1 wt% (117.19 MPa and 7.78 MPa). On

the other hand, increase of SP nanocrystalline cellulose content from 0 to 0.1 wt% decreased elongation at break factor from 38.1 to 24.01 %. Mohammed et al. [92] studied the impact of microwave treatment on SPF composites with thermoplastic polyurethane matrix at three different temperatures, results showed that tensile strength at 70°C 80 °C and 90 °C reached 18.42 MPa, 17.128 MPa and 18.168 MPa, respectively, while the highest strength obtained for untreated fibers was 11.71 MPa.

De Farias et al. [137] obtained 47% tensile strength reduction by adding more PE-P powder, whereas the size and orientation of fiber affected the obtained tensile strength. Hence, woven fibers specimens with 5 and 10 mm fibers' lengths exhibited an increase of 100% and 220% compared to specimens prepared with randomly oriented fibers with 25 mm fibers' length, while maximum young's modulus was observed in woven specimens with 5 mm fiber size. Santos et al. [123] observed that chemical treatments had negligible improvement in fibers' tensile strength, while 21% increase in young's modulus was recorded in fibers treated with C_3H_3N and NaOH. However, H_2O_2 caused property deterioration. Leman et al. [91] treated the fibers with freshwater for 1 month and observed about 55% improvement in tensile strength reaching a value of 21266.5 KPa. The results listed in Table 11 show that, for OPF composites, young's modulus ranged from 425 MPa to 3.31 GPa for OPF/Jute/epoxy hybrid specimens [126]. However, SPF soaked in 0.25 M NaOH for 4 h and reinforced with epoxy provided the highest young's modulus in this palm type. However in DPF, HDPE matrix provided the lowest young's modulus range of 1.22 - 1.5 GPa, which was comparable with DPF/RPP specimens [105]. Peak value was reported by Ibrahim et al. [112] in glycerol matrix with 50 wt% DPF. PE-P fiber (PE-PF) weaves with 5mm fiber size reinforced with polyester exhibited the highest young's modulus among all PNFCs (4.18 GPa). NaOH, C_3H_3N , seawater and 70 °C microwave treatments, hybridization

with ijuk, jute and glass fibers as well as adding nano-fillers contributed in tensile strength and young's modulus improvement. However, 50 wt% fiber content, 5 mm fiber size and woven layers was the optimum combination. It is worthy to mention that, the highest TS values were obtained in epoxy and polyester matrices.

Single fiber pull-out was conducted in PNFC studies by testing the fibers before and after their treatment, in order to evaluate the effects of treatments on fiber properties. As clearly shown in Table 11, single fiber pull-out was mostly considered to test DP extracts, results ranged from 366 MPa up to 1246.7 MPa. Highest tensile strength (1246.7 MPa) was revealed in 1% NaOH treated palm fibers, with a young's modulus of 26.1 GPa [87]. Hence, peak elastic modulus (160 GPa) with 800 MPa tensile strength was observed in date palm meshes [88]. Alsaeed et al. [117] conducted single fiber pull tests on DPFs with four different fiber lengths (5, 10, 15 and 20 mm) and three NaOH soaking concentrations. The highest tensile strength (400 MPa) was obtained in fibers with a length of 10 mm and soaking time of 6 h. Abdal-hay et al. [118] observed 57% improvement in the tensile strength of DP single fiber upon treatment with alkaline solution, nevertheless, this solution reduced the young's modulus. Izani et al. [98] observed an increase in the tensile strength of OP single fiber treated with alkaline. Alawar et al. [88] reported that soda treatment (NaOH) cleaned DP mesh from the impurities resulting in tensile strength improvement, where the highest TS was observed in fibers treated with 1% soda.

2.2 Luffa and Its Composite Materials

Luffa is a type of Cucurbitaceae family, its mature fruit is being used around the world as an organic cleaning sponge. Luffa has a natural 3D network structure, which contributes in its high strength, toughness, and stiffness.

2.2.1 Fiber Treatment

Water absorption and moisture retention harm the fiber/matrix adhesion in composite materials. Moreover, NFs have high moisture absorption behavior as they are naturally hydrophilic. Such properties cause a reduction in bond strength, thereby matrix and fibers detach from each other. Hence, these composite materials exhibit negligible mechanical characteristics in wet environments [167]. Therefore, treating a NF with a convenient chemical solution can influence its chemical composition, remove surface impurities, as well as reduce its water absorption characteristics. Table 12 shows the treatments applied to luffa fibers in LNFC studies.

Table 12: Luffa Fiber Treatments

Treatment	Reference
Sodium Hydroxide (NaOH)	[25, 61, 66-68, 168-190]
Hydrogen Peroxide (H ₂ O ₂)	[27, 168, 169, 179-181]
Acetic Acid (CH ₃ COOH)	[27, 168, 169]
Carbamide CO(NH ₂)	[169]
Methacrylamide	[174, 183]
Benzoyl Chloride Permanganate (KMnO ₄)	[68, 189]
Acetic Anhydride, and Acetone	[179]
Furfuryl Alcohol followed by oxidation (sodium chlorite + acetic acid)	[67]
CaCl ₂ , H ₂ SO ₄ , and Na ₂ HPO ₄	[171]
Hypochlorite (NaClO)	[172]
Ethanol, BTDA Dianhydrides	[178]
HCl	[170]
Chlorine Bleach	[63, 191]
Calcium Phosphate and Calcium Carbonate	[192]
CaOH ₂ and Silane	[185]
Thermo-mechanical treatment and thermo-hydromechanical treatment	[193]
Heat treatment	[194]

Sodium hydroxide (NaOH)/alkaline treatment evidenced its capability in improving luffa fibers' microstructure by changing its chemical composition as well as removing all impurities [66, 173-177, 184]. Treating luffa fibers with 4% NaOH at 120 °C for 3 h revealed the highest fiber crystallinity index. In addition, combined chemical

treatments switched luffa from a mat into a filament structure [181]. Contrary to other chemical solutions, methacrylamide treatment caused a serious deterioration in luffa fiber integrity [183]. Mixing NaOH with other solutions like CH_3COOH can drastically improve LNFC mechanical performance as well as significantly decrease its water absorption. In contrast, mixing with H_2O_2 deteriorated its mechanical characteristics [169]. The tensile strength of LNFC prepared with HCl treated fibers was lower than that of LNFC treated with alkaline [170]. Cyanoethylating and acetylation improved fiber/matrix adhesion, resulting in an enhancement in mechanical characteristics [179, 180]. Furfuryl alcohol followed by oxidation treatment revealed higher performance compared to alkaline, where it improved the surface structure and reduced hemicellulose, lignin, and wax quantities [67]. As shown in Table 12, sodium hydroxide was mostly utilized to chemically treat luffa fibers, followed by hydrogen peroxide and acetic acid.

2.2.2 Matrices Selected for LNFCs

Composites have a combination of fibers and matrix properties, and in addition to matrix properties, they behave as a structure that holds all fibers together, as well as a protection from the surrounding environment (water, heat, etc.) [1, 195-197]. Thus, studying the performance of a new NFC involves choosing a suitable matrix that exhibits good properties with a considerable interaction with the selected NF. Several studies investigated luffa as a pure mat (without a matrix), however, others studied different thermoplastics and thermosets like epoxy, polyester, resorcinol-formaldehyde, vinyl ester, and so on [198-200]. Matrices considered in recent LNFC studies are listed in Table 13.

LNFC studies have involved diverse polymeric matrices with different weight ratios (fibers volume fraction), which ranged from 2 wt% to 50 wt%, however, the most

common weight composition was 30 wt% [24, 66, 67, 176, 184]. Although the majority of studies considered luffa as rectangular mat, some utilized it as randomly chopped fibers between 2 mm and 6 cm.

Table 13: Thermoplastics and Thermosets Used in Luffa Natural Fiber Composite (LNFC) Development

Matrix	Reference
Epoxy	[25, 61, 66-68, 168, 173, 175-177, 201-205] [186-189, 198, 206, 207]
Polyester	[24, 170, 174, 179, 180, 184, 185, 198, 208-210]
Resorcinol-formaldehyde	[171, 192, 211]
Polylactic acid	[172, 194]
Bio-based polyethylene (HDPE)	[212]
Vinyl ester	[7, 178]
Polyurethane foam	[62]
Polyurethane (PU)	[213]
Polypropylene	[182]
Geopolymer	[214]
Pre-gelatinized cassava starch	[215]
Eva resin	[216]
Bismuth nitrate pentahydrate (Bi(NO ₃) ₃ ·5H ₂ O) and potassium iodide	[190]
Concrete	[217]

As clearly shown in Table 13, epoxy resin was selected most often in the LNFC field, followed by polyester and resorcinol-formaldehyde, which is due to matrix properties as well as matrix/fiber compatibility.

2.2.3 Tensile Properties of LFCs

Mechanical characteristics of an NFC are specified through different testing procedures [218, 219]. The tensile properties of LNFCs are summarized and discussed in this section. Tensile testing results obtained in recent LNFC studies are compiled and classified in Table 14, all the listed tests were conducted following the standard of American Society for Testing Materials (ASTM).

Table 14: Mechanical Properties of Luffa Natural Fiber Composites

Resin/Fiber Treatment	Fiber Size, Shape, and Composition $V_f/\text{wt}\%$	Hybrid/Filler	Tensile (MPa)	Ref.
Epoxy/NaOH	Particles, short fibers, and mat shaped fibers (0.3–0.5 V_f)		23	[173]
Epoxy/NaOH	10–20 mm (0.1 – 0.5 V_f)	Ground nut (1:1)	20	[176]
Epoxy/NaOH	Mat (0.3 V_f)	Flax	24	[66]
Epoxy/NaOH		Ceramic B_4C (10 wt%)	13.56 E: 73.29	[61]
Epoxy	Rectangular mat (8, 13 and 19 wt%)		18 E: 699	[204]
Epoxy	Rectangular mat (19.87–30.86% V_f)	Glass fiber	35.34	[205]
Epoxy/NaOH, and furfuryl alcohol followed by oxidation (sodium chlorite + acetic acid)	100 × 100 mat (30 wt%)		226.40 E: 5865.70	[67]
Epoxy/NaOH, benzoyl chloride, and potassium permanganate KMnO_4	Rectangular mat (13 wt%)		28 E: 910	[68]
Epoxy/NaOH	Chopped randomly (30%, 40% and 50% V_f)		18	[177]
Epoxy/NaOH	6 cm (0.3 V_f)	Silica nanoparticles	13 E: 3284	[175]
Epoxy/NaOH, acetic acid	2 mm (8, 9, 9.5 and 10 wt%)	Lignite Fly Ash filler	17.28	[168]
Epoxy	Rectangular mat (8, 13, and 19 wt%)		16.76	[202]
Epoxy/NaOH	2–5 mm (3.2–9.6 wt%)		E: 5560	[25]
Epoxy		Ceramic fibers	140.68	[198]
Epoxy/NaOH	2 mm	Carbon fibers	60.48	[220]
Polyester	30 wt%	Natural fillers (ground nut shell, rice husk, and wood powder) (3, 7 and 11 WT%)	31.5	[24]
Polyester/NaOH, methacrylamide	Short fibers and mat (24.5–42.6% V_f)		22 E: 5200	[174]
Polyester/methyl ethyl ketone peroxide	Mat 250 × 100 mm		23.893	[170]
RF/Calcium phosphate and calcium carbonate	50 wt%		14.88 E: 680	[192]
RF/NaOH, CaCl_2 , H_2SO_4 , and Na_2HPO_4	2 cm (10–50 wt%)		29.438 E: 1662	[171]
Polyurethane	Mat	Glass fiber	12.7	[213]
PP/NaOH and silane coupling agent	2–15 wt%		35	[182]
Bio-based polyethylene (HDPE)	(10, 20, 30 and 40 wt%)		21.2 E: 2082	[212]
Vinyl ester/ethanol, NaOH, BTDA dianhydrides	Mat (15 wt%)		21.2	[178]
Polylactic acid/ NaClO	2 cm (2, 5 and 10 wt%)		36.44 E: 2997.45	[172]

Table 14: Mechanical Properties of Luffa Natural Fiber Composites (Continued)

Resin/Fiber Treatment	Fiber Size, Shape, and Composition $V_t/wt\%$	Hybrid/Filler	Tensile (MPa)	Ref.
Pre-gelatinized cassava starch	3–5 mm (5, 10, 15, and 20 wt%)		1.24	[215]
Pure luffa/NaOH, H ₂ O ₂ , CH ₃ COOH,	30–40 mm/Bundle		74.23 E: 820	[169]
Pure luffa/glacial acetic acid and hydrogen peroxide	2 20 and 30 mm		91.63 E: 1897	[27]
Pure luffa/thermo-hydrromechanical treatment	3 mm		177.93	[193]
Pure luffa	30 mm		120 E: 2300	[64]

Luffa natural fiber composite studies have mostly considered the tensile behavior compared to other mechanical properties, aiming to define the elastic behavior of this NFC, i.e., ultimate tensile strength as well as young's modulus. Tensile strength of LNFCs increased by increasing fiber content up to 40 wt%, but it started to decrease at 50 wt% [173, 176]. Thus, Mani et al. [221] reported an increment in the tensile strength of luffa mat/epoxy NFC followed by a decrement when adding fibers beyond 40 wt%. However, by considering chopped luffa fibers, 50 wt% revealed the highest strength. In a sandwich structure, the tensile strength of LNFC increased by increasing fiber content up to two luffa layers then decreased by adding a third layer [204]. Generally, LNFC developed with NaOH-treated fibers exhibited higher tensile strength compared to that of untreated fibers [66, 68, 174]. Moreover, benzoyl treatment showed better property improvement than alkali and KMnO₄ treatments [68]. In addition, BTDA dianhydrides (tetracarboxylic benzophenone dianhydrides) revealed the best TS increment compared to ethanol and NaOH treatments [178]. However, Furfuryl Alcohol-grafted LNFC revealed a notable improvement in tensile strength (100%) and tensile modulus (123%), which were higher than that observed in NaOH-treated LNFC [67]. Superior TS can be obtained by hybridizing LNFC with

natural or synthetic fibers such as ceramic B₄C, which improved TS around 8.6% [61], glass fiber (up to 100.4%) [202, 205], and ground nut shell. In contrast, hybridization of LNFC with wood powder or rice husk reduced its tensile strength [24]. Adding silane coupling agent into luffa/polypropylene NFC can deteriorate its TS, whereas increasing the luffa fiber volume fraction reduced the tensile strength [182]. In single luffa fiber testing, 10% NaOH treatment for 30 min at 40 °C showed best enhancement in the fiber's tensile strength [169].

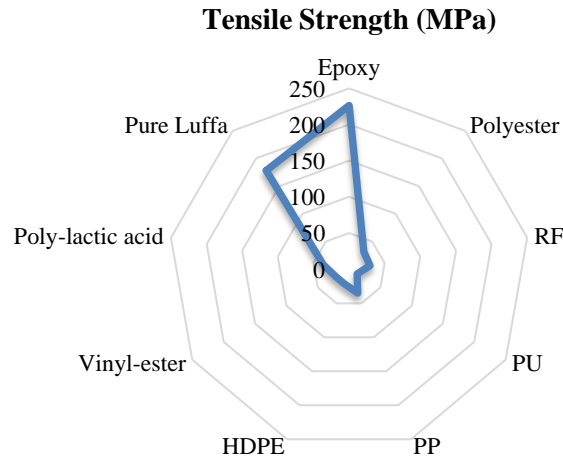


Figure 10: Tensile Strength of Luffa Natural Fiber Composites

As clearly shown in Table 14 and Figure 10, peak tensile strength of LNFC was observed in epoxy matrix, followed by polylactic acid and polypropylene. However, the highest LNFC tensile strength reported was 226 MPa in an epoxy matrix, followed by 140 MPa in a ceramic/luffa/epoxy hybrid NFC. Hence, LNFC with polylactic acid matrix reached a tensile strength of 36.44 MPa and a tensile modulus of around 3 GPa. Thus, luffa in a polypropylene matrix exhibited 35 MPa TS. Luffa NFC revealed a tensile strength of 31.5 MPa with a polyester matrix, 29 MPa in resorcinol-formaldehyde, 21 MPa in bio-based high-density polyethylene as well as in vinyl ester, and lower tensile strength was observed in a polyurethane matrix (12.7 MPa). In terms

of pure luffa, the peak tensile strength observed was 177.93 MPa after treating the fibers through a thermo-hydro-mechanical technique. Paglicawan et al. [222] mentioned that the stress and strain curve of luffa/polyester NFC was similar to the curve of a brittle materials, hence it behaves elastically as stress and strain increases in linear trend.

2.3 Modeling and Simulation

The growing utilization of natural fibers composites (NFC) highlighted the essentiality of effectively designing and developing NFC for optimum performance [223]. Since testing all aspects of an NFC is expensive, scientists and engineers are involving computational techniques to simulate the thermal, physical and mechanical properties of their developed materials, thereby validating their findings experimentally [28, 224]. Application of analytical and numerical methods is profusely increasing in the natural fibers modeling as well as the design of natural fibers composites[225-228]. Hence, a wide set of models and approaches is now available for predicting various characteristics of NFCs [229-232]. Though researchers have focused on predicting the macroscopic (elastic) properties of NFCs such as young's modulus, shear modulus and Poisson's ratio, which revealed high accuracy in the prediction of properties and exhibited good agreement with experimental results [8, 218, 233]. Chen et al. reported a significant agreement between FEA and experimental results of luffa fibers [64]. Kebir et al. [234] highlighted the capability of FEA in predicting the micro-mechanical properties of hemp/polypropylene NFC. Adeniyi et al. [235] observed a notable agreement between FEA and phenomenological analytical model while predicting the elastic properties of banana/polystyrene NFC.

NFC analytical studies investigated models in 1, and 3 dimensions, while 2D was mostly considered. However, a range of analytical theories were involved in the analysis of mechanical, thermal and acoustic properties of NFC, for example, Rule of Mixture, Puck failure theories, Halpin, Tsai–Wu, Tsai–Hill, Nairn Shear-lag, Mendels et al. stress transfer, fatigue-life (S–N) curves, and Hirsch were utilized for studying stiffness, elastic modulus, strength, fatigue-life response, etc. while, Johnson-Champoux-Allard was utilized for inspecting the sound absorption of coconut coir as well as rice husk NFC. Moreover, several analytical models contribute in calculating the mechanical properties of woven fibers composites i.e. Halpin Tsai, Hirsch's, and Cox [236]. However, Fourier's heat conduction equation was previously utilized to study the temperature variation of hemp/kenaf/epoxy hybrid NFC. Not only, Mesoscale Damage Theory was used for calculating the mechanical response, inelasticity, and stiffness degradation of Flax NFC [236-240]. Furthermore, Cox and Halpin-Tsai models has an adequate accuracy in predicting the elastic properties, similarly Hirsch's model is able to calculate the elastic modulus [236]. Hence, less error was revealed while computing the elastic modulus using Halpin-Tsai approach compared to Rule of Mixture, Nairn shear lag analysis, and Stress transfer [241]. Comparing with Tsai-Wu and Tsai-Hill theories, Puck and Hashin exhibits higher accuracy in predicting failure criteria of NFC [237]. However, Rule of Mixture and Tsai based rules were commonly used. Hence, Halpin-Tsai approach can be considered as the best approach in predicting micro-mechanical properties. In terms of woven NFC, Hirsch's model was the best analytical technique for predicting young's modulus, yet Cox and Halpin-Tsai models exhibited analogous remarkable accuracy in calculating the tensile strength. Johnson-Champoux-Allard model was most accurate model for analyzing the sound absorption of NFC, Fourier's heat conduction

equation was significantly convenient to predict the thermal behavior of natural fibers composites, Hashin's model was notably reliable in predicting the fatigue criteria. Only few researches implemented optimization theories as well as design of experiments.

In NFC numerical analysis, most researches tend toward using finite element analysis as well as representative volume elements due to the high accuracy of this method in predicting composites' properties. Some studies involved analytical theories besides the numerical methods, such as Rule of mixtures (ROM), Chamis model, Fick's law, Hamilton's principle, Halpin-tsai model, Hashin and Rosen model. Numerically analyzing the mechanical properties of NFC was the major focus of a notable number of studies. Major natural fiber selected was flax fiber, and epoxy matrices were mostly chosen. While several researches involved more than one type of natural fibers to develop a hybrid natural fibers composite, though NFCs were hybridized with synthetic fibers like E-glass. Despite the fact that composites and NFC are orthotropic, materials were mostly considered as Isotropic in M&S of NFC studies, apparently, due to the lack of data about these newly developed materials.

Various boundary conditions were assigned like clamped, free, and simply supported boundary conditions, as well as periodic boundary conditions in representative volume element [242-244], Diverse boundaries were taken into account like topologies, material properties, weight, cost, mass, cost, easy manufacturing, mesh density, element order, microwave exposure time and location of specimen in the microwave. ANSYS was majorly utilized as a simulation platform, whereas several element types were used such as wedge elements (C3D6), linear hexahedral elements (C3D8R), quadratic tetrahedral elements (C3D10), SHELL 181, Solid 95, Solid 185, Solid 186

and Solid 187, yet most studies analyzed NFC as a 3D solid model. Some optimization algorithms were applied, viz. Genetic Algorithm, Topsis, parametric optimization and APDL, regardless of the distinct aspects optimized through the aforementioned algorithms, the implementation of those techniques proved its reliability and effectiveness. while very few studies included the design of experiment by using Taguchi method (ANOVA) for selecting the parameters combination that gives maximum load enduring capacity at failure, for instance, Parsad et al. considered three factors, viz. three fiber lengths, three CNSL percentages (5, 10 and 15%), and three fiber to matrix ratios (20, 30 and 40 wt%), then utilized Taguchi (DOE) method in order to obtain the analysis number [245]. A significant number of researches indicated that predicted and experimental findings were in strong agreement.

Majority of the researches focused on investigating the mechanical properties of natural fibers composites, multiple simulation platforms were utilized such as ANSYS, ABAQUS, MATLAB, LS- DYNA, Nastran/Patran, Siemens PLM NX 10.0, NISA and so on. In addition, several analytical techniques were involved like experimental modal analysis, Newton-Raphson non-linear, Maximum strain and Tsai-Wu, J-Integral, Rule of mixture, Weibull distribution, Chamis model, Nielsen Elastic model, Halpin–Tsai model, etc. Table 15 shows the summary of research on numerical M&S of tensile strength, joint strength, stress and strain characteristics of natural fibers composites.

Table 15: Numerical M&S of Tensile and elastic behavior of NFCs

Fiber type, size and orientation	Epoxy/ Hardener	Analytical	Numerical Analysis	Objective of The Study	Platform	Boundary Conditions	Optimization Algorithms/ Physical Experiments and Validation/ Key Findings and Remarks	Ref.
Flax 46.2 WT%	POM		FEA RVE (homogenized)			Periodic Boundary Conditions	<ul style="list-style-type: none"> Tensile, SEM Results obtained from RVE and FEA models significantly agreed with experimental results. 	[246]
Flax one by one top-hat stiffened composite plate	Epoxy	Grillage	FEA	Stresses & strain	Abaqus	Simply Supported Boundary Conditions	<ul style="list-style-type: none"> Parametric study is 5% lower in accuracy comparing to finite element analysis. 	[247]
Flax	PP	Maximum Strain failure criterion	FEA	Strain	Abaqus		<ul style="list-style-type: none"> Stamping & Aramis monitoring system FLC & MSF criteria can accurately predict failure regions in all specimens. 	[248]
Hemp Naca cowling of an acrobatic ultra-light airplane	Epoxy	Maximum strain and Tsai-Wu	FEA	Mechanical properties	Fluent and ANSYS)		<ul style="list-style-type: none"> Tensile, 3-point bending & SEM FEA and experimental results were different. 	[249]
Hemp 30 WT%	PP		FEA (RVE)	Mass Fraction, Tensile	Kebir Simulation Platform		<ul style="list-style-type: none"> Tensile PF approach could be considered as a complementary technique to micro-mechanical approaches 	[234]
Hemp/ Jute Hybrid 30°,45° & 90°	Epoxy & Polyester			Mechanical Properties	ANSYS		<ul style="list-style-type: none"> Tensile, flexural, impact, Specific gravity, water test & hardness tests High agreement was exhibited between FEA and experimental results. 	[250]
Jute 45° - 90°	Epoxy		FEA	Tensile behavior	Siemens PLM NX 10.0		<ul style="list-style-type: none"> Tensile Testing & SEM Simulation outputs significantly agreed with tensile testing results. 	[251]
Jute	Epoxy and (PU joints)	J-Integral (Compliance Calibration Method, Cubic polynomial & Corrected Beam Theory	FEA	Tensile fracture toughness of adhesive joints & CZM	Matlab Sub-routine		<ul style="list-style-type: none"> Bulk tensile Trapezoidal law reproduces the experimental behavior with a reasonable level of accuracy 	[252]
Jute	Epoxy	Rule of mixture, Weibull distribution	FEA	Tensile, Strain, & Elastic modulus	MENTAT & MARC		<ul style="list-style-type: none"> Predicting failure stress and tensile strength were significantly improved by updating fibers' strength with accordance to their length post-failure. 	[253]

Table 15: Numerical M&S of Tensile and elastic behavior of NFCs (Continued)

Fiber type, size and orientation	Epoxy/ Hardener	Analytical	Numerical Analysis	Objective of The Study	Platform	Boundary Conditions	Optimization Algorithms/ Physical Experiments and Validation/ Key Findings and Remarks	Ref.
Jute/ banana hybrid	Cashew nut shell resin		FEA	Strength	Solidworks, ANSYS & Minitab		<ul style="list-style-type: none"> Tensile FEA and experimental results are close 	[245]
Banana	Polystyrene	Chamis model, Nielsen Elastic model, Halpin–Tsai model, and Rule of Mixture	FEA (RVE)	Elastic properties	ABAQUS	Periodic Boundary Conditions	<ul style="list-style-type: none"> The phenomenological analytical model estimations highly agreed with FEA results 	[235]
Sisal & Banana	Epoxy	Rule of mixture & Halpin-Tsai	FEA	Elastic Properties	ANSYS		<ul style="list-style-type: none"> Tensile & SEM The FEA combined with the micromechanical analysis had the ability to describe the interface state of the NFC phases. 	[254]
Sisal/ Coir Hybrid	Epoxy		FEA (RVE)	Mechanical Properties	ANSYS		<ul style="list-style-type: none"> Tensile Significant agreement between FEA & Experimental results. 	[255]
Agave	Epoxy	linear elastic orthotropic model	FEA	effect of joint geometry on the strength	ANSYS		<ul style="list-style-type: none"> Tension tensile strength of lap shear joints was extremely lower than plain NFC, dissimilar to intermingled fiber joints & laminated fiber joints 	[256]
Nettle &grewia optiva	polylactic acid & polypropylene		FEA	Joint Strength	COMSOL		<ul style="list-style-type: none"> Microwave heating & adhesive bonding by considering experimental and numerical results, the proposed model may be utilized to study the joining performance of composite materials using microwave. 	[257]
Pineapple	Epoxy	ROM, MROM, chamis, halpin-tsai, Hashin and Rosen model	FEA (RVE)	Mechanical properties	ANSYS & Matlab	x, y, z = 0	<ul style="list-style-type: none"> Electronic tensometer & Single fiber pull-out MROM as well as Chamis model showed high accuracy. 	[258]
Pulp Ellipsoidal	Poly lactic acid		FEA	Dimensions and orientation of fiber agglomerates	ANSYS		<ul style="list-style-type: none"> Tensile test, SEM The predicted strength using the stress concentration factor theory disagreed with experimental findings. 	[259]
Henequen Laminates	PE	Photoelastic	FEA	Fiber curvature effect on the tensile properties	NISA		<ul style="list-style-type: none"> Tensile test Much better agreement was obtained after decreasing the fiber efficiency by using an average length value to compensate for the fiber curvature in the strength properties. 	[260]
Wood 60 WT%	18% PE & 12% PP		FEA	Joint Strength	Yamada-Sun failure criterion in ABAQUS	Simply supported	<ul style="list-style-type: none"> Tension Predicted and experimental results are in high agreement 	[261]
Wheat straw 4 fiber lengths	PP		FEA	microstructural behavior & microcellular-voided	AutoCAD & Abaqus		<ul style="list-style-type: none"> Tensile & SEM The FEA curves are well matched in general to the experiments. 	[262]

Numerical modeling and simulations of NFCs were barely reported compared to glass and carbon composite materials. However, initial FEA steps consist of; creating the model geometry followed by assigning the characteristics of the material. FEA that considers the mechanical behavior of an NFC requires specific failure criteria, which defines the failure initiation as well as propagation. It is worthy to mention that in terms of tensile properties, natural fibers behave in a different manner compared to synthetic fibers. Failure criteria of strong synthetic fibers are usually involved in NFC analyses, as the specific failure criteria of NF are not proposed. Thus, the aforementioned criteria contributes in predicting the ultimate tensile strength, yet it ignores other characteristics like nonlinear tensile response of a NF [263]. As clearly shown in table 15, numerical M&S of NFC was mostly focusing on the tensile behavior compared to other mechanical properties. The tensile strength, and stress/strain properties of numerous natural fibers were simulated i.e., flax, hemp, jute, banana, sisal, wood and so on. Several analytical approaches were considered along with the numerical techniques, such as Maximum Strain failure criterion, Tsai-Wu, Weibull distribution, Chamis model, Nielsen Elastic, Halpin–Tsai, Rule of Mixture, Hahsin, Rosen, etc. Different polymeric matrices were selected, for example epoxy, polypropylene, POM, polystyrene, and PLA.

Thus, Petrone et al. [264] numerically analyzed the mechanical properties of flax/polyethylene laminates (250 x 15 x 1 mm) NFC using Structural Dynamic Toolbox (SDT) in MATLAB software, authors had to modify the mechanical properties assigned to the finite element model due to the discrepancies between FEA and experimental results. After two parameter's update stages, it was observed that outcomes may be enhanced by including further information through the model update procedure like panel shape and thickness dimensions. Xiong et al. [246] studied the

micro-mechanical characteristics of flax/ polyoxymethylene NFCs using RVE micro-scale. The multi-scale constitutive model was conducted in 2 stages; primarily, utilizing an orientation averaging technique to calculate micromechanical characteristics of the twisted yarn, then the outputs of stage 1 were shifted into a meso-scale representative volume element of a single ply NFC in order to inspect its elastic behavior. Results showed that elastic properties of this NFC are highly affected by the twist angle of the yarn. The latter has a simultaneous effect on the distributed stress throughout the RVE.

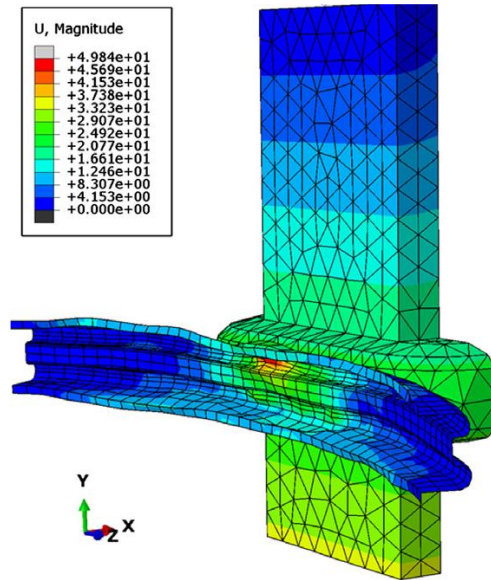


Figure 11: Displacement profile of double hat profile after impact [265]

Further mechanical performance have the potential to be inspected through finite element analysis at costs lower than experimental testing, for example Davoodi et al. [265] numerically studied the impact properties of a car bumper made from hybrid kenaf/glass/epoxy using Catia and Abaqus platforms. Figure 11 illustrates the displacement profile of a car beam after applying an impact load. Usually, The variation between experimental and finite element analysis results is due to unconsidered material properties, it is worthy to mention that natural fibers are

orthotropic, as well as NFCs contain voids, discontinuity and porosity [266]. In order to examine the sound transmission loss, it is conceivable to create a mechanical model in FEA using the data obtained from mechanical testing and assign identical boundary conditions imposed in the impedance tube [267].

2.4 Machine Learning Application for Composite Materials

Nowadays, machine learning as well as artificial intelligence are being implemented not only by the AI researchers, yet scientists and engineers in other researcher areas are also utilizing these tools for achieving their own targets. Previously machine learning was utilized for detecting C60 solubility, however it is currently involved in predicting molecular characteristics of designed materials. Despite the fact that experimental testing is significantly essential for developing a new material, machine learning contributes in decreasing the cost as well as the computational time throughout an experiment, as the required tools for running the machine learning algorithms are free to access and easily available [268].

Recently, artificial intelligence was applied by several researchers in composite materials and natural fibers composites. Antil et al. [269] utilized ANN and RSM to study the erosion behavior of S Glass composites, inputs included nozzle diameter, impingement angle, and slurry pressure. Pati et al [270] applied ANN for predicting the wear behavior of glass/epoxy composites, input parameters consisted of; erodent temperature, erodent size, RBD content, impingement angle, and impact velocity. While Baseer et al. [271] assigned shear strength, failure stress and strain, tensile modulus, and tensile strength as input parameters for evaluating the interfacial and tensile properties of hybrid composite material. Atuanya et al. [272] emphasized the reliability of using ANN to predict the mechanical behavior of NFCs, authors

implemented artificial neural networks for predicting the mechanical properties of date fibers' reinforced low-density polyethylene (recycled), input data consisted of fibers' weight percentages, while the output was tensile strength, young's modulus, elongation, flexural modulus, and hardness. Daghigh et al. [273] utilized k-nearest neighbor regressor for predicting the heat deflection temperature of latania NFCs, pistachio shell NFCs, and date seed NFCs. Also, Daghigh et al. [274] applied decision tree regressor and adaptive boosting regressor for studying the fracture toughness of the aforementioned natural fibers composites. Garg et al. [275] implemented extreme machine learning to investigate the mechanical factor of jute as well as coir natural fibers composites. Wang et al. [276] used random forest machine learning approach for analyzing the acoustic emission of flax NFCs.

Chapter 3

METHODOLOGY

In this research the mechanical properties of the natural fiber composites were studied. The methodologies included experimental investigations, modelling and simulation, and machine learning. The micro-mechanical properties such as longitudinal modulus, transverse modulus, shear modulus and poissons' ratio were investigated analytically and numerically, in addition to the tensile strength that was obtained experimentally. Specimen preparation and tensile property testing were carried out as per ASTM standards (ASTM D3039). The tensile properties of the considered NFCs were utilized for training machine learning models i.e. Artificial Neural Networks, Multiple Linear Regression, Adaptive Neuro-Fuzzy Inference System, and Support Vector Machine in order to generate the design space as well as evaluate the aforementioned models in predicting tensile strength of natural fibers composites that were considered in the experiment. The overall research is divided in 6 phases as shown in Fig. 12.

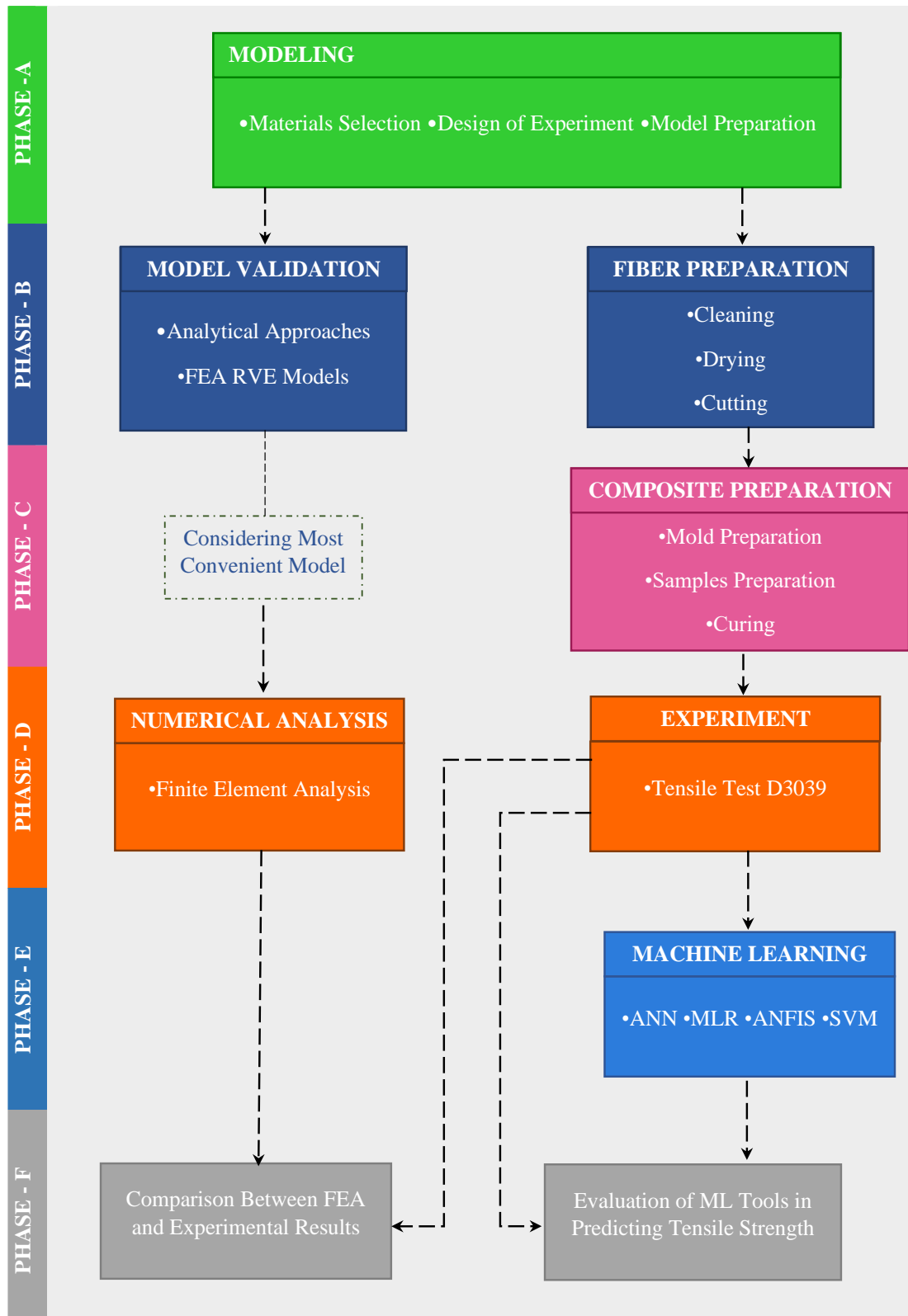


Figure 12: Research Methodology

3.1 Modeling and Simulation

Prediction of NFC properties can be performed through many analytical approaches such as rule of mixture, Halpin-Tsai, Nielsen, Chamis, Tsai-Hil, Mendels et al. stress transfer, Hirsch, Tsai-Wu, and Nairin. Finite element analysis and other numerical techniques helps conducting virtual experiments on a simulation platform [277-280]. Since NFC structures are complicated due to their diverse length scales, it is of a high importance to develop a homogenized computational method. Thus, representative volume element is the most effective homogenized multiscale FEA, which includes analyzing the properties of a natural fiber composite unit cell at nano, macro, or micro-scale [253, 281-284].

3.1.1 Finite Element Analysis

Finite element analysis is a modeling and simulation tool widely used in academia and industry, any material model, boundary conditions and complex shape structures can be easily solved by finite element analysis [285-288]. FEA is a tool where an experiment can be conducted virtually, hence the graphs obtained can be read and analyzed easily [289]. Highly accurate and optimized results can be obtained by conducting several iterations, so that the product development down time will be reduced, and its lifetime will be enhanced [290-292]. Figure 13 shows the steps in finite element analysis process [243].

The preprocessing of a FEA is a very important step, it determines the quality of the simulation and thereby the accuracy of the results, it consists of: geometry preparation, material definition, element and mesh selections. Next, loads and constraints are assigned based upon the considered analysis type [293].

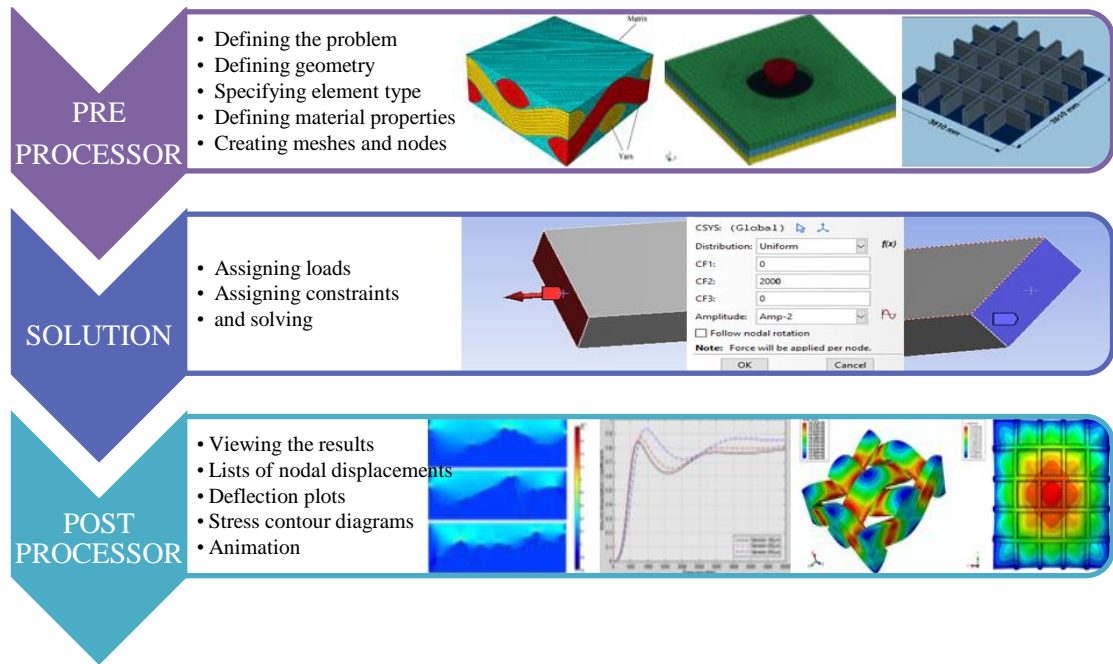


Figure 13: Overview of Finite Element Analysis (FEA) Adapted from [294]

3.1.2 FEA of Natural Fibers Composites

In modeling and simulation, a range of properties can be predicted and a diversity of analysis methods can be utilized, viz. multi-physics analysis, electrical analysis, buckling analysis, electromagnetic analysis, heat transfer analysis, fluid analysis, thermal analysis, structural analysis, and acoustic. Mostly in M&S of NFC researches focused on mechanical properties [242, 295-298], while few investigated the acoustic and thermal properties [299, 300]. Analytically, a model can be studied from one dimension up to three dimensions. But for accurate results, three-dimensional models are recommended for natural fibers composites analysis, especially when loads are applied in the out-of-plane direction [301]. The model preparation is easy since the imported geometry is usually three-dimensional [302].

Matrix as well as natural fibers' characteristics are specified in modeling and simulation based on requirements of the type of analysis [303, 304], for example: studying the mechanical properties requires poisson's ratio, young's modulus,

elongation at break, shear strength, and density. Whereas, analyzing the thermal behavior of a natural fiber composite needs to assign the thermal conductivity values (K) of both components. However, inspecting the sound absorption coefficient can require orthotropic mechanical characteristics [267, 305]. Since it is hard to define the exact orthotropic properties of a newly developed NFC, some researchers considered their materials as isotropic, where a material behaves similarly in all force directions, unlike orthotropic materials that exhibit dissimilar properties upon different load directions [306, 307], where it is simpler to assign a single value for young's modulus as well as for Poisson's ratio [12, 308, 309].

Finite element analysis has become very valuable engineering tool. Commercially available FEA Software's are: ANSYS, SDRC/IDEAS, NASTRAN/PATRAN, HYPERMESH, LS DYNA, ABAQUS, SIEMENS PLM NX, NISA, COMSOL, KEBIR and so on. While MATLAB have been used for some modeling and optimization purposes (using fmincon solver). ABAQUS capabilities for geometry modelling are quite general (cables, trusses, shells, 2D & 3D continua and so on), includes a wide range of materials, limited support and reasonable control in meshing [310]. However, ANSYS workbench is vastly automated and very flexible for users to modify according to their application/analysis type. Its materials library consists of reactive material, creep, viscoelasticity, elasticity, plasticity, linear materials, etc. Moreover, ANSYS includes Thin- sweep meshing and automatic meshing (hexa-dominant, swept hex, hex-core, tetrahedral, and surface meshing) [311]. Furthermore, based on the geometry shape and dimensions in NFC studies, elements' numbers ranged between 15000 and 180000 with element size from 20 to 70 μm . Solid models involve typical solid elements where the material is assigned to all regions of the model, while shell models consider the external shell of the model only [312].

Researchers utilized diverse solid and shell elements in ANSYS such as, Solid 20 Node 186, Solid 95, Solid 46 , Shell 281, Shell 181, Shell 99, etc. [313]. while numerous elements types were used in ABAQUS like, hexahedral elements (C3D8R), tetrahedral elements (C3D6), tetrahedron (TET10 or C3D10) and eight node hexahedron (HEX8). Figure 14 illustrates the main element types involved in finite element analysis.






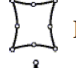





Element Order	2D Solid	3D Solid	3D Shell	Line Elements
Linear	 PLANE42 PLANE182	 SOLID45 SOLID185	 SHELL63 SHELL181	 BEAM3/44  BEAM188
Quadratic	 PLANE82/183  PLANE2	 SOLID95/186  SOLID92/187	 SHELL93	 BEAM189

Figure 14: Elements Type [314]

Hence, the load applied depends on the natural fiber composites' analysis type (Acoustic, fatigue load, buckling load, thermal load or structural load), so that this load indicates which property of the NFC is examined [315], for example in mechanical loadings; the direction of applied forces indicates if this analysis is tensile, shear, flexural, impact, or compression [316].

3.1.3 Representative Volume Element (RVE)

RVE comprise investigating the performance of an NFC or a composite material's unit cell at Nano-scale, Micro-scale or Macro-scale. Main 3-dimensional RVE boundary conditions are: periodic (PBC), homogeneous (HBC), and displacement boundary conditions [243]. When PBC is selected, the simulation outputs characterize a macro structure containing repeated periodical cells. Whereas, by selecting HBC, the simulation outcomes will deem that the RVE itself is the macro structure and take into consideration its micro-components [244]. However, in another NFC analysis types,

the boundary conditions of the electrical conductivity problem included an applied voltage on one face and a ground on the opposing face. That generated some current density within the RVE model and that current density was used along with Ohm's law and the dimensions of the RVE to calculate the overall conductivity of the composite [317]. Currently, various helpful tools like EasyPBC in ABAQUS and Material Designer in ANSYS are being utilized in order to study the RVE of natural fibers composites [235]. These tools require materials' properties, fiber size and volume fraction as an input, thereby it can automatically define the corresponding RVE dimensions, most convenient mesh size and type, and lastly it solves the RVE model.

3.1.4 Numerical and Analytical Simulation of Palm and Luffa NFC

First, the simulation model utilized in this research was validated through comparing the performance of multiple analytical approaches and two RVE models, input properties were identified from the literature, all models' results were evaluated using experimental findings from the literature as well. Table 16 illustrates the properties of the materials utilized to validate the model of predicting the elastic characteristics of palm/HDPE, palm/PP, palm/epoxy, palm/ecopoxy, luffa/HDPE, luffa/PP, luffa/epoxy, and luffa/ecopoxy composites.

Table 16: Input Properties of The Selected Materials for Model Validation

Materials	Young's Modulus	Poisson's Ratio	Shear Modulus
Date Palm Fibers	5065.6 MPa [318]	0.169 [318]	2165 MPa [318]
Luffa Fibers	2300 MPa [64]	0.3	885 MPa
High Density Polyethylene (HDPE)	720 MPa [319]	0.4	260 MPa
Polypropylene (PP)	630 MPa [320]	0.36	232 MPa
Epoxy	1980 MPa (jawaid et al. 2011)	0.35	730 MPa
EcoPoxy	2540 MPa (Plastic Liquid 2:1 Data sheet)	0.33	950 MPa

The selected materials in this research for the simulation are: epoxy, ecopoxy, high density polyethylene and polypropylene as a matrix and date palm and luffa fibers as a reinforcement. The matrices and fibers were assumed to be homogenized and isotropic. Different fiber volume fractions were considered (0.1 to 0.5) in order to evaluate the effect of fiber content on NFC elastic properties. The results obtained from representative volume element (RVE) with unidirectional and random chopped orientations were compared with those of analytical models. After model validation, most accurate model was implemented for predicting the elastic properties of biopoxy/palm, biopoxy/luffa, epoxy/palm, epoxy/luffa, PP/palm, PP/luffa, HDPE/palm, and HDPE/luffa considered in the tensile test upon a fibers volume fraction of 0.1, 0.2, and 0.3. Orthotropic output of RVE chopped was assigned into a 120 x 20 x 5 mm beam (following ASTM D3039), thereby a tensile load was applied on the beam till its failure in order to measure its tensile strength. Materials properties considered for the simulation are displayed in Table 17.

Table 17: Input Properties of The Selected Materials for Simulation

Materials	Young's Modulus	Poisson's Ratio
Date Palm	700 MPa	0.19
Luffa	80 MPa	0.3
BioPoxy 36	1850 MPa	0.3
Epoxy	23 MPa	0.3
PP	630 MPa	0.3
HDPE	150 MPa	0.28

3.1.4.1 Analytical Models

Analytical models are able to mathematically compute the properties of the end composite material through assigning characteristics of matrix and reinforcement as input, for example in some basic micromechanics theories, main inputs include volume fraction, shear modulus, poisson's ratio, and elastic modulus of each component in the

considered composite. Further parameters might be required in some models, such as fiber orientation, aspect ratio, density, orthographic properties, viscoelastic behavior and so on. Predicting properties of woven fibers composites is much complex comparing to continuous fibers composites. The wide variety of theoretical models includes: Rule of mixtures (ROM) which is the easiest existing method to analyze the elastic properties of a fiber-reinforced composite [241], ROMs can only be used on continuous and unidirectional fiber. Similarly, Halpin and Tsai equations are vastly implemented in order to predict elastic properties of composite materials [236]. Cox's model is an ancient analytical model that can be used to determine short fibers impact on the modulus and strength of a composite materials [236]. The analytical models considered in this research are Chamis model, Nielsen elastic model, Rule of Mixture, and Halpin-Tsai model.

3.1.4.1.1 Rule of Mixture

Rule of mixture is the application of mathematical equations to compute the elastic characteristics of composites based on orientation, volume fraction, and properties of fibers and matrix.

Longitudinal properties:

$$E_1 = E_f V_f + E_m V_m \quad (1)$$

$$\nu_{12} = \nu_f V_f + \nu_m V_m \quad (2)$$

where E_m is the young's modulus of HDPE and PP, E_f is the Young's modulus of palm and luffa fibers, ν_m is the poisson's ratio of HDPE and PP, ν_f is the poisson's ratio of palm and luffa fibers, V_m is the volume fraction of HDPE and PP and V_f is the volume fraction of palm and luffa fibers.

Transverse properties:

$$E_2 = \frac{E_m E_f}{E_m V_f + E_f V_m} \quad (3)$$

Shear properties:

$$G_{23} = \frac{G_m G_f}{G_m V_f + G_f V_m} \quad (4)$$

where G_m and G_f are the shear moduli of matrices and fibers, respectively.

3.1.4.1.2 Halpin Tsai

Halpin–Tsai approach is a semi-empirical model developed to modify transversal modulus by correcting factors η and ζ . This approach involves predicting the longitudinal modulus and poisson's ration based upon the rule of mixture [321].

Longitudinal properties:

$$E_1 = E_f V_f + E_m V_m \quad (5)$$

$$\nu_{12} = \nu_f V_f + \nu_m V_m \quad (6)$$

Transverse properties:

$$E_2 = E_m \left(\frac{1 + \zeta \eta V_f}{1 + \eta V_f} \right) \quad (7)$$

$$\text{where } \eta = \left(\frac{\frac{E_f}{E_m} - 1}{\frac{E_f}{E_m} + \zeta} \right) \text{ with } \zeta = 2$$

Shear modulus:

$$G_2 = G_m \left(\frac{1 + \zeta \eta V_f}{1 + \eta V_f} \right) \quad (8)$$

$$\text{where } \eta = \left(\frac{\frac{G_f}{G_m} - 1}{\frac{G_f}{G_m} + \zeta} \right) \text{ with } \zeta = 2 \quad (9)$$

3.1.4.1.3 Nielsen

Nielsen elastic model is in fact the modified and upgraded version of the equation of Halpin–Tsai by taking into account maximum packing fraction ϕ_{max} , a function of the geometry of the model. ϕ_{max} is 0.785 for a squared cell of circular fibers [322].

Longitudinal properties:

$$E_1 = E_f V_f + E_m V_m \quad (10)$$

$$v_{12} = v_f V_f + v_m V_m \quad (11)$$

$$\text{Transverse properties: } E_2 = E_m \left(\frac{1+\zeta\eta V_f}{1+\psi\eta V_f} \right) \quad (12)$$

$$\text{where } \eta = \left(\frac{\frac{E_f}{E_m} - 1}{\frac{E_f}{E_m} + \zeta} \right) \text{ with } \zeta = 2 \quad (13)$$

$$\text{and } \psi = 1 + \frac{(1-\phi_{\max})}{\phi_{\max}^2} V_f$$

$$\text{Shear modulus: } G_2 = G_m \left(\frac{1+\zeta\eta V_f}{1+\psi\eta V_f} \right) \quad (14)$$

$$\text{where } \eta = \left(\frac{\frac{G_f}{G_m} - 1}{\frac{G_f}{G_m} + \zeta} \right) \quad \text{with } \zeta = 2 \quad \text{and } \psi = 1 + \frac{(1-\phi_{\max})}{\phi_{\max}^2} V_f$$

3.1.4.1.4 Chamis

Chamis model is derived from ROM through substituting the volume fraction of fibers by its square root. As a semi-empirical model, it is the most commonly used and trusted model [323].

Longitudinal properties:

$$E_1 = E_f V_f + E_m V_m \quad (15)$$

$$v_{12} = v_f V_f + v_m V_m \quad (16)$$

Transverse properties:

$$E_2 = \frac{E_m}{1 - \left\{ \sqrt{V_f} \left[1 - \left(\frac{E_m}{E_f} \right) \right] \right\}} \quad (17)$$

Shear modulus:

$$G_{23} = \frac{G_m}{1 - \left\{ \sqrt{V_f} \left[1 - \left(\frac{G_m}{G_f} \right) \right] \right\}} \quad (18)$$

3.1.4.2 Finite Element Analysis

Finite element analyses of luffa as well as palm fibers reinforced thermoplastic composites were conducted using ANSYS “material designer” plugin, which applies an automatic implementation of RVE homogenization concepts. Moreover, the analysis was carried out based on the following criteria.

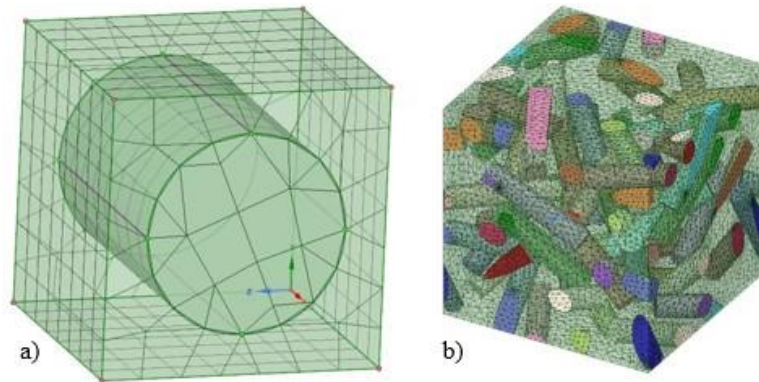


Figure 15: a) RVE with Unidirectional Fibers, B) RVE with Chopped Fibers

Square geometry was selected for RVE and fibers' diameter was considered as 5 μm . Natural fibers composites were considered to be free of voids, and interlinkage between fibers and matrix was considered to be free of flaws. RVE chopped model was meshed with conformal meshing, while conformal as well as block meshing was applied for RVE unidirectional along with periodic boundary condition. Figures 15a and 15b show RVEs with unidirectional structure and chopped fiber orientations.

3.2 Composite Materials Preparation

In this research, date palm meshes and luffa were considered as reinforcements, while biopoxy 36, epoxy, polypropylene, high-density polyethylene were selected as a matrix. This section describes main stages of tensile testing samples' preparation, which includes; fibers' extraction, matrices materials' supply, molds' preparation, and natural fibers composite specimens' preparation.

3.2.1 Composites' Components

Date palm meshes that surround the stem were extracted from a palm tree located in north Lebanon, the fibers were kept to dry for 72 hours and then washed with cold water in order to remove all the dust and impurities. Next, the cleaned palm fibers were dried through placing them under the sunlight on a mosquito net for 23 days [324]. The aim of using a mosquito net was to let the air ventilate the bottom of palm fibers, and avoid any water drop from staying below the fibers, which thereby could harm the fibers by creating moisture. Luffa sponge was supplied from a local store, it was dry and peeled, its length was 46 cm and its average diameter was 16 cm. Regarding the matrices, biopoxy 36 was offered by the manufacturer of this green resin i.e. EcoPoxy, Canada. Aquaglass epoxy resin and its hardener were supplied from Colortek, Lebanon. Moreover, polypropylene 528k and high-density polyethylene F00952 were supplied from Sabic.

3.2.2 Molds Development

Since both thermoplastic and thermoset matrices are considered in this research, and each of the aforementioned has its specific preparation technique, it was compulsory to utilize two different mold's types. For natural fibers' reinforced thermosets, 36 silicon molds were developed by the following steps: 1) silicon sealant was added into water/dish soap mixture, 2) putty was then mixed well till it reached an unsticky dough structure, 3) next, a wooden pattern that has same dimensions of the specimens was inserted in the putty and pressed well around the corners, 4) lastly, the putty was rested on a plastic tray for 15 mins to dry before removing the pattern (Figure 16a).

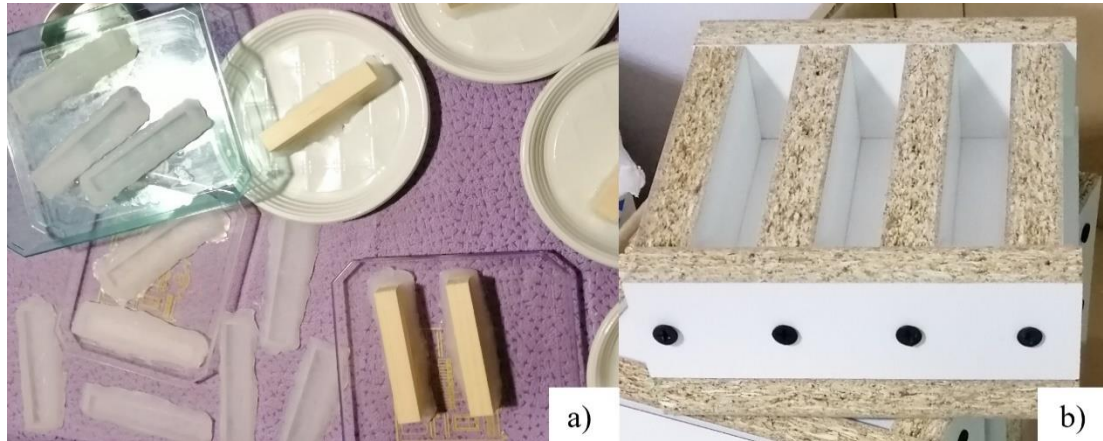


Figure 16: Silicone and Wood Molds Preparation

Meanwhile for the thermoplastic NFCs, the mold required a female mold along with its male part that contributes in compressing the molten NFC till it solidifies. Hence, a plywood board was trimmed into small parts that included the inner and outer walls of the mold, and their base. Thereby, these parts were assembled using wood screws to create 15 female molds that consist of 3 cavities each (Figure 16b).

3.2.3 Samples Preparation

Luffa as well as date palm fibers were chopped using a waring blender in order to attain a homogeneous mixture with the considered matrices, the approximate fibers' length was 1 cm, and the desired fibers' orientation was random. Treating the surface of luffa and date palm fibers with chemical solutions was not applied in order keep these NFCs as green materials, especially NFCs with BioPoxxy 36 matrix. In terms of NFCs with thermoset matrices, the resin was mixed with its hardener for 5 minutes, the resin to hardener mixing ratio was 4:1 for biopoxxy 36 and 1.8:1 for epoxy. Since the micro-mechanical behavior of the considered NFCs observed through the simulation model validation showed notable variations throughout 0.1, 0.2, 0.3 V_f , the aforementioned fibers' volume fractions were considered in for the experimental specimens.

As shown in Table 18, volume fraction was ensured through calculating the specific volume for the fiber and matrix from the total sample's volume i.e. 12 cm³, then multiplying the obtained volume by the corresponding density, which thereby defines the weight of matrices as well as the fibers. Thus, a digital micro-scale was utilized for weighing the components while preparing the natural fibers' composites. For example, for developing a 0.1 palm/biopoly sample, volume of palm fibers was considered to be 10% of the whole specimen whilst that of biopoly was 90%. Thus, out of 12 cm³, volume of palm fibers had to be 1.2 cm³ and BioPoxy had to be 10.8 cm³. Then, the desired volume of palm fibers in this specimen "1.2 cm³" was multiplied by its density "0.19 g/cm³" in order to identify its weight at this volume, which was observed to be 0.228 g. Similarly, weight of biopoly was obtained by multiplying its volume "10.8 cm³" by its density "1.1 g/cm³", thus the obtained weight was 11.88g.

Table 18: Fibers Volume Fraction and Weights Calculations

Matrix	Fibers	V _f	Matrix Density (g/cm ³)	Fibers' Density (g/cm ³)	Matrix Volume (cm ³)	Fibers' Volume (cm ³)	Matrix Weight (g)		Fibers' Weight (g)
							Main	Including Shrinkage Allowance	
BioPoxy	Palm	0.1	1.1	0.19	10.8	1.2	11.88		0.23
		0.2	1.1	0.19	9.6	2.4	10.56		0.46
		0.3	1.1	0.19	8.4	3.6	9.24		0.68
Epoxy	Palm	0.1	1.1	0.19	10.8	1.2	11.88		0.23
		0.2	1.1	0.19	9.6	2.4	10.56		0.46
		0.3	1.1	0.19	8.4	3.6	9.24		0.68
PP	Palm	0.1	0.905	0.19	10.8	1.2	9.774	10.165	0.23
		0.2	0.905	0.19	9.6	2.4	8.688	9.036	0.46
		0.3	0.905	0.19	8.4	3.6	7.602	7.906	0.68
HDPE	Palm	0.1	0.952	0.19	10.8	1.2	10.282	10.693	0.23
		0.2	0.952	0.19	9.6	2.4	9.139	9.505	0.46
		0.3	0.952	0.19	8.4	3.6	7.997	8.317	0.68
BioPoxy	Luffa	0.1	1.1	0.178	10.8	1.2	11.880		0.21
		0.2	1.1	0.178	9.6	2.4	10.560		0.43
		0.3	1.1	0.178	8.4	3.6	9.240		0.64
Epoxy	Luffa	0.1	1.1	0.178	10.8	1.2	11.880		0.21
		0.2	1.1	0.178	9.6	2.4	10.560		0.43
		0.3	1.1	0.178	8.4	3.6	9.240		0.64
PP	Luffa	0.1	0.905	0.178	10.8	1.2	9.774	10.165	0.21
		0.2	0.905	0.178	9.6	2.4	8.688	9.036	0.43
		0.3	0.905	0.178	8.4	3.6	7.602	7.906	0.64
HDPE	Luffa	0.1	0.952	0.178	10.8	1.2	10.282	10.693	0.21
		0.2	0.952	0.178	9.6	2.4	9.139	9.505	0.43
		0.3	0.952	0.178	8.4	3.6	7.997	8.317	0.64

Hence, while preparing this specimen, the components were weighed on a digital micro-scale in order to ensure highest precision before adding them in the mold. It is worthy to note that shrinkage allowance was taken into account for samples with thermoplastic matrix. Furthermore, rule of mixture was implemented in order to evaluate the precision of fiber volume fraction of the prepared specimens [325].

$$\rho_c = \rho_f V_f + \rho_m V_m \quad (19)$$

ρ_c is the density of end composite material, ρ_f is fiber's density, ρ_m is matrix density, V_f is fibers volume fraction, and V_m is matrix density.

Following equation 19, the remaining factor that was not defined while preparing the samples is their final dimensions, therefore dimensions of end NFCs were measured using INSIZE digital caliper.

Since the silicone molds may have a small variety in their heights, the specimens' thickness was ensured using a tiny stick marked on 5 mm from its tip. First, coat of silicone spray was applied to the bottom of the mold and a small layer of resin/hardener mixture was poured, then the fibers were added upon a specific volume fraction i.e. 0.1, 0.2, or 0.3, next, the remaining quantity of the resin was added and the fibers were pushed downward in order to release any available air bubbles. The specimens were prepared at a room temperature of 21°C and humidity of 66%, all 36 specimens were kept for 1 week to fully cure. Figure 17 describes the main stages of samples preparation.

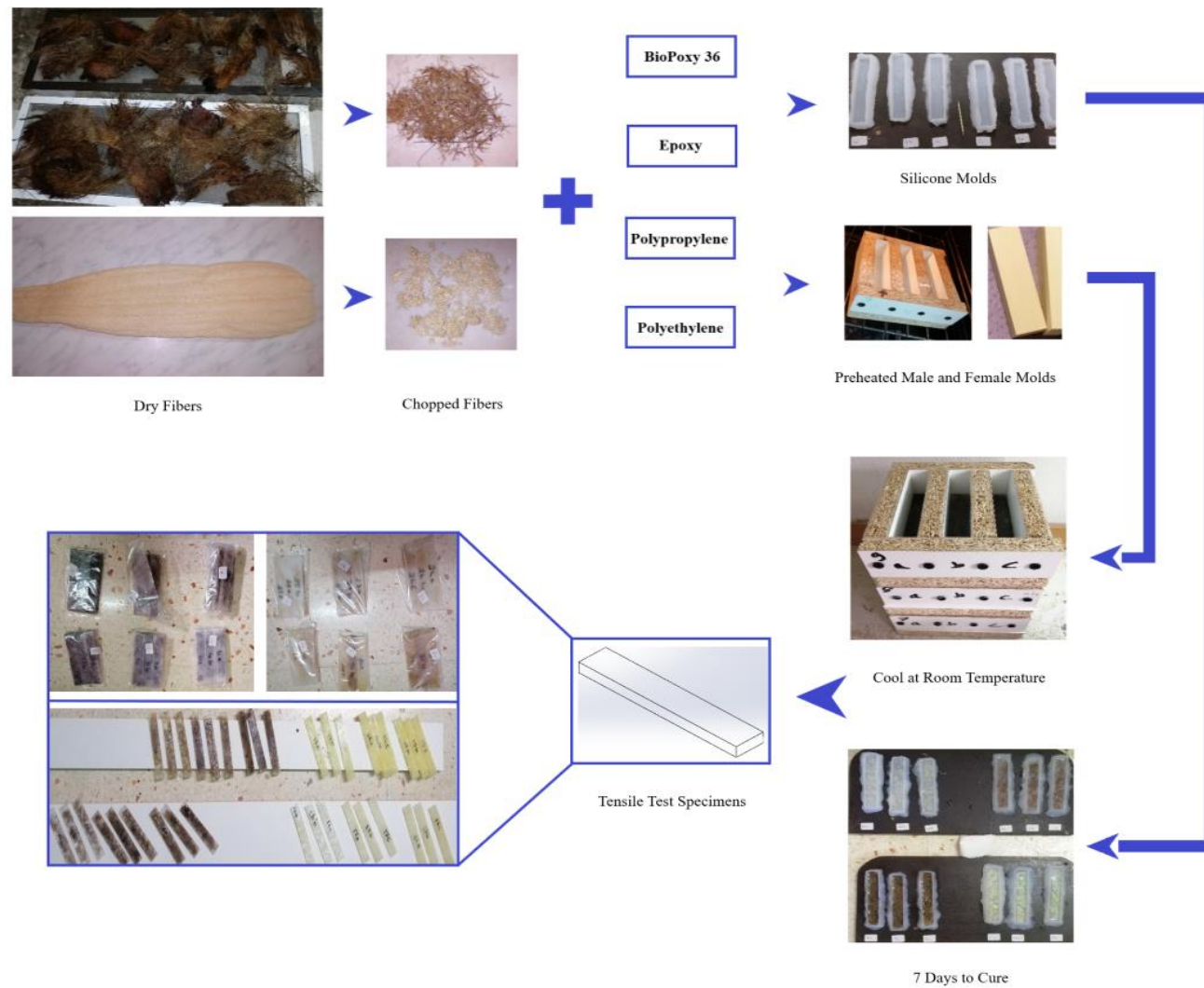


Figure 17: Palm and Luffa NFCs Specimens Preparation

Regarding the specimens with PP matrix, the granules were put in an aluminum foil sprayed with silicone realizing agent, and then placed in a toaster at 230 °C for 5 mins to melt, then the fibers were added into the molten plastic and kept in the toaster for 3 more minutes for getting the most soft structure that helps in taking the mold's shape, next, the molten NFC was placed in a preheated female mold at 80 °C and pressed using a screw clamp on the male part of the mold. Thus, the aforementioned NFC was cooled down inside the mold for 15 minutes at a room temperature of 18 °C. Meanwhile, specimens with HDPE matrix were prepared through similar process, yet the first melting stage was 3 minutes, and 2 minutes after adding the fibers, which was due to the low melting temperature of HDPE (190 °C).

Furthermore, specimens' dimensions were 120 x 20 x 5 mm following the ASTM 3039 standard. A total of 72 samples were prepared for the tensile test by considering 8 different NFCs i.e. palm/epoxy, palm/biopoxy, palm/PP, palm/HDPE, luffa/epoxy, luffa/biopoxy, luffa/PP, and luffa/HDPE with fibers volume fraction of 0.1, 0.2, and 0.3. Thus, each NFC combination had 3 replicated samples.

3.3 Tensile Test

The tensile test was conducted using a Hounsfield universal machine and a laser extensometer as shown in the Figure 18. Two reflective tapes were taped to each specimen in order to test strain variations through the extensometer. The considered gage length was 60 mm, and the speed rate was 5 mm/min [326].

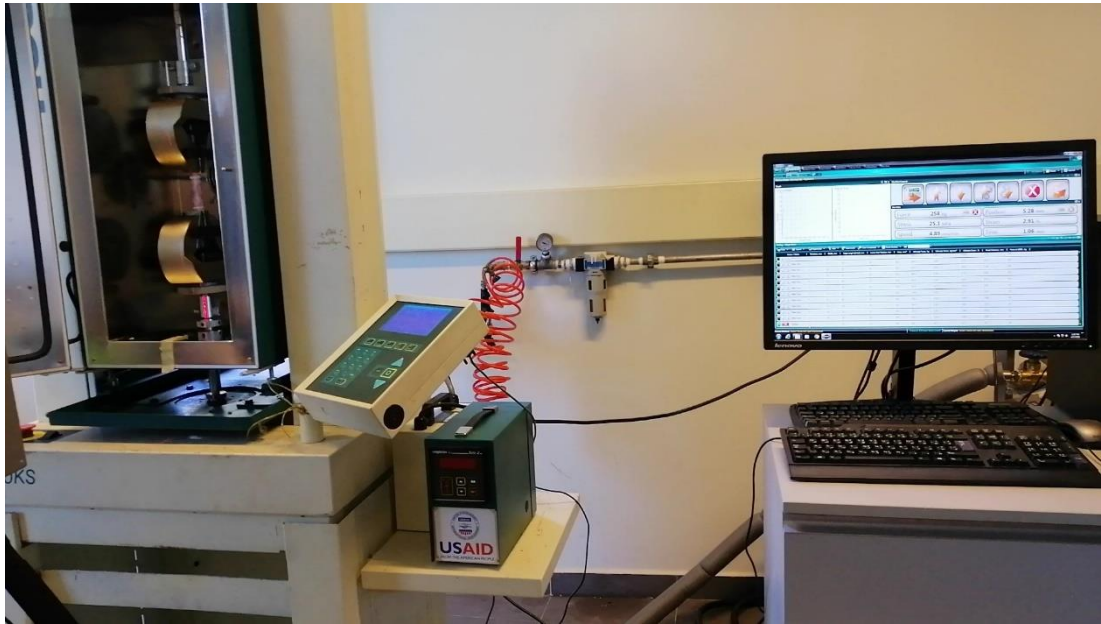


Figure 18: Tensile Testing Machine

Following ASTM D3039 standard concerning chopped and randomly oriented composite materials, both sides of all 72 specimens were covered with emery cloth (grade 100 sand papers), which contributed in increasing the grip and preventing the samples from slipping out of the machine clamps. After tightening the machine clamps on the specimens' edges, the applied force as well as the strain rate were adjusted to be zero. Hence, tension load was applied upon the specified speed rate and the specimens extended till failure. Results were revealed through stress-strain graphs as well as excel files that included whole details of force, break distance, ultimate tensile strength, and strain.

3.4 Design of Experiment

Selection of a suitable natural fiber for reinforcing a polymeric matrix and developing a natural fibers composite is complicated and may include diverse problems as it is influenced by multiple criteria, therefore it is considered as multi criteria decision making problem. Evaluating natural fibers upon several criteria includes many advantages, such as determining better characteristics, and make suitable informative

decisions while utilizing natural fibers composites in the industry. In other words, utilization of a suitable design of experiment approach while developing a new natural fibers composite can contribute in defining the optimum specimens' number required for specifying the design space of the considered parameters. Thereby, it reduces the overall cost, and wastes [327]. Table 19 lists different design of experiment approaches that can be implemented in NFCs development.

Table 19: Design of Experiment Approaches [328]

Approach	Suitability
RCBD	Focusing on a primary factor using blocking techniques
Latin squares	Focusing on a primary factor cheaply
Full Factorial	Computing the main and the interaction effects, plotting response surface
Fractional factorial	Estimating the main and the interaction effects
Central Composite	Plotting response surface
Box-Behnken	Plotting quadratic response surfaces
Plackett-Burman	Estimating the main effects
Taguchi	Addressing the influence of noise variables
Random	Plotting response surface
Halton, Sobol, Faure	Plotting response surface
Latin hypercube	Plotting response surface
Optimal design	Plotting response surface

In this research full factorial design of experiment approach was implemented to determine the design space that covered all component combinations and fiber volume fractions.

3.5 Machine Learning Models

Machine learning is a subcategory of artificial intelligence, it is a technique where the computers learn the way of doing something that is generally particular to human and gained through experience. Usually, the efficiency of the algorithm increases by increasing the quantity of learning samples [329]. Deep learning became popular in many research areas since 2006, where it was implemented for determining the performance in fields like speech recognition, object recognition, image segmentation,

and machine translation. Majority of deep learning approaches are usually presented as deep neural networks as they involve neural network architecture. There are two types of machine learning algorithms, supervised and unsupervised. Supervised machine learning proved its convenience in most manufacturing applications as the aforementioned provide labeled data [330]. Machine learning algorithms are classified in Figure 19.

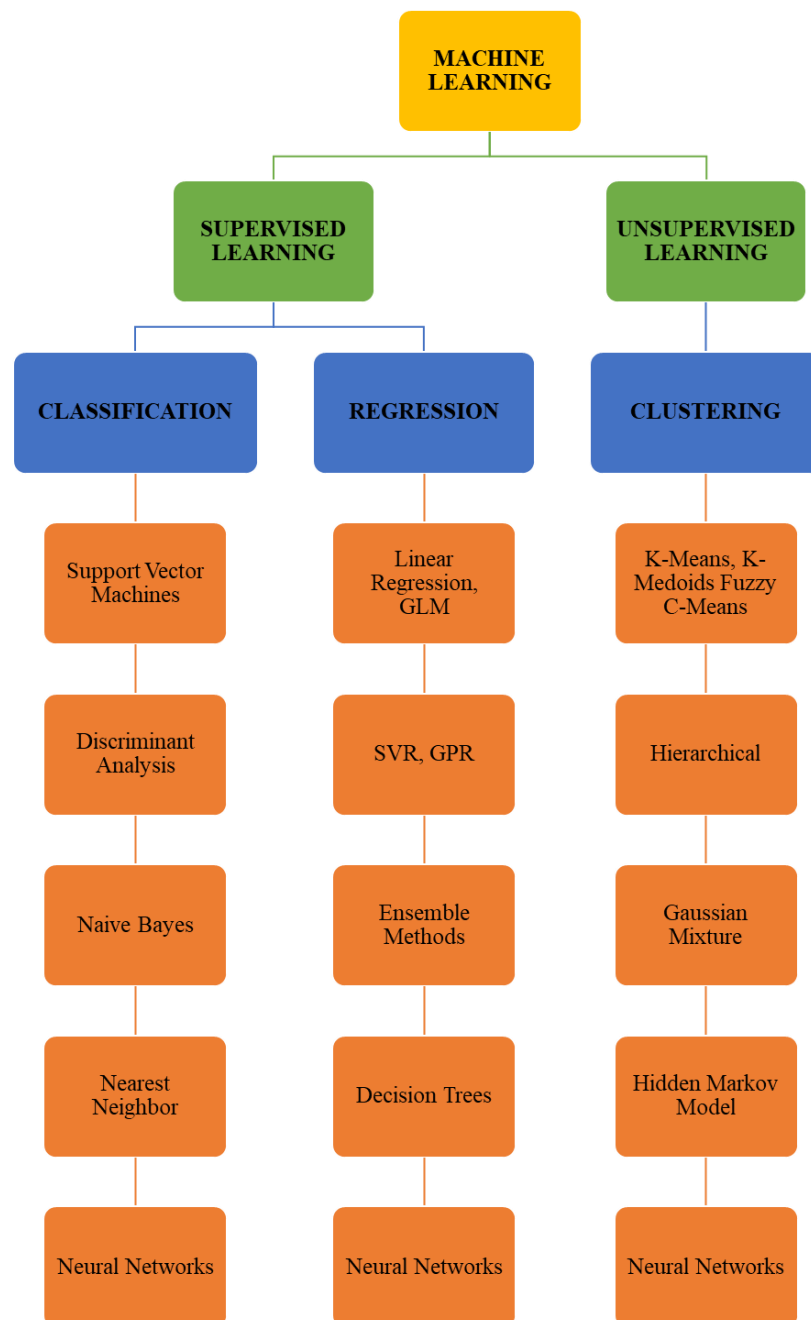


Figure 19: Classification of Machine Learning Algorithms

$$\text{Prediction error\%} = \frac{|Expt.Value - Pred.Value|}{Expt.Value} \times 100 \quad (20)$$

Prediction error is a simple method that evaluates the reliability of a training model, where the prediction model is validated through new input data that were unconsidered previously in testing the model. Therefore, the error percentage of a training model can be defined using this tool. Moreover, a common technique for defining the error of a model is Root Mean Square Error (RMSE).

$$\text{RMSE} = \sqrt{\frac{1}{N} \sum_{i=1}^N (p_i - q_i)^2} \quad (21)$$

Where q_i is the actual value, p_i is the prediction of the deliberate information, and N is the complete training data.

Artificial Neural Network, Response Surface Metamodel, Adaptive Neuro-Fuzzy Inference System, and Support Vector Machine were implemented in this research to define the design space upon the considered parameters, and determine most convenient approach in predicting tensile strength values of input parameters that were unconsidered in the experimental tensile test of natural fibers composites.

3.5.1 Artificial Neural Network

Artificial Neural Network is a mathematical model adapted from the human brain neurons' behavior and their structure. Basic components of an ANN are organized layers in a hierarchical structure. ANN layers are categorized into three main types; input layer, hidden layers and output layer. Synapses are links that connect neurons together, each synapse includes a specific weight factor. Multilayer ANN is considered as a supervised learning model, which is able to learn a nonlinear function through input data that can be utilized for regressions and classifications. Usually artificial neural networks are involved in solving complex functions in diverse applications [331]. Levenberg–Marquardt algorithm was utilized in this research for training all

components of ANN prediction model, which exhibited a swift and stable convergence. The design of the ANN model is shown in Figure 20. The model includes 3 inputs, 8 hidden layers, and 1 output.

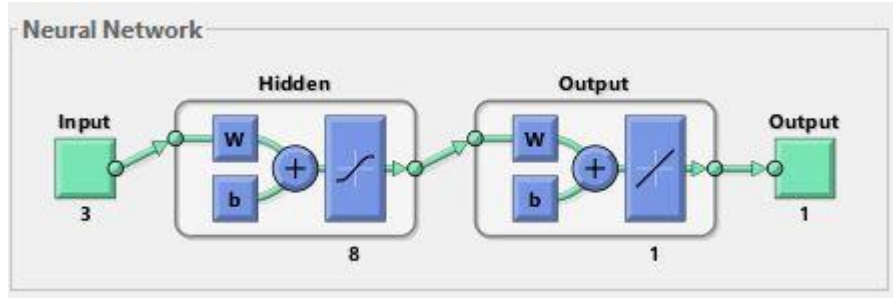


Figure 20: Artificial Neural Network Model Structure

The model was generated using neural network fitting tool in MATLAB. Input data consisted of: matrix type, fibers' type, and fibers' volume fraction, while the output was tensile strength. Data of all experimentally tested NFC specimens were considered, 70% of the data were used for training the model, 15% for testing, and 15% for validation.

3.5.2 Multiple Linear Regression

Multiple Linear Regression (MLR) is a tool that provide several advantages, such as Inter-correlation between the predictor variables and the error, homoscedasticity, predicting normality hypotheses, the ability to be tuned over reasoning, and parametric transformations, interpretability, and clarity. Response surface models are regression models that were developed over fifty years ago for the exploration and exploitation of stochastic response functions [332, 333]. They are used in conjunction with response surface methodology, which is the most commonly used approach to metamodel-based simulation optimization. This metamodel family consists of first or second-order polynomial probability models fitted to observed values of the system response Y . A full second-order response surface model would be

$$Y(\theta) = \beta_0 + \sum_{j=1}^p \beta_j \theta_j + \sum_{i=1}^p \sum_{k=i}^p \beta_{ik} \theta_i \theta_k + \varepsilon, \quad \varepsilon \sim NID(0, \sigma^2) \quad (22)$$

where *NID* indicates that the deviations have independent (and identical) normal distributions. Suppose that an experiment has been conducted, with simulation that runs at parameter settings $\theta^1, \theta^2, \dots, \theta^n$ and corresponding observed responses (perhaps averages of replications) of y^1, \dots, y^n . Let y represent the vector of responses. For metamodel prediction, maximum likelihood (equivalently, least squares) estimators for the $\beta_0, \beta_i, \beta_{ik}$ and σ^2 are computed, and used in the prediction equation.

$$g(\theta) = \beta_0 + \sum_{j=1}^p \beta_j \theta_j + \sum_{i=1}^p \sum_{k=i}^p \beta_{ik} \theta_i \theta_k \quad (23)$$

Response surface metamodels can be fit using standard statistical packages.

In this research, regression model was implemented using curve fitting tool in MATLAB. In order to reach a better curve fitting results, two different response surface models were generated using cubic polynomial approximation functions, one for palm NFCs and the other for luffa NFCs. Therefore, input data included matrix type and fibers volume fraction, whereas the output was the corresponding TS values.

3.5.3 Adaptive Neuro-Fuzzy Inference System

Adaptive Neuro-Fuzzy Inference System is also known as ANFIS. When assigning a data set with known input and output, ANFIS toolbox function generates a fuzzy inference system (FIS), where its membership functions involves backpropagation algorithm or in integration with least squares type technique. Thereby, the mentioned application of fuzzy rules leads the system to train from the data they modeled. Though, neural networks operate in a similar way as adaptive neuro-fuzzy inference system. The considered ANFIS model consists of; 3 inputs (matrix type, fibers' type, and V_f), 4 membership function for the first input, 2 for the second input, and 3

membership functions for the third input. Structure of the ANFIS model is illustrated in Figure 21.

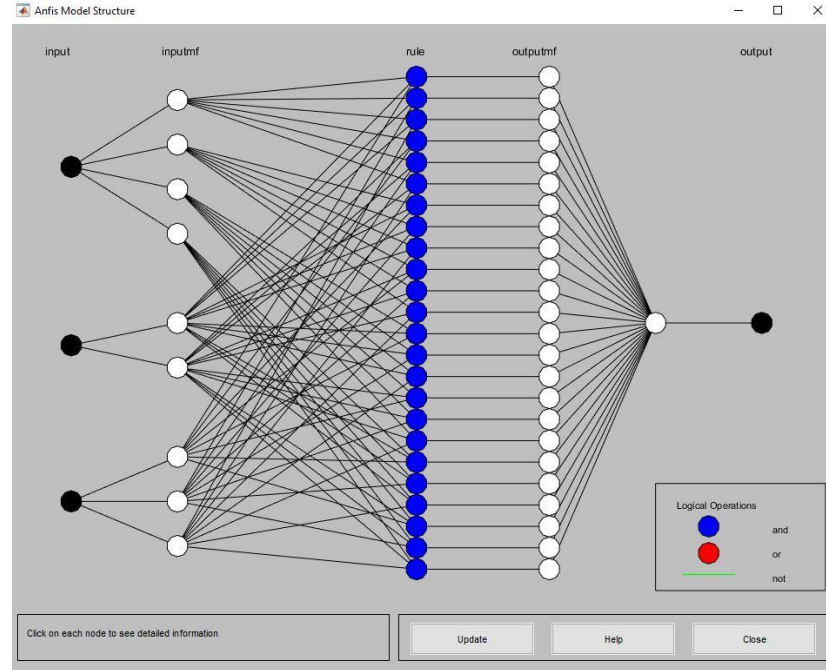


Figure 21: ANFIS Model Structure

Neuro fuzzy designer tool in MATLAB was utilized for applying ANFIS model. 80% of the experimental results were utilized for training the model and the remaining 20% were used for the testing.

3.5.4 Support Vector Machine

Support Vector Machine (SVM) is based on structural risk minimization principal. SVM builds single or multiple hyperplanes in a high-dimensional space. Support Vector Regression or SVR is a technique for regressions in SVM. The objective is to find a solution that simplifies the training examples. SVM are utilized in several machine learning implementation i.e., time series prediction, object classification, and pattern recognition. The support vector machine model in this research was generated through regression learner tool in MATLAB. 4 Matrix types, 2 fibers' type, and 3 fibers volume fraction were considered as input parameters. Figure 22 shows the

training and testing output datasets developed by the SVM model. Blue dots illustrates the true data, while the yellow dots are the predicted data.

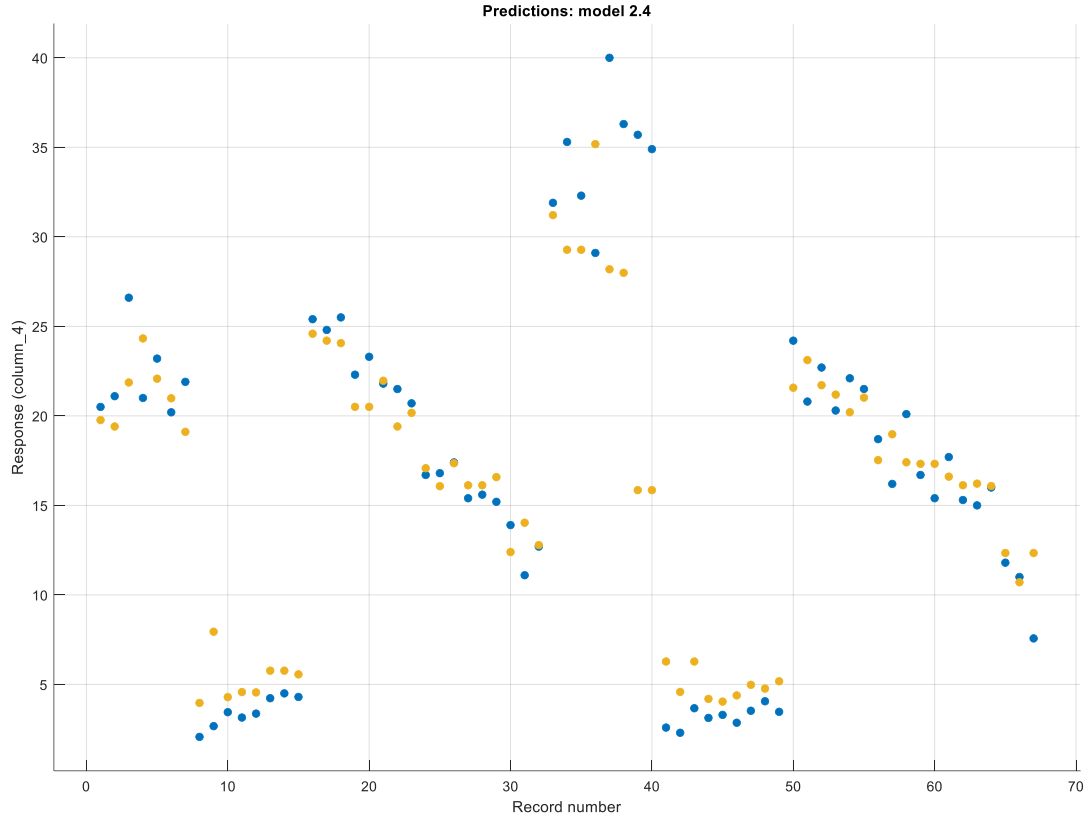


Figure 22: Predict versus Real SVM Data

In other words, inputs of the proposed model are matrix types, fibers' types, and fibers' volume fraction. Results of all experimentally tested specimens were applied for training, testing, and validation. Several machine learning methods were utilized for developing the tensile strength prediction model i.e., ANN, MLR, ANFIS, and SVM. Reliability of TS prediction model was evaluated using the mean absolute percentage error.

Chapter 4

RESULTS AND DISCUSSION

This section presents the experimental findings, machine learning results, FEA simulation results as well as the results of elastic properties obtained from analytical and numerical simulation, i.e. longitudinal moduli, transverse moduli, shear moduli, and poisson's ratio of palm and luffa NFCs in epoxy, ecopoxy, HDPE and PP matrices, obtained through representative volume element chopped and unidirectional FEA, Rule of Mixture, Chamis, Halpin-Tsai, and Nielsen analytical models.

4.1 FEA and Analytical Simulation Model Validation

It is worthy to mention that the longitudinal modulus obtained from RVE chopped model was in accordance with the experimental findings of Mulinari et al. [319] in pure HDPE and 0.1 V_f Date palm fibers (Table 20).

Table 20: E_1 of Palm/HDPE Obtained from RVE Chopped Model and Literature

Fibers' Volume Fraction (V_f)	E_1 RVE Chopped (MPa)	E_1 (MPa) [319]
0	720	~730
0.1	879.89	~870
0.2	1075.10	~940

However, at 0.2 volume fraction, the aforementioned model revealed a close E_1 value to that of experimental results, which was the closest among all utilized techniques.

4.1.1 Longitudinal Modulus

The proportion of longitudinal strength to longitudinal strain is defined as longitudinal modulus which is the reaction of palm and luffa fiber-reinforced composites

throughout the application of a stress parallel with the fibers' direction. Figure 23 shows E_1 of palm/epoxy and luffa/epoxy obtained from analytical, RVE UD, and RVE chopped models.

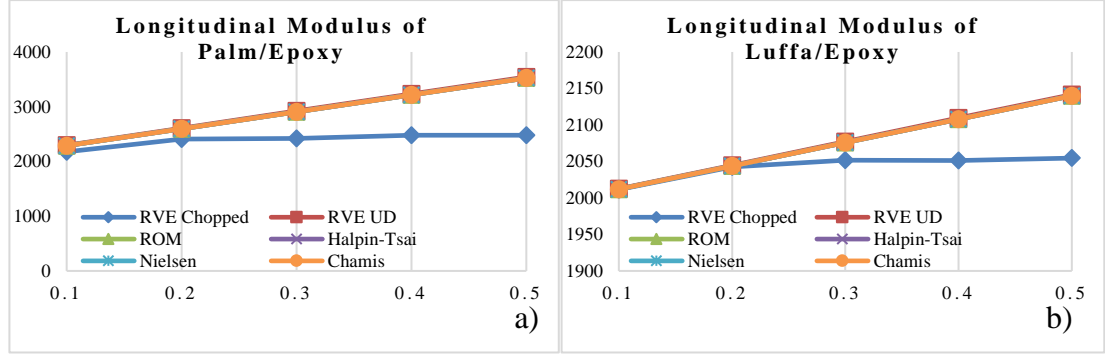


Figure 23: Longitudinal Modulus of a) Palm/Epoxy and b) Luffa/Epoxy Natural Fibers Composites

As clearly shown in Figure 23a and 23b, findings of RVE UD model drastically agreed with results of analytical techniques, where they revealed a continuous increment in the longitudinal modulus of palm/epoxy as well as luffa/epoxy NFCs while increasing their fibers volume fraction. Moreover, E_1 of palm/epoxy NFC increased from 2288 MPa to 3523 MPa at 0.5, while E_1 of luffa NFC in epoxy matrix was 2012 MPa at 0.1, hence it raised to 2140 MPa by increasing the fibers' volume fraction up to 0.5. On the other hand, results of RVE chopped model were slightly inferior from that of the analytical approaches and RVE UD model. However, the aforementioned model showed a slight increase in E_1 of Palm/Epoxy by increasing its fibers volume fraction, yet the longitudinal modulus decreased at 0.3 and recovered back at 0.4 where it revealed a value of 2479 MPa, thereby decreased back at 0.5. While in terms of luffa NFC in epoxy matrix, RVE Chopped results agreed with the considered approaches at 0.1 and 0.2 fibers volume fractions, but it stayed steady beyond 0.2 at around 2051

MPa. Figure 24 displays the findings of longitudinal modulus of palm/ecopoxy as well as luffa/ecopoxy from analytical models as well as RVE.

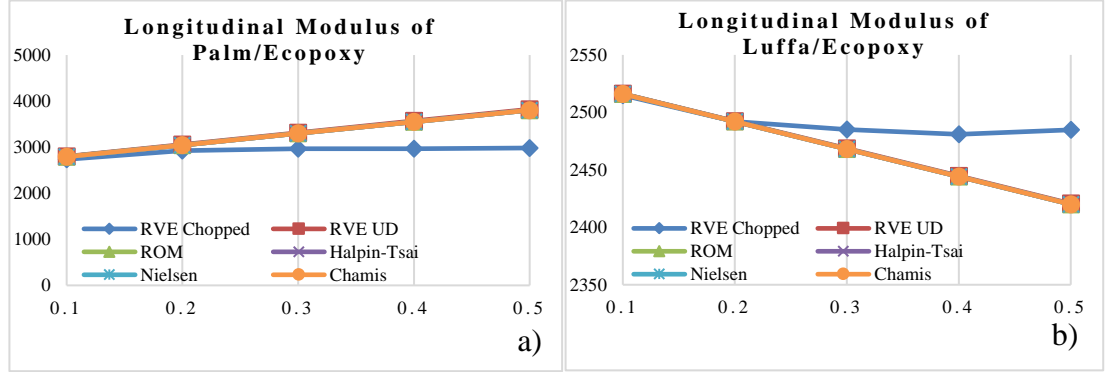


Figure 24: Longitudinal Modulus of a) Palm/EcoPoxy and b) Luffa/EcoPoxy Natural Fibers Composites

Correspondingly, E_1 of palm/ecopoxy as well luffa/ecopoxy obtained from analytical models agreed with that of RVE UD. While these models showed that longitudinal modulus of palm/ecopoxy NFC increased from 2792 MPa to 3802 MPa while increasing fibers volume fraction from 0.1 to 0.5 (Figure 24a). However, E_1 of luffa NFC in ecopoxy matrix decreased from 2516 MPa to 2420 MPa by adding fibers up to 50% (Figure 24b). In contrast, RVE chopped model followed its diverse trend, as E_1 of palm/ecopoxy decreased from 3045 MPa to 2969 MPa beyond 0.2 and remained steady up to 0.5. In terms of predicting E_1 of luffa/ecopoxy, results of RVE chopped agreed with the analytical and RVE UD models at 0.1 and 0.2, thereby the RVE chopped model showed a gradual decrease in E_1 from 2492 MPa to 2484 MPa at 0.5. Comparing longitudinal moduli of luffa and palm reinforced epoxy, these two natural fibers composites showed similar behaviors, while the addition of date palm fibers resulted in higher E_1 (3522 MPa). Yet, addition of luffa fibers in ecopoxy matrix decreased its longitudinal modulus. Hence, the decline in E_1 of luffa/ecopoxy may be due to the superior properties of ecopoxy resin compared to luffa fibers. Figure 25

shows the longitudinal moduli of palm/PP and luffa/PP obtained from RVE and analytical models.

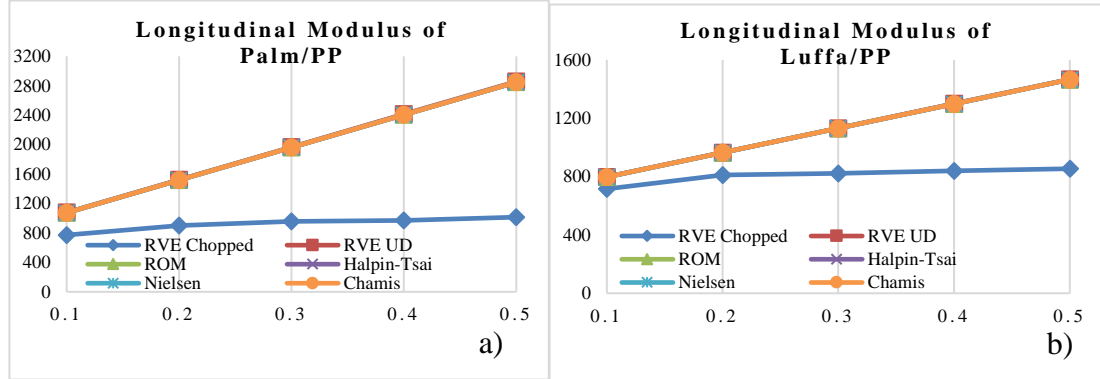


Figure 25: Longitudinal Moduli of a) Palm/PP and b) Luffa/PP NFCs

As shown in Figures 25a and 25b, results of analytical approaches presented strong agreement with that of RVE UD; however, significant increments in the longitudinal moduli of both palm/PP and luffa/PP NFCs were observed by increasing fiber volume fraction. Moreover, E_1 of palm/PP NFC increased from 1074 MPa to 2848 MPa by increasing fiber content up to 0.5. Also, considering 0.1 luffa fibers in PP matrix revealed an E_1 of 797 MPa, while increasing fiber content up to 50%, increased E_1 to 1466 MPa. E_1 results obtained from RVE of chopped palm NFC were lower than those obtained from other methods, noticing a slight increment while increasing fiber content. Figure 26 displays the results of E_1 of luffa/HDPE and palm/HDPE obtained from RVE chopped and UD as well as analytical models.

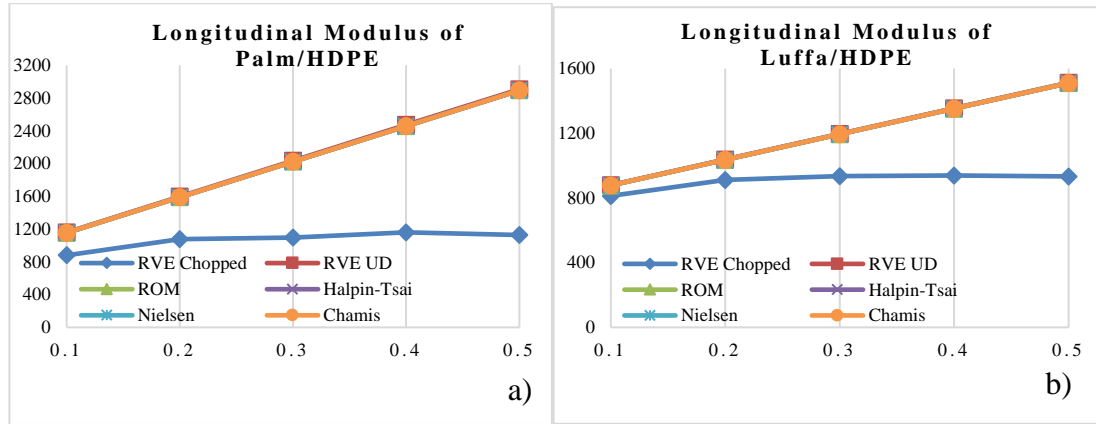


Figure 26: Longitudinal Moduli of a) Palm/HDPE and b) Luffa/HDPE Reinforced Composites

Similarly, longitudinal moduli of palm/HDPE and luffa/HDPE obtained from RVE UD significantly agreed with analytical findings. Furthermore, increasing fiber volume fraction improved the longitudinal moduli of both NFCs. However, the results obtained from RVE UD revealed a value slightly higher than analytical results. As shown in Figure 26a, E_1 of palm/HDPE increased from 1155 MPa at 0.1 to 2893 MPa at 0.5. While, as shown in Figure 26b, addition of 0.1 luffa fibers into HDPE exhibited an E_1 value of 878 MPa and 0.5 V_f fiber content increased E_1 to 1512 MPa.

Results of RVE chopped model exhibited an E_1 value lower than those obtained by RVE UD and analytical methods for palm/HDPE and luffa/HDPE, thus increasing fiber volume fraction had an inferior impact on improving longitudinal modulus. Yet, RVE chopped palm/HDPE showed a decrement in E_1 beyond 0.3, such that it decreased from 1095 MPa at 0.3 to 1128 MPa at 0.5. Moreover, E_1 of luffa/HDPE reached its peak at 0.4 fiber content, then it began to decrease at 0.5. Comparing E_1 of luffa and palm reinforced HDPE revealed that these two NFCs displayed similar E_1 trends, yet the addition of palm fibers contributed in higher E_1 improvement in both matrices. Peak E_1 obtained was 3802 MPa in ecopoxy matrix with 0.5 palm fibers.

Generally, increasing the fibers volume fraction of both natural fibers increased the longitudinal modulus, which is due to the stiffness increase occurring while increasing V_f of luffa as well as palm fibers [7].

4.1.2 Transverse Modulus

The proportion of transverse strength to transverse strain is defined as transverse modulus. It is the reaction of luffa and palm fiber-reinforced thermoplastic composites when a perpendicular stress is applied. Figure 27 shows the transverse moduli of palm and luffa reinforced epoxy upon fibers' volume fractions from 0.1 to 0.5.

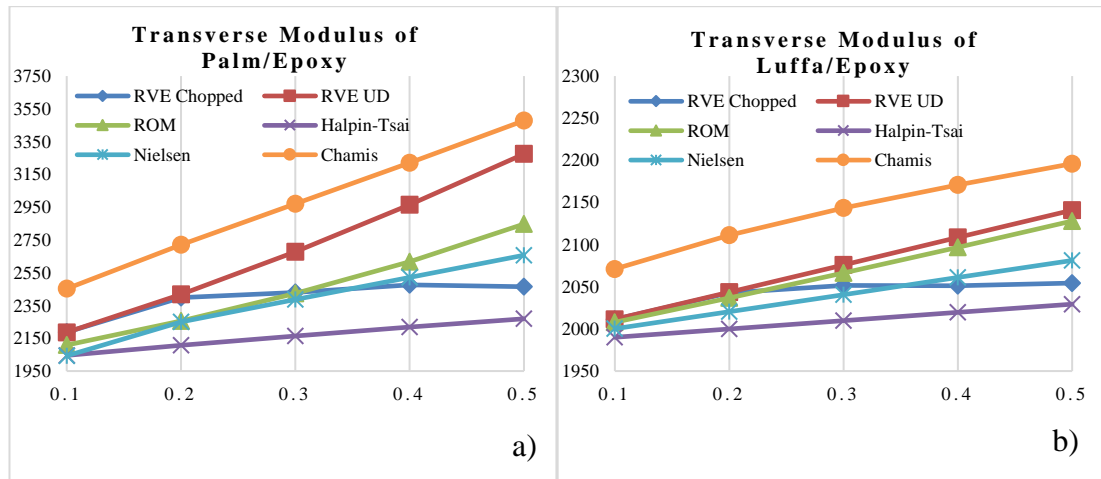


Figure 27: Transverse Modulus of a) Palm/Epoxy and b) Luffa/Epoxy Natural Fibers Composites

In terms of transverse modulus Palm/Epoxy as well as Luffa/Epoxy NFCs, all the considered analytical and numerical models followed their independent trends. Where least E_2 values were observed through Halpin-Tsai model, while Chamis model showed the highest values. As Figure 27a and 27b show, RVE UD as well as all analytical models exhibited a growing trend while increasing the fibers' volume fraction. Least transverse modulus was 1990 MPa obtained in epoxy matrix with 0.1 luffa fibers through Halpin-Tsai model. While epoxy with 0.5 palm fibers exhibited the peak E_2 a value of 3418 MPa, while the highest E_2 of luffa/epoxy was 2196 MPa

at 0.5. In contrast with all the utilized models, RVE chopped model showed that E_2 of palm/epoxy significantly increased by increasing fibers volume fraction from 0.1 to 0.2, thereby it remained constant throughout 0.3 and 0.4 to drop down at 0.5. Thus, E_2 of luffa/epoxy increased to 2042 MPa by increasing the fibers' loading up to 0.2, then it remained steady at around 2051 MPa upon 0.3, 0.4, and 0.5 fibers volume fractions. Figure 28 shows the transverse moduli of palm/ecopoxy and luffa/ecopoxy NFCs while considering fibers' volume fractions from 0.1 to 0.5.

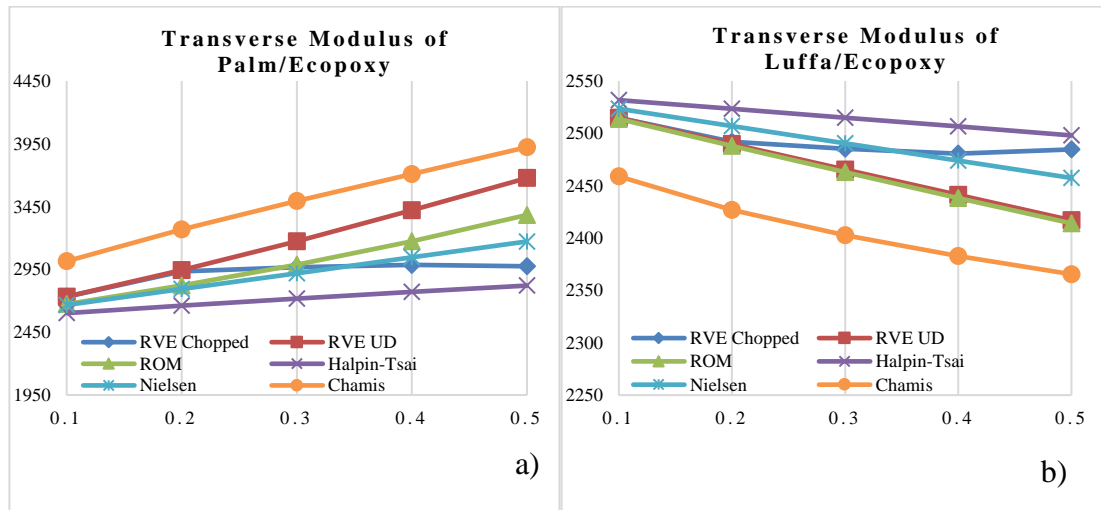


Figure 28: Transverse Modulus of a) Palm/EcoPoxy and b) Luffa/EcoPoxy Natural Fibers Composites

As shown in Figure 28a, based on RVE UD as well as the considered analytical approaches, increasing fibers volume fraction led to an increase in the transverse modulus of palm/ecopoxy NFC. Moreover, Chamis model showed higher E_2 values compared with other methods, thus it revealed the peak E_2 (3923 MPa) in ecoepoxy with 0.5 palm fibers. While Halpin-Tsai displayed the lowest transverse moduli, yet, the least E_2 was 2601 MPa in palm/ecopoxy at 0.1. However, RVE chopped model showed that increasing the fibers content from 0.1 to 0.2 increased E_2 from 2732 to 2933 MPa, thereby it slightly increased at 0.3 before reaching a peak of 2986 MPa at

0.4, whilst it decreased to 2974 MPa at 0.5. Regarding luffa NFC with ecopoxy matrix (Figure 28b), addition of luffa fibers in ecopoxy resulted in a drastic decrease in the transverse modulus. Lowest E_2 was 2365 MPa observed through Chamis model in luffa/ecopoxy at 0.5. Whereas highest transverse modulus was 2531 MPa in ecopoxy with 0.1 luffa fibers, which was obtained using Halpin-Tsai model. RVE chopped model showed a constant E_2 between 0.2 and 0.5 luffa fibers content. In other words, addition of palm fibers contributed in higher transverse modulus of ecopoxy, yet luffa fibers led to a drastic decrease in E_2 . Moreover, results of rule of mixture model showed an agreement with that of RVE UD in predicting the transverse modulus of luffa/epoxy and luffa/ecopoxy, while ROM agreed with Nielsen model in predicting E_2 of palm NFC with epoxy as well as ecopoxy matrices. Figure 29 shows the transverse moduli of palm and luffa-reinforced polypropylene considering fiber volume fractions ranging from 0.1 to 0.5.

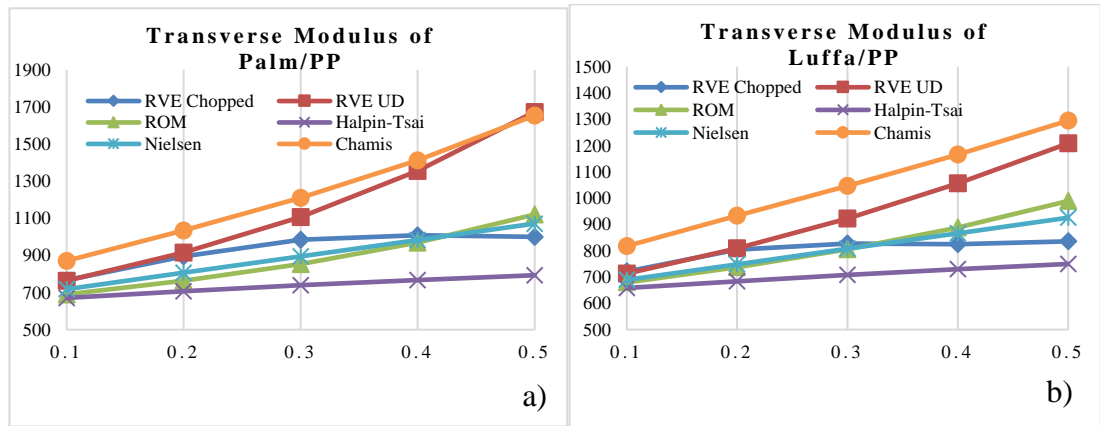


Figure 29: Transverse Moduli of a) Palm/PP and b) Luffa/PP Reinforced Composites

Diverse transversal modulus results were obtained for palm and luffa fibers in PP. Results of Chamis technique revealed the highest E_2 values compared to other analytical approaches, while Halpin-Tsai method showed the least values. Furthermore, as exhibited in Figures 29a and 29b, almost all analytical methods and

RVE UD displayed an increasing trend when increasing fiber content. In contrast, based on Halpin-Tsai approach, E_2 of palm/PP and luffa/PP remained constant by the increase of fiber volume fraction. The lowest transverse moduli observed through Halpin-Tsai were 671.28 MPa in palm/PP at 0.1 and around 684 MPa with 0.1 luffa fibers. palm/PP exhibited highest E_2 value of 1673.6 MPa, observed through RVE UD model. However, Chamis model revealed peak E_2 luffa/PP (1294.75 MPa). E_2 values obtained from RVE chopped luffa/PP and palm/PP were in agreement with E_2 values observed in RVE UD model at 0.1, thereby E_2 slightly increased by increasing fiber loading. Thus, E_2 of palm/PP started to decrease as fiber content was beyond 0.4. Furthermore, E_2 of luffa in PP matrix increased gradually from 720 MPa to 827 MPa by increasing fiber volume fraction up to 0.3, then E_2 decreased to 824 MPa at 0.4 and increased to 835 MPa at 0.5. Results of RVE UD model showed a good agreement with those of Chamis analytical model. Figure 30 illustrates the transverse moduli of luffa and palm-reinforced HDPE taking into consideration different fiber volume fractions (0.1 to 0.5).

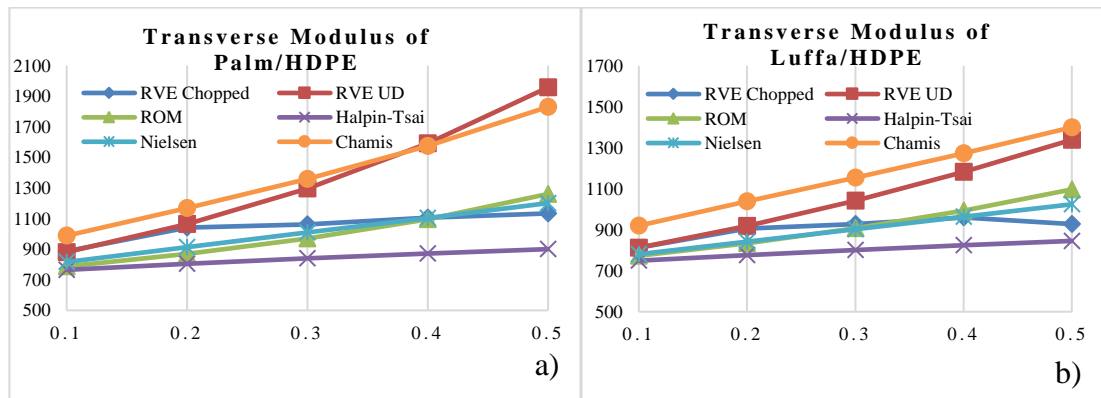


Figure 30: Transverse Moduli of a) Palm/HDPE and b) Luffa/HDPE Reinforced Composites

Figures 30a and 30b show different E_2 results of luffa/HDPE and palm/HDPE NFC obtained from analytical analysis and RVE UD. Based on RVE UD model and

analytical methods, increasing fiber volume fraction from 0.1 to 0.5 contributed in improving the transverse modulus of both natural fiber composites, but Halpin-Tsai findings showed a negligible difference in E_2 . Moreover, Halpin-Tsai showed the least transverse moduli of 749 MPa for 0.1 V_f luffa/HDPE and 765 MPa for 0.1 palm/HDPE. However, peak E_2 result of 1957.50 MPa was observed in RVE UD for 0.5 palm/HDPE while peak E_2 value of luffa/HDPE was 1400 MPa at 0.5 obtained by Chamis model. Based on RVE chopped model, transverse modulus of luffa in HDPE matrix increased by increasing fiber loading up to 0.4, then it began to decrease when fiber content was further increased. Furthermore, RVE UD results were in accordance with Chamis model findings. Compared with considered luffa NFCs, palm reinforced NFCs revealed superior transverse moduli.

4.1.3 Shear Modulus

The proportion of shear strength to shear strain is known as in-plane shear modulus which defines the capability of a material to endure transversal deformations. Figure 31 shows the shear modulus of palm/epoxy and luffa/epoxy obtained using RVE and analytical approaches.

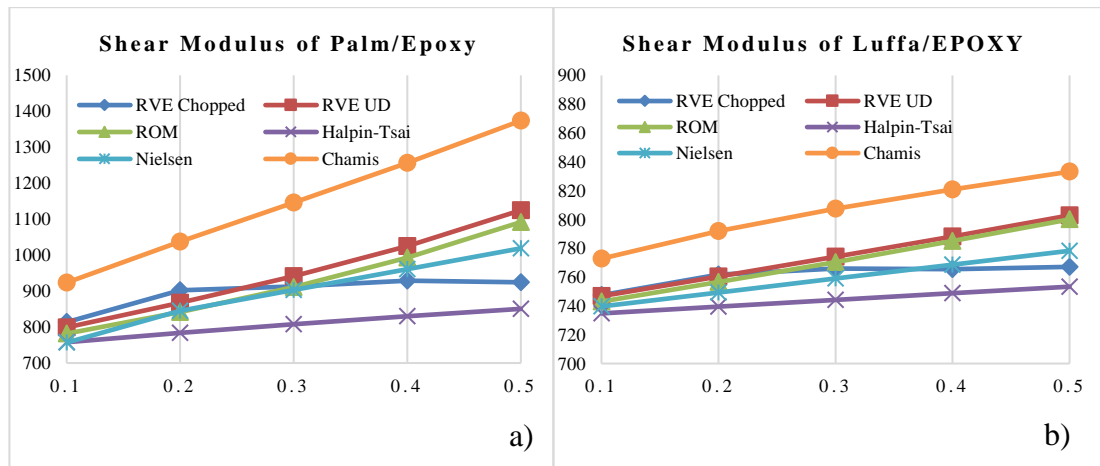


Figure 31: Shear Modulus of a) Palm/Epoxy and b) Luffa/Epoxy Natural Fibers Composites

Based on the analytical models as well as RVE UD, the shear modulus of palm as well as luffa NFCs in epoxy matrix followed an ascending trend while increasing the fibers volume fraction. As exhibited in Figure 31a and 31b, Chamis model showed the highest G_{23} compared to other analytical approaches as well as RVE models, thus Halpin-Tsai approach exhibited the lowest G_{23} values. Moreover, highest shear modulus observed was 1373 MPa in palm/epoxy at 0.5, while least G_{23} was 734 MPa in epoxy with 0.1 luffa fibers. RVE chopped findings showed that shear modulus of palm/epoxy increased by increasing V_f and reached a peak of 928 MPa at 0.4, thereby dropped down at 0.5. Whereas, G_{23} of luffa/epoxy NFC remained constant at around 765 MPa between 0.2 and 0.5. A good agreement was observed between RVE UD model and rule of mixture in predicting G_{23} of Palm/Epoxy as well as luffa/epoxy NFCs.

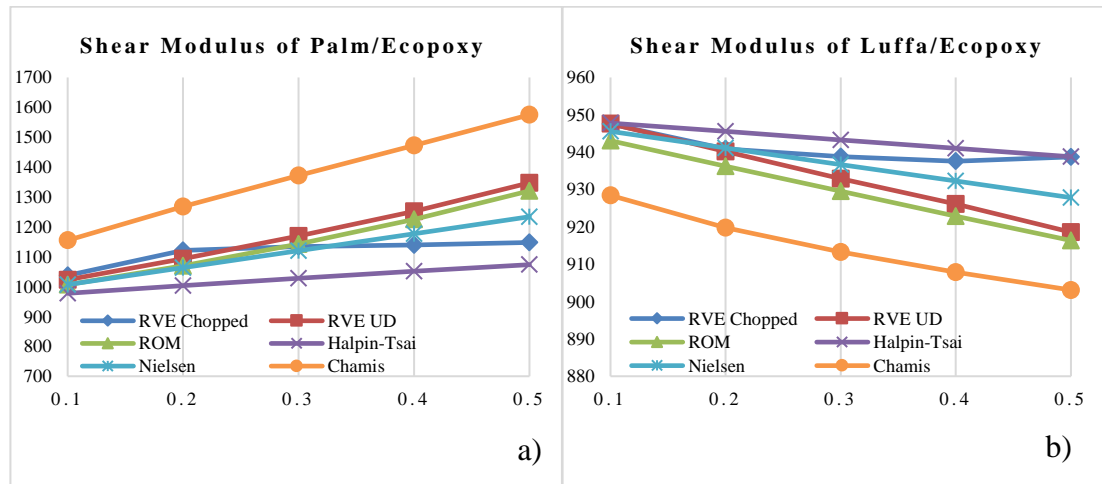


Figure 32: Shear Modulus of a) Palm/EcoPoxy and b) Luffa/EcoPoxy Natural Fibers Composites

As exhibited in Figure 32a, increasing the fibers volume fraction increased the shear modulus of palm/ecopoxy. Highest G_{23} was 1575 MPa in palm/ecopoxy at 0.5, that was observed through Chamis analytical approach. While lowest G_{23} (977 MPa) was obtained in Halpin-Tsai results at 0.1. RVE chopped results displayed a slight increase

in G_{23} from 0.2 to 0.5 where it hit its peak of 1147 MPa. Figure 32b shows that increasing the luffa fibers content in ecopoxy matrix reduced the shear modulus. Chamis model revealed lowest G_{23} values compared with other models throughout the 5 fibers volume fractions. Whereas Halpin-Tsai results showed the highest shear moduli. 903 MPa was the minimal G_{23} , which was observed in ecopoxy with 0.5 luffa fibers, while the greatest shear modulus was 947 MPa. However, RVE chopped findings exhibited a decline in G_{23} by increasing luffa fibers content from 0.1 to 0.2, thereby it remained steady at around 938 MPa by increasing fibers content up to 0.5. Though the decline in G_{23} of ecopoxy throughout the addition of luffa fibers is apparently due to the superior characteristics of this matrix. Figure 33 illustrates the shear moduli of palm and luffa in PP matrix observed through analytical approaches and RVE models.

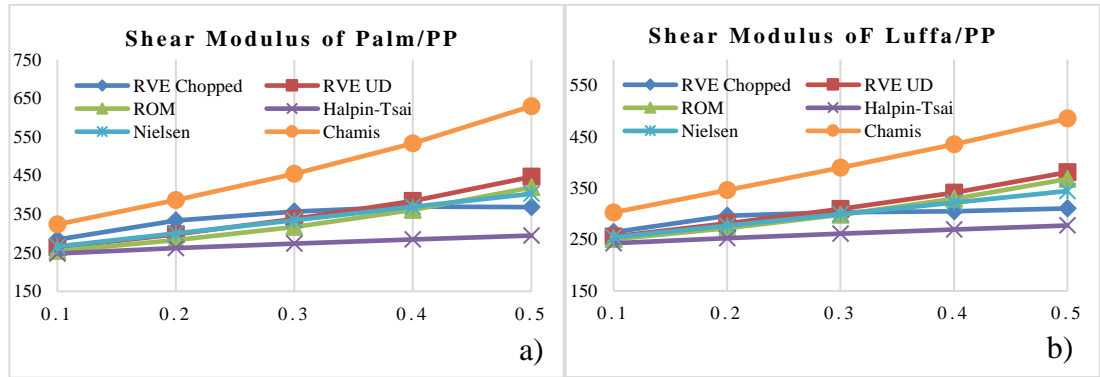


Figure 33: Shear Moduli of a) Palm/PP and b) Luffa/PP Reinforced Composites

Regarding the shear moduli of palm and luffa fiber-reinforced PP, G_{23} followed an ascending trend in all utilized methods. As clearly shown in Figures 33a and 33b, G_{23} values obtained from Chamis model were higher than those obtained from other analytical techniques and RVE UD, while Halpin-Tsai model revealed the least G_{23} values. According to the majority of the considered methods, addition of palm and luffa fibers improved the shear modulus of PP, though a slight improvement was

observed through Halpin-Tsai results. Furthermore, Chamis model revealed peak G_{23} values of 629 MPa for 0.5 palm/PP and 485 MPa for 0.5 luffa/PP. RVE chopped results showed that G_{23} of palm/PP increased gradually to hit a peak of 369 MPa at 0.4 and then decreased at 0.5. Thus, G_{23} of luffa/PP remained constant at around 303 MPa beyond 0.2. RVE model showed a significant agreement with ROM analytical model in predicting the shear moduli of palm and luffa reinforced thermoplastic composites.

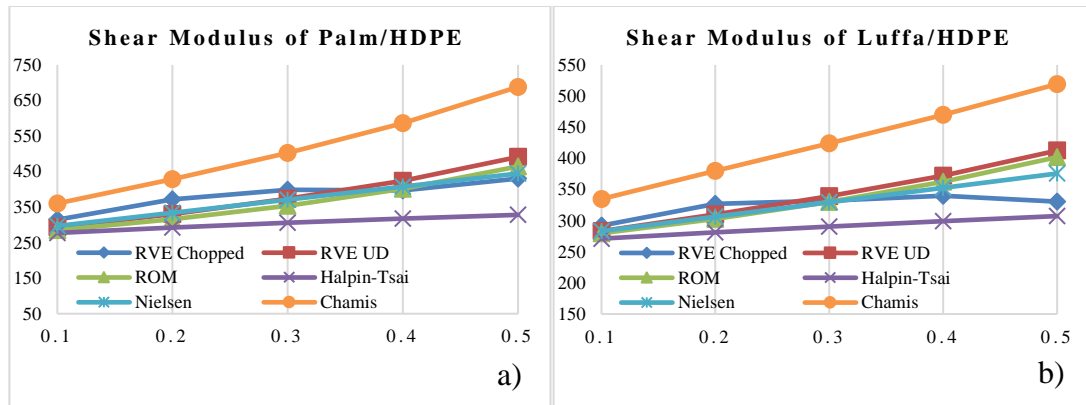


Figure 34: Shear Moduli of a) Palm/HDPE and b) Luffa/HDPE Reinforced Composites

As shown in Figures 34a and 34b, G_{23} values of palm/HDPE and luffa/HDPE were increased by increasing fiber content up to 0.5. Similar to the previously mentioned PP NFCs shear moduli, G_{23} values obtained from Chamis model were higher than other models for all five specimen compositions. However, peak G_{23} of 688 MPa was observed in HDPE matrix with 0.5 palm fibers. Thus, RVE UD results showed a drastic agreement with those of ROM in predicting G_{23} of luffa/HDPE and palm/HDPE. RVE chopped model presented its independent trend shape, such that G_{23} of palm/HDPE increased from 314.5 MPa to 399 MPa by increasing fibers' volume fraction from 0.1 to 0.3, then dropped to around 396 MPa at 0.4, and increased back to 430 MPa at 0.5, though shear modulus of luffa/HDPE decreased by further increasing fiber content beyond 0.4. It is worthy to mention that palm in HDPE matrix

revealed higher shear moduli than those of luffa/HDPE (around 688 MPa). Palm fibers with ecopoxy matrix exhibited the greatest shear moduli compared to all the considered natural fibers composites. Generally, increasing palm fibers content slightly improved G_{23} , this is caused by the limited endurance of NFCs towards transversal loads [334].

4.1.4 Poisson's Ratio

Poisson ratio defines the contraction or expansion of a composite material along the perpendicular direction to applied load. The poisson's ratio results of palm as well as luffa natural fibers composites are listed in Table 21. As clearly shown in Table 21, based on all the considered analytical and numerical models, poisson's ratio of epoxy, ecopoxy, PP, and HDPE decreased while increasing the fibers volume fraction of palm or luffa, which was witnessed in almost all utilized methods (analytical and RVE UD). v_{12} of Palm/Epoxy NFC decreased from 0.33 to 0.26 by rising the fibers' volume fraction from 0.1 to 0.5. Increasing the palm fibers' content in ecopoxy matrix decreased the poisson's ration from 0.31 to 0.25. Moreover, v_{12} of luffa reinforced thermoplastics were higher than that of Palm/Epoxy and palm/ecopoxy. Increasing luffa fibers' volume fraction from 0.1 to 0.5 decreased the Poisson's ratio of epoxy from 0.35 to 0.33, and v_{12} of ecopoxy from 0.33 to 0.32. RVE UD model markedly agreed with the analytical approaches in predicting v_{12} of palm as well as luffa reinforced thermosets, yet a small variance occurred between the analytical and RVE UD findings in palm/epoxy at 0.3 and 0.4, as well as in palm/ecopoxy at 0.4. Hence, results of RVE chopped model were higher than those obtained from other models. Not only, the aforementioned model showed a common behavior in poisson's ratio of all the considered natural fibers composites, as v_{12} decreased by increasing fibers volume fraction from 0.1 to 0.2, thereby it remained constant by increasing to 0.3, 0.4

and up to 0.5. It is worthy to mention that RVE chopped model agreed with all the utilized models in predicting v_{12} of luffa/ecopoxy NFC. HDPE matrix with luffa and palm fibers resulted in higher poisson's ratios compared to PP NFCs. However, luffa reinforced samples revealed Poisson's ratios slightly higher than those obtained with palm fibers. A noteworthy agreement between RVE UD and analytical findings was observed while predicting the Poisson's ratio of natural fiber-reinforced thermoplastic composites. A slight difference was detected between the results obtained from analytical techniques and RVE UD for palm/HDPE at 0.1 and 0.4. While RVE chopped model revealed the highest results among all considered techniques, v_{12} of palm/PP decreased by increasing fiber volume fraction up to 0.3 and increased at 0.5 (0.33), while palm in HDPE had a constant Poisson's ratio (0.38) at almost all compositions, which then dropped to 0.35 at 0.5. v_{12} of luffa/PP NFC was constant at the majority of fiber volume fractions, but it dropped to 0.34 at 0.3. Hence, Poisson's ratio of luffa/HDPE NFC followed a decreasing trend by increasing fiber content to up to 0.4, and then increased at 0.5 to reach a value of 0.38. However, Increasing the fibers' content of luffa and palm led to a reduction in the poisson's ratio of the NFCs, this is caused by the resistance increase of the natural fibers composite material. Hence, poisson's ratio contributes in specifying a material's elasticity, therefore the elasticity of the considered NFCs is decreasing while increasing the fibers volume fraction [32].

Table 21: Poisson's Ratio of Palm and Luffa Reinforced Thermosets

Fiber	Matrix	V _r	RVE UD	RVE Chopped	ROM	Halpin-Tsai	Nielsen	Chamis
Palm	Epoxy	0.1	0.33	0.34	0.33	0.33	0.33	0.33
		0.2	0.31	0.32	0.31	0.31	0.31	0.31
		0.3	0.29	0.32	0.30	0.30	0.30	0.30
		0.4	0.27	0.32	0.28	0.28	0.28	0.28
		0.5	0.26	0.31	0.26	0.26	0.26	0.26
	Ecopoxy	0.1	0.31	0.31	0.31	0.31	0.31	0.31
		0.2	0.30	0.30	0.30	0.30	0.30	0.30
		0.3	0.28	0.30	0.28	0.28	0.28	0.28
		0.4	0.26	0.30	0.27	0.27	0.27	0.27
		0.5	0.25	0.30	0.25	0.25	0.25	0.25
	PP	0.1	0.35	0.34	0.34	0.34	0.34	0.34
		0.2	0.33	0.32	0.32	0.32	0.32	0.32
		0.3	0.32	0.30	0.30	0.30	0.30	0.30
		0.4	0.32	0.28	0.28	0.28	0.28	0.28
		0.5	0.33	0.26	0.26	0.26	0.26	0.26
	HDPE	0.1	0.38	0.37	0.38	0.38	0.38	0.38
		0.2	0.38	0.35	0.35	0.35	0.35	0.35
		0.3	0.38	0.33	0.33	0.33	0.33	0.33
		0.4	0.38	0.30	0.31	0.31	0.31	0.31
		0.5	0.35	0.28	0.28	0.28	0.28	0.28
Luffa	Epoxy	0.1	0.35	0.35	0.35	0.35	0.35	0.35
		0.2	0.34	0.34	0.34	0.34	0.34	0.34
		0.3	0.34	0.34	0.34	0.34	0.34	0.34
		0.4	0.33	0.34	0.33	0.33	0.33	0.33
		0.5	0.33	0.34	0.33	0.33	0.33	0.33
	Ecopoxy	0.1	0.33	0.33	0.33	0.33	0.33	0.33
		0.2	0.32	0.32	0.32	0.32	0.32	0.32
		0.3	0.32	0.32	0.32	0.32	0.32	0.32
		0.4	0.32	0.32	0.32	0.32	0.32	0.32
		0.5	0.32	0.32	0.32	0.32	0.32	0.32
	PP	0.35	0.35	0.35	0.35	0.35	0.35	0.35
		0.35	0.35	0.35	0.35	0.35	0.35	0.35
		0.34	0.34	0.34	0.34	0.34	0.34	0.34
		0.35	0.33	0.34	0.34	0.34	0.34	0.35
		0.35	0.33	0.33	0.33	0.33	0.33	0.35
	HDPE	0.39	0.39	0.39	0.39	0.39	0.39	0.39
		0.39	0.38	0.38	0.38	0.38	0.38	0.39
		0.38	0.37	0.37	0.37	0.37	0.37	0.38
		0.37	0.36	0.36	0.36	0.36	0.36	0.37
		0.38	0.35	0.35	0.35	0.35	0.35	0.38

4.2 Tensile Test Results

Tensile test findings are listed in this section, which includes tensile strength, strain, and young's modulus of luffa as well as palm natural fibers composites in biopoxy, epoxy, HDPE and PP matrices. First, some stress and strain charts are displayed to show the tensile behavior of these NFCs, then the effect of increasing the natural fibers volume fraction in the considered matrices. Figure 35 shows the stress-strain behavior of BioPoxy NFC with 0.1 luffa fibers.

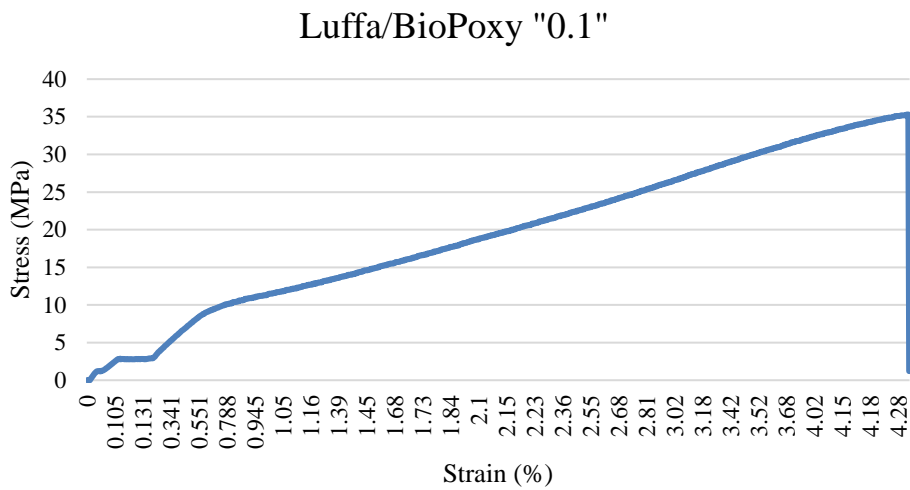


Figure 35: Stress and Strain Curve of Luffa/BioPoxy "0.1"

As shown in Fig. 35, the stress increased gradually to reach a yield strength of 3.77 MPa at 0.262 %, then it followed a continuous increase to attain an ultimate tensile strength of 35.3 MPa at 4.31 % straight before its brittle failure. Figure 36 displays the stress-strain behavior of epoxy NFC with 0.3 palm.

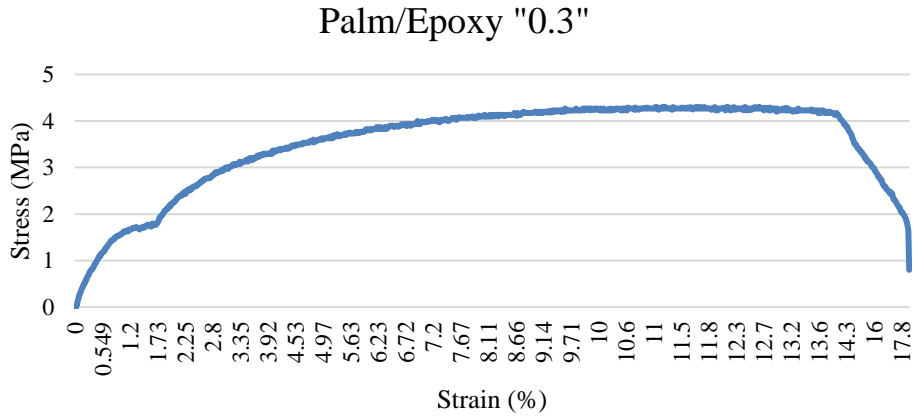


Figure 36: Stress and Strain Curve of Palm/Epoxy "0.3"

As exhibited in Fig. 36, a yield strength of 1.67 MPa was observed at 1.8 %, then the stress increased to reach a 4.13 MPa ultimate tensile strength at 14.1 %, which emphasizes the notable ductility of this material, thereby the Palm/Epoxy NFC performed a plastic failure at 17.5 %. Figure 37 displays the stress-strain curve of polypropylene NFC with 0.1 palm fibers.

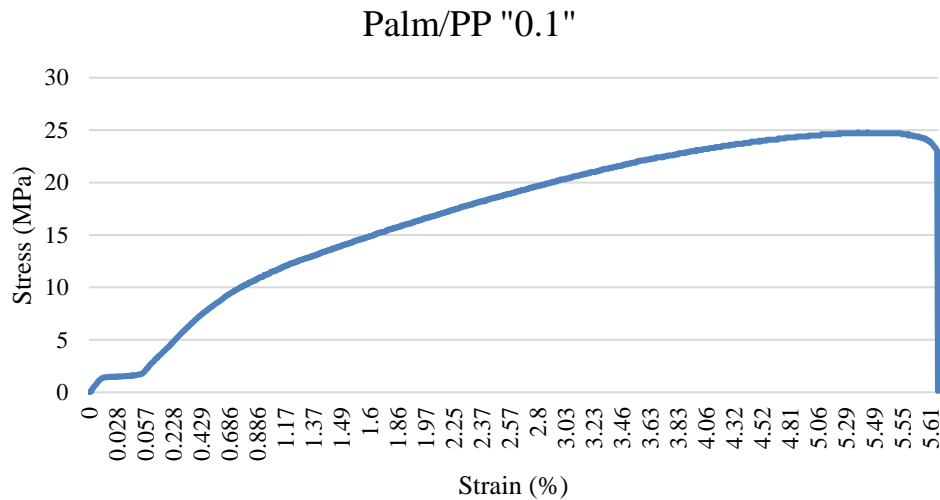


Figure 37: Stress and Strain Curve of Palm/PP "0.1"

As exhibited in Fig. 37, polypropylene with 0.1 pam fibers revealed a yield strength of 3.07 at 0.143 %, then the stress drastically increased to attain an ultimate tensile

strength of 24.7 MPa at 5.52 %, next it decreased to 23 MPa at 5.58 % right before its brittle failure at 5.61 %. Figure 38 shows the stress-strain behavior of high-density polyethylene reinforced with 0.1 luffa fibers.

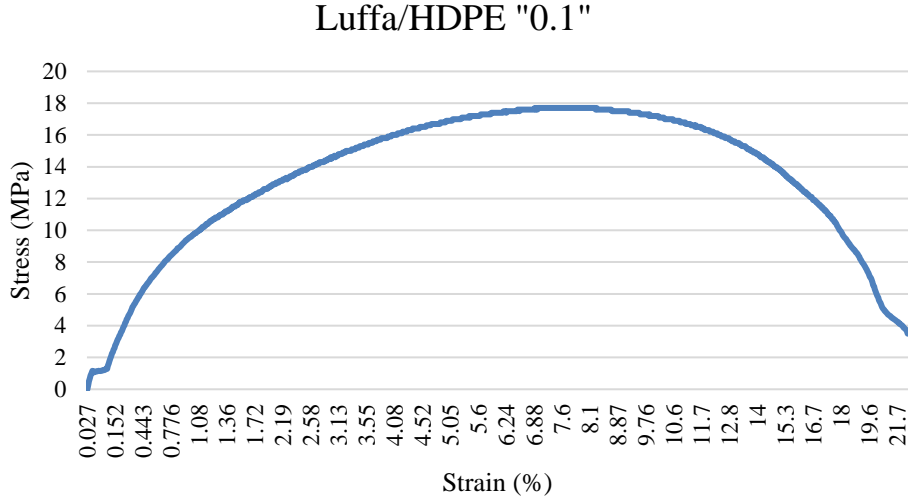


Figure 38: Stress and Strain Curve of Luffa/HDPE "0.1"

As observed in Figure 38, a yield strength of 1.28 MPa was observed at 0.027 %, then a gradual increase in the stress was observed along with an increase in the strain to reach an ultimate tensile strength of 17.7 at 7.15 %. Hence, the stress followed a descending trend till its ductile failure at 21.7 %. It is worthy to mention that natural fibers composites with HDPE matrix revealed the highest ductility.

Moreover, in order to achieve an accurate validation of TS results with that observed by other researchers, equation 24 was involved for converting weight percentage into fibers volume fraction.

$$V_f = \frac{\rho_m}{\rho_f \times \left(\frac{1}{wt\%} - 1 \right) + \rho_m} \quad (24)$$

Where ρ_m is the density of the matrix, ρ_f is the density of the fibers, V_f is the fibers volume fraction, and wt% is the weight percentage. It was observed through equation

24 that 10 wt% of the considered NFCs is around 1.1 V_f . Table 22 lists the tensile test results. As shown in table 22, natural fibers' reinforced biopoxy displayed the highest tensile strengths along with the least strain values.

Table 22: Tensile Test Outcome

Matrix	Fibers	V_f	TS (MPa)	Strain (%)	E (MPa)
BioPoxxy	Palm	0.1	20.800	1.24765	1667.134
		0.2	23.600	1.3597	1735.677
		0.3	21.050	2.3325	902.465
Epoxy	Palm	0.1	2.370	7.6615	30.934
		0.2	3.323	9.081667	36.594
		0.3	4.343	9.971333	43.558
PP	Palm	0.1	25.233	3.986667	632.943
		0.2	22.467	3.834667	585.883
		0.3	21.100	2.391	882.476
HDPE	Palm	0.1	16.967	11.13833	152.327
		0.2	15.400	9.224	166.956
		0.3	12.567	7.746	162.234
BioPoxxy	Luffa	0.1	33.167	3.266667	1015.306
		0.2	35.133	1.281667	2741.222
		0.3	35.300	2.4735	1427.128
Epoxy	Luffa	0.1	2.853	16.36	17.441
		0.2	3.097	16.48	18.790
		0.3	3.687	17.08333	21.580
PP	Luffa	0.1	22.567	2.646333	852.752
		0.2	21.300	3.654	582.923
		0.3	18.333	2.555667	717.360
HDPE	Luffa	0.1	16.600	7.764	213.807
		0.2	15.433	7.600333	203.061
		0.3	10.123	5.11	198.108

While palm as well as luffa reinforced epoxy exhibited the lowest TS compared to the selected matrices, yet it provided the highest strain record in this study. Moreover, PP matrix revealed a notable TS (between 18 and 25 MPa), while the tensile strength of HDPE samples ranged between 10 and 17 MPa.

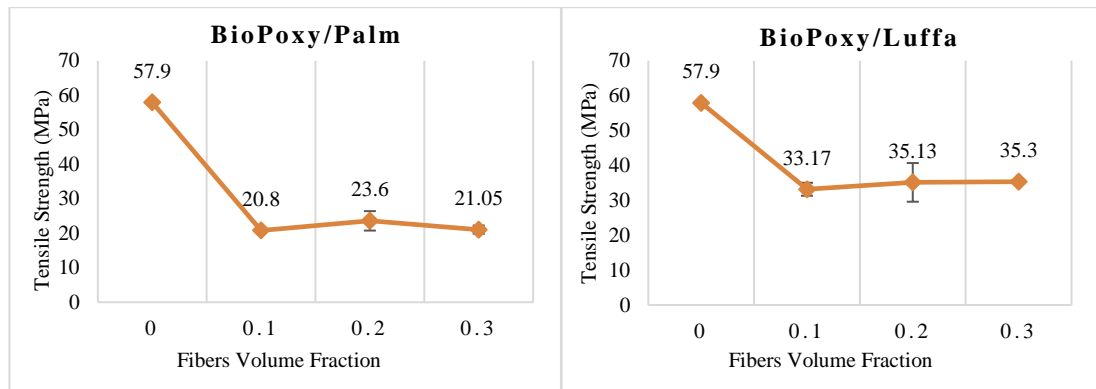


Figure 39: Tensile Strength Variation of BioPoxy/Palm and BioPoxy/Luffa

In terms of biopoxy/palm NFC, the tensile strength increased from 20.8 MPa to 23.6 by increasing the fibers volume fraction from 0.1 to 0.2, thus it decreased back to 21.05 MPa by reaching 0.3. Whereas reinforcing biopoxy with luffa fibers exhibited the highest TS outcome in this research, increasing the fibers volume fraction of luffa from 0.1 to 0.3 increased the tensile strength from 33.16 to 35.5 MPa, respectively. It is worthy to mention that TS of pure BioPoxy 36 is 57.9 MPa. However, highest TS observed in biopoxy/palm was 23.6 MPa at 0.2, and in biopoxy/luffa was 35.3 MPa at 0.3. Addition of luffa fibers into biopoxy resin contributed in higher tensile strengths compared to palm fibers.

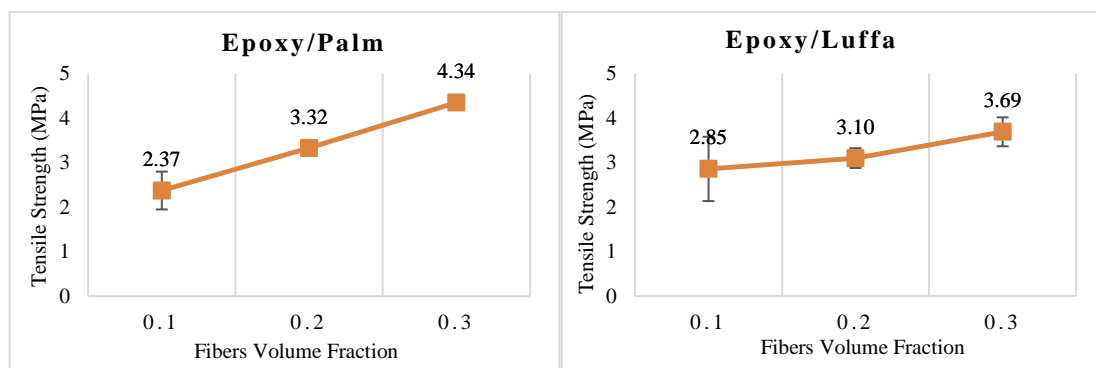


Figure 40: Tensile Strength Variation of Epoxy/Palm and Epoxy/Luffa

Epoxy with 0.1 palm exhibited a tensile strength of 2.37 MPa, by growing the fibers' content, TS increased to 3.32 MPa at 0.2 and 4.34 MPa at 0.3. While luffa reinforced

epoxy displayed a TS 2.85 MPa at 0.1 fibers volume fraction, then reached 3.69 MPa by growing the fibers content up to 0.3. Adding luffa as well as palm fibers into epoxy matrix improved the tensile strength, yet, palm had a better impact than luffa fibers. Highest TS observed in NF reinforced epoxy was 4.34 MPa in epoxy with 0.3 palm fibers.

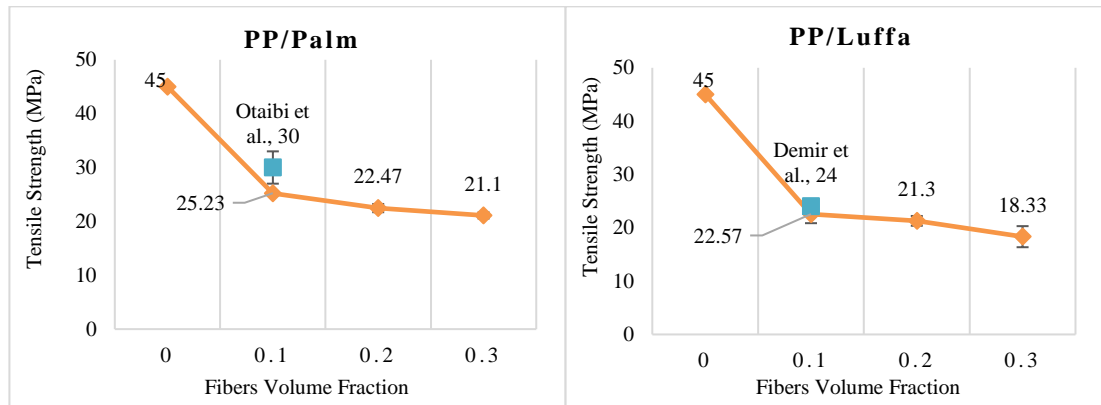


Figure 41: Tensile Strength Variation of PP/Palm and PP/Luffa

Regarding palm fibers reinforced polypropylene, increasing the fibers' content from 0.1 to 0.3 decreased the tensile strength from 25.23 to 21.1 MPa, respectively. Similarly, increasing V_f of luffa fibers in PP reduced TS from 22.57 MPa at 0.1 to 18.33 MPa at 0.3, respectively. Furthermore, addition of palm fibers in PP matrix resulted greater TS values than that of PP/luffa, thus peak TS was 25.23 MPa observed in PP with 0.1 palm fibers. It is worthy to mention that the tensile test findings of PP/luffa were in accordance with Demir et al. [182] at 0.1 fibers' volume fraction, whereas the results of PP/palm agreed with the findings of Otaibi et al [335] at 10 wt%, which was the closer to 0.1 in the literature.

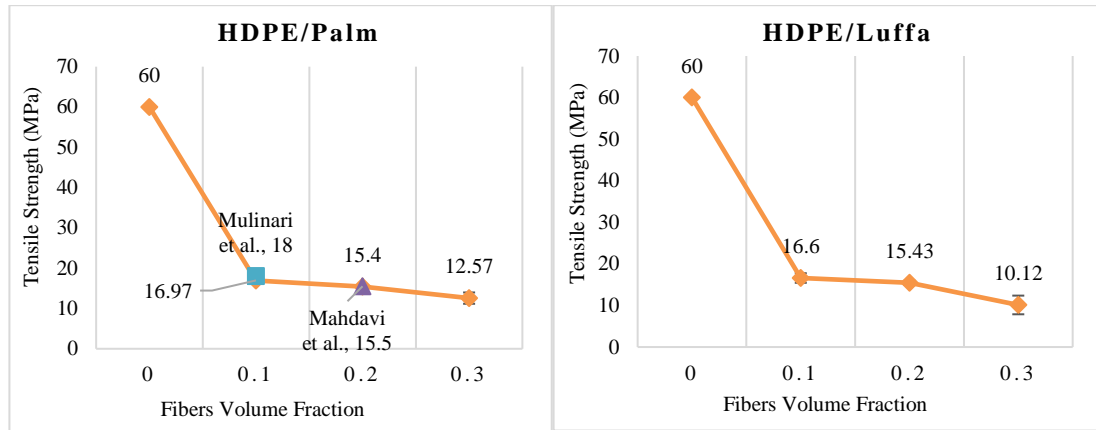


Figure 42: Tensile Strength Variation of HDPE/Palm and HDPE/Luffa

As clearly shown in Figure 42, loading palm fibers into HDPE matrix reduced the tensile strength to 12.57 MPa at a volume fraction of 0.3, yet it was 16.97 MPa at 0.1 and 15.4 MPa at 0.2. Reinforcing HDPE with luffa fibers reduced the tensile strength from 16.6 MPa at 0.1 to 10.12 MPa at 0.3, respectively. HDPE/palm and HDPE/luffa exhibited identical TS values at 0.1 and 0.2 fibers' volume fraction, whilst palm fibers had a better effect at 0.3. Results of HDPE/palm agreed with Mulinari et al. at [319] 10 wt% and Mahdavi et al. [113] at 20 wt%, which was the closer to 0.1 and 0.2 in the literature.

However, the observed results highlight the potential of Palm/BioPoxy to be used in industrial applications, Luffa/BioPoxy for aircraft minor components, palm/epoxy and luffa/epoxy for appliances coating applications, palm/PP and luffa/PP for automotive parts, and palm/HDPE and luffa/HDPE for bio-packaging.

4.3 FEA and Experimental Results

Since RVE chopped was observed to be the most accurate model due to its non-linear trends and its agreement with the literature, this model was involved in analyzing the elastic properties of the materials utilized for conducting the tensile test. In ANSYS Explicit Dynamics space, orthotropic output of RVE chopped was assigned as an input

into a 120 x 20 x 5 mm beam following ASTM D3039 (Fig. 43). After meshing the sample with linear elements order, the total number of nodes was 693 and the number of elements was 384. Moreover, bottom of the sample was fixed through applying a nodal displacement of 0 mm, and a nodal force was applied on the top of the sample similar to the real tensile test. Furthermore, all models were analyzed by firstly applying a low nodal force on the beam, thereby increasing it till its failure in order to measure its tensile strength. However, each natural fiber composite required different nodal force to break the sample.

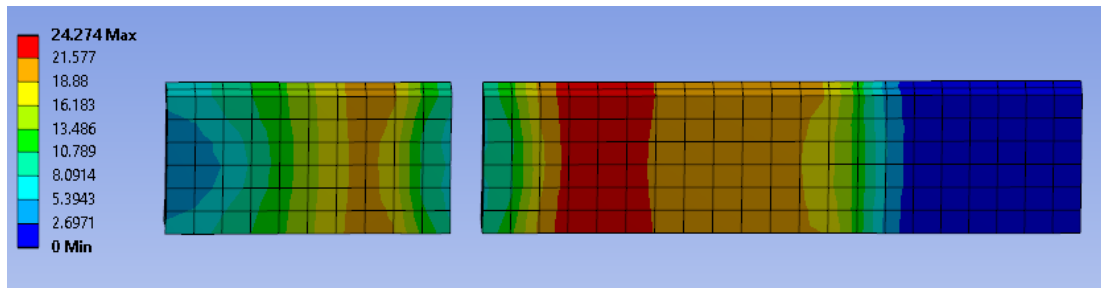


Figure 43: FEA Beam Model Following ASTM D3039

This section compares the tensile strength obtained through representative volume element chopped model followed by finite element analysis simulation, and the conducted experiment.

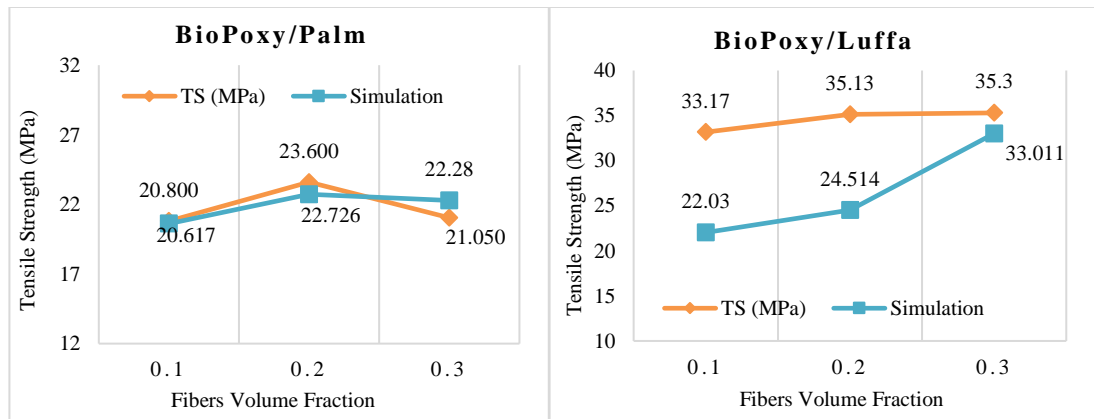


Figure 44: Experimental versus FEA Tensile Strength of BioPoxy/Palm and BioPoxy/Luffa

As shown in Figure 44, experimental tensile strength of biopoxy/palm increased from 20.8 MPa to 23.6 MPa by increasing the fibers' volume fraction from 0.1 to 0.2, then it dropped to reach a TS of 21.050 MPa at 0.3. A common behavior was displayed by FEA model, TS increased from 20.617 to 22.726 MPa at 0.2, thereby decreased to 22.28 MPa at 0.3. Whereas experimental TS of biopoxy/luffa increased from 33.17 to 35.3 MPa through increasing V_f from 0.1 to 0.3, similarly FEA tensile strength followed an ascending trend to reach a TS value of 33.011 MPa at 0.3. Tensile strength results obtained from FEA showed a good agreement with the experimental findings.

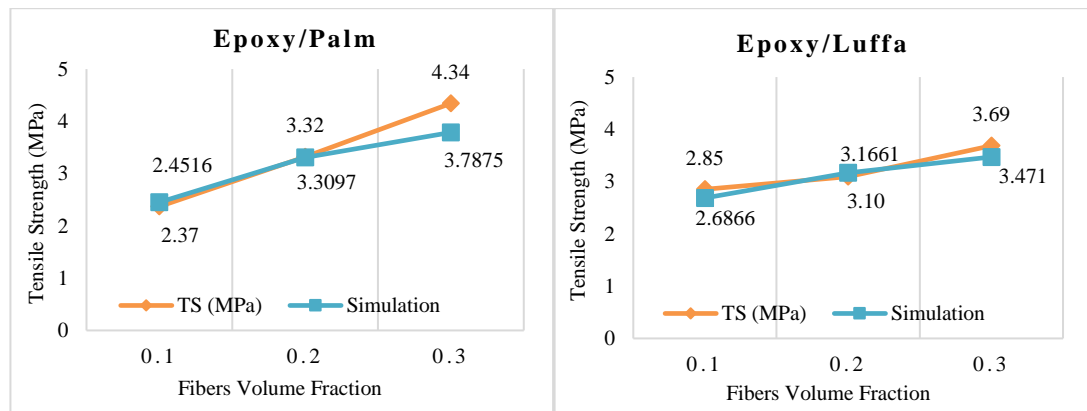


Figure 45: Experimental versus FEA Tensile Strength of Epoxy/Palm and Epoxy/Luffa

As shown in figure 45, both methods showed increasing trends while increasing the fibers' content of luffa as well as palm. However, tensile strength of epoxy/palm observed in FEA model increased from 2.45 to 3.31 MPa by increasing V_f from 0.1 to 0.2, and to 3.79 MPa by increasing V_f up to 0.3, whilst the experimental TS of epoxy/palm increased to 3.32 MPa and 4.34 MPa, respectively. In terms of Epoxy/Luffa, the numerically observed tensile strength increased to 3.17 MPa at 0.2, and 3.47 MPa from 0.2 to 0.3, thus the corresponding experimental results increased to 3.1 MPa by increasing the fibers' volume fraction from 0.1 to 0.2, and 3.69 MPa from 0.2 to 0.3. FEA findings significantly agreed with the tensile test results.

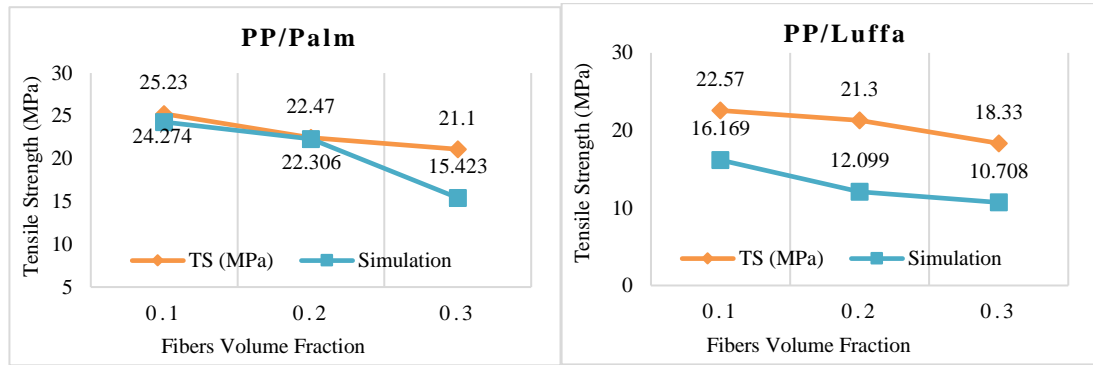


Figure 46: Experimental versus FEA Tensile Strength of PP/Palm and PP/Luffa

As seen in Figure 46, considering both FEA and experimental results, increasing the fibers' content to 0.3 decreased TS of both PP/palm and PP/luffa, respectively. In terms of experimental TS of PP/palm NFC, increasing V_f to 0.3 reduced the tensile strength to 22.47 MPa and 21.1 MPa respectively, similarly FEA TS followed a descending trend, TS decreased from 24.274 to 22.3 MPa by increasing the fibers' content to 0.2, and to 15.423 MPa at 0.3. While Regarding TS of PP/luffa, both methods displayed a continuous decline in tensile strength while increasing the fibers volume fraction. Moreover, the simulation results notably agreed with the experimental findings.

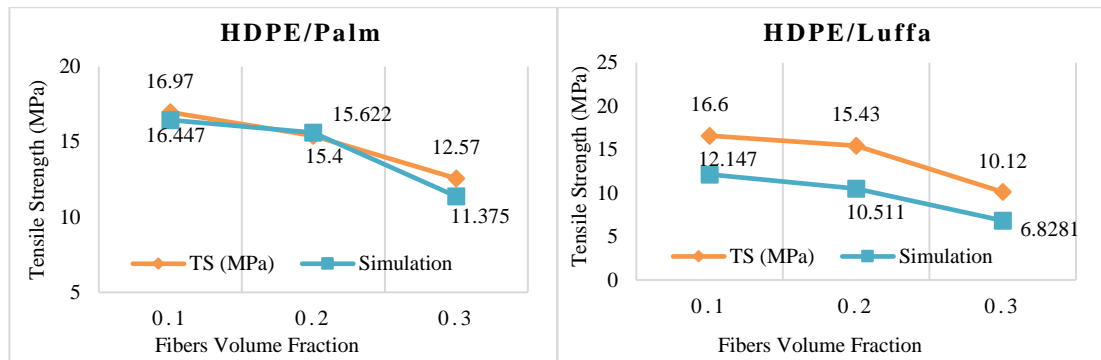


Figure 47: Experimental versus FEA Tensile Strength of HDPE/Palm and HDPE/Luffa

As shown in Figure 47, increasing V_f of palm from 0.1 to 0.2 in HDPE matrix decreased the tensile strength from 16.97 to 15.622 MPa, consequently it decreased to 12.57 MPa at 0.3, similarly TS of HDPE/palm observed in FEA model exhibited a

continuous decline to reach a TS value of 11.375 MPa at 0.3. Furthermore, addition of luffa fibers in HDPE reduced the tensile strength, that was observed through FEA simulation as well as FEA model. It is worthy to mention that the overall agreement between FEA simulation and tensile test results is quite acceptable [336, 337]. Although FEA and experimental TS were following same trends in PP/luffa and HDPE/luffa, the predicted values were slightly lower than the experimental.

4.4 Machine Learning Findings

Artificial neural network, multiple linear regression, support vector machine, and adaptive neuro-fuzzy inference system were adapted in this research to determine the design space as well as to specify most convenient ML approach in predicting TS of NFCs. This section introduces the outcome of the aforementioned ML tools in predicting the tensile strength of palm NFCs as well as luffa NFCs. Figure 48 displays the schemes of tensile strength regressions for all considered NFCs throughout three different fibers' volume fractions, i.e. 0.1, 0.2, and 0.3. This figure highlights the correlation between the ANN output and the experimental data (target). The correlation between the output values and target values were represented through the solid line, while best correlation that can be generated is represented through the dotted line. The overall regression coefficient of ANN model was observed to be 0.989, which means it is satisfactory as it is close to 1. Moreover, response surface metamodel provides a surface fitting that covers the design in order to predict responses for inputs not considered throughout the experiment. A cubic polynomial approximation function is involved in study to develop the response surfaces shown in Figure 49 and Figure 50.

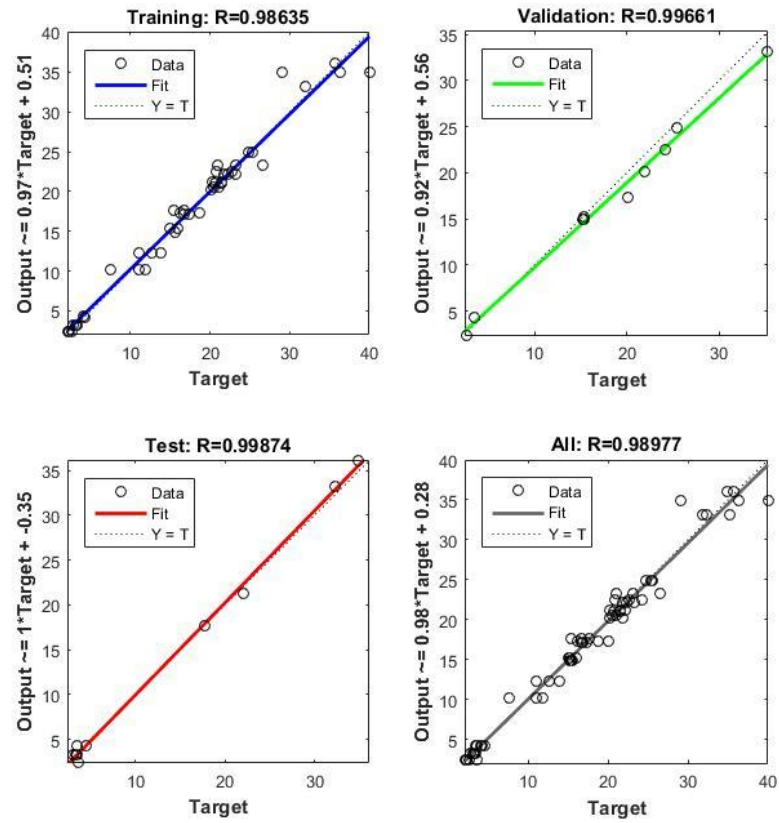
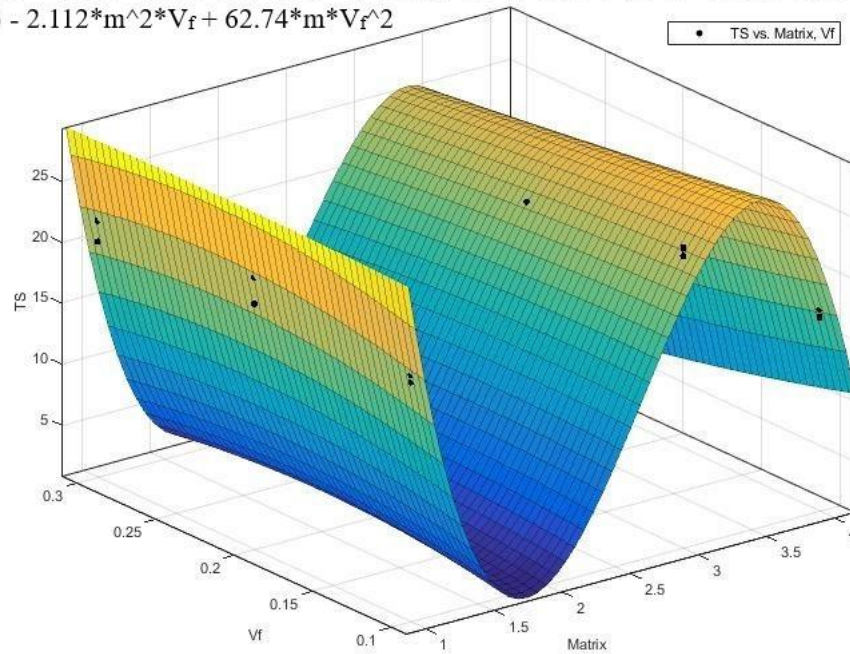


Figure 48: Regression Plot of ANN Model

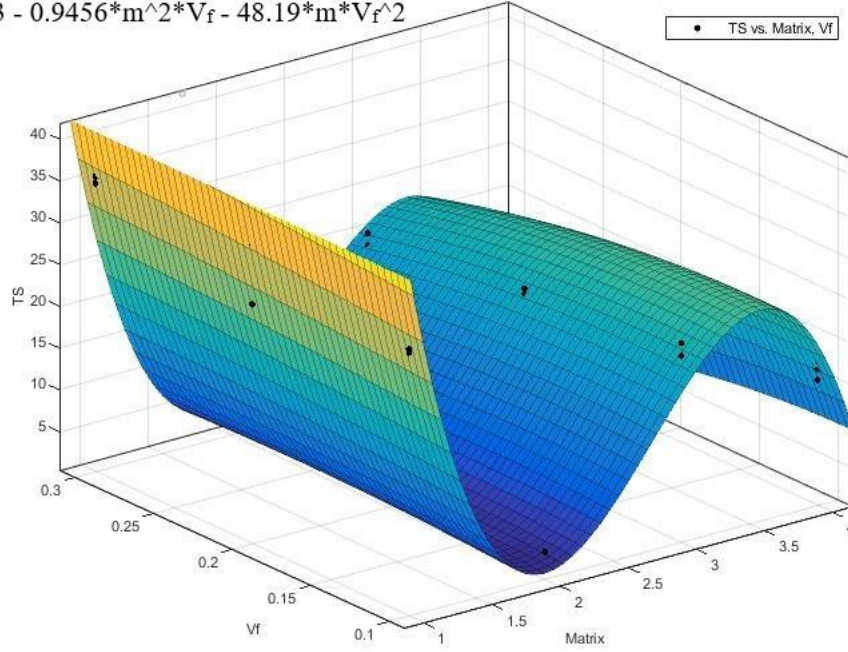
$$f(m, V_f) = 135.7 - 194.1 \cdot m + 91.5 \cdot V_f + 85.17 \cdot m^2 - 24.74 \cdot m \cdot V_f - 210.2 \cdot V_f^2 - 10.95 \cdot m^3 - 2.112 \cdot m^2 \cdot V_f + 62.74 \cdot m \cdot V_f^2$$



Goodness of fit: SSE: 44.32 R-square: 0.9781 Adjusted R-square: 0.9705

Figure 49: Response Surface Fitting of Palm NFCs

$$f(m, V_f) = 184 - 238.2*m + 12.51*V_f + 97.75*m^2 + 8.274*m*V_f + 31.59*V_f^2 - 12.18*m^3 - 0.9456*m^2*V_f - 48.19*m*V_f^2$$



Goodness of fit: SSE: 104.6 R-square: 0.977 Adjusted R-square: 0.9699

Figure 50: Response Surface Fitting of Luffa NFCs

MATLAB cftool was utilized for developing the RSM for TS of palm NFCs as well as luffa NFCs. Goodness of fit were evaluated using sum of square error (SSE), R-square adjusted, and root mean square error (RMSE). The values of R-square adjusted ranges between 0 and 1, where a good fit would get a value close 1. In contrast, RMSE and SSE values should be close to zero in order to have a good surface fit. Moreover, the utilized function in developing the RSM for palm NFCs was:

$$f(m, V_f) = p_{00} + p_{10}*m + p_{01}*V_f + p_{20}*m^2 + p_{11}*m*V_f + p_{02}*V_f^2 + p_{30}*m^3 + p_{21}*m^2*V_f + p_{12}*m*V_f^2 \quad (25)$$

Where m is the matrix type, V_f is the fibers volume fraction, $p_{00} = 135.7$, $p_{10} = -194.1$, $p_{01} = 91.5$, $p_{20} = 85.17$, $p_{11} = 24.74$, $p_{02} = -210.2$, $p_{30} = -10.95$, $p_{21} = -2.112$, and $p_{12} = 62.74$. The goodness of fit included an SSE of 44.32, R-square of 0.9781, Adjusted R-square of 0.9705 and RMSE of 1.388.

While regarding the RSM model of luffa NFCs, the approximation function was:

$$f(m, V_f) = p00 + p10*m + p01*V_f + p20*m^2 + p11*m*V_f + p02*V_f^2 + p30*m^3 + p21*m^2*V_f + p12*m*V_f^2 \quad (26)$$

Where m is the matrix type, V_f is the fibers volume fraction, $p00 = 184$, $p10 = -238.2$, $p01 = 12.51$, $p20 = 97.75$, $p11 = 8.274$, $p02 = 31.59$, $p30 = -12.18$, $p21 = -0.9456$, and $p12 = -48.19$, with SSE: 104.6, R-square: 0.977, Adjusted R-square: 0.9699, and RMSE: 2.006.

ANFIS model was implemented using MATLAB Neuro-Fuzzy Designer, all fibers, matrices, and fibers' volume fractions were considered. FIS model was generated using Gaussmf membership function with a constant output. Training was completed at epoch 2, and average testing error was observed to be 1.4876. ANFIS model plot that displays the training data as well as the FIS output data is shown in figure 51.

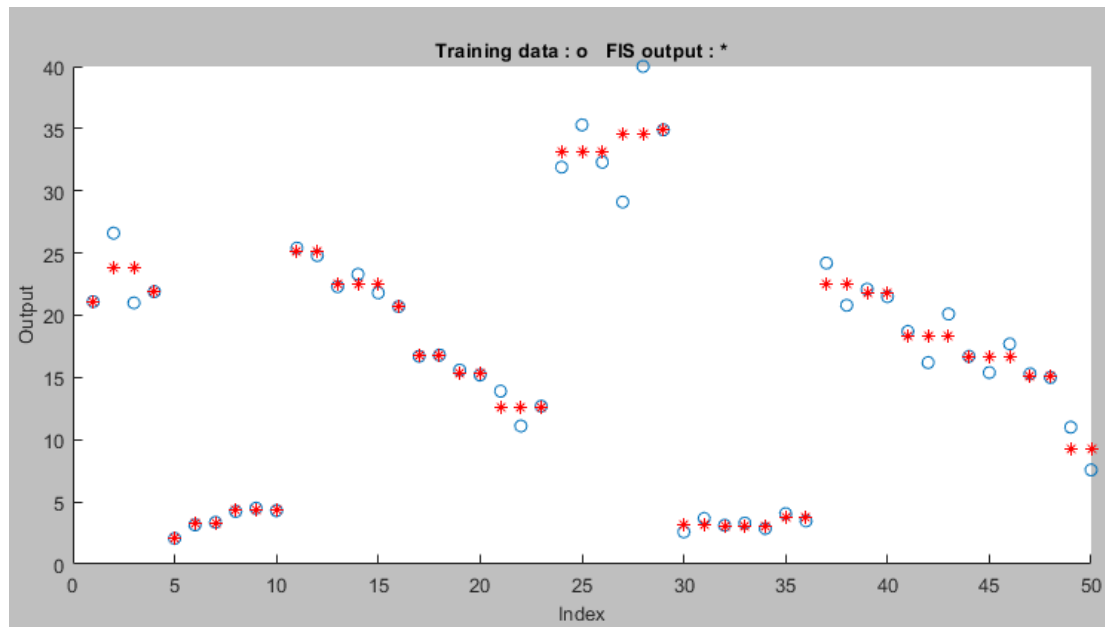


Figure 51: Adaptive Neuro-Fuzzy Inference System Plot

Hence, experimental results of all NFCs were utilized for training the SVM model, the kernel function used was the Gaussian, and the involved preset was the fine Gaussian SVM. Moreover, the obtained RMSE was 2.7296, R-squared was 0.93, and MSE was 7.4509. Table 23 shows the predicted data using machine learning methods as well as real tensile strength results of palm and luffa NFCs, where matrix 1 is biopoxy 36, matrix 2 is epoxy, matrix 3 is PP, matrix 4 is HDPE, fiber 1 is palm, and fiber 2 is luffa.

Table 23: Predicted Tensile Strength Using ANN, MLR, ANFIS, and SVM

Matrix	Fibers	V_f	Experimental	ANN	MLR	ANFIS	SVM
			TS (MPa)	TS (MPa)	TS (MPa)	TS (MPa)	TS (MPa)
1	1	0.1	20.800	20.550	20.810	21.100	19.835
1	1	0.2	23.600	23.250	22.851	23.800	22.256
1	1	0.3	21.050	20.150	21.943	21.900	20.646
2	1	0.1	2.370	2.423	3.090	2.070	3.928
2	1	0.2	3.323	3.275	3.906	3.260	4.411
2	1	0.3	4.343	4.235	3.027	4.343	5.489
3	1	0.1	25.233	24.850	23.887	25.100	24.242
3	1	0.2	22.467	22.150	23.055	22.467	22.043
3	1	0.3	21.100	20.950	21.783	20.700	20.245
4	1	0.1	16.967	17.110	17.502	16.750	16.828
4	1	0.2	15.400	14.900	14.600	15.400	16.459
4	1	0.3	12.567	12.320	12.513	12.567	12.642
1	2	0.1	33.167	33.150	33.188	33.167	31.041
1	2	0.2	35.133	34.980	34.674	34.550	30.356
1	2	0.3	35.300	36.090	35.828	34.900	33.637
2	2	0.1	2.853	2.419	3.040	3.130	3.852
2	2	0.2	3.097	3.282	3.624	3.097	4.370
2	2	0.3	3.687	4.266	2.912	3.765	4.730
3	2	0.1	22.567	22.440	22.042	22.500	22.060
3	2	0.2	21.300	21.210	21.535	21.800	20.835
3	2	0.3	18.333	17.370	18.768	18.333	17.460
4	2	0.1	16.600	17.630	17.116	16.600	16.661
4	2	0.2	15.433	15.280	15.328	15.150	16.255
4	2	0.3	10.123	10.230	10.318	9.285	10.546
Prediction Error %				3.21%	6.86%	2.17%	12.65%

As clearly shown in table 23 the predicted TS using ANN, and ANFIS, displayed a strong agreement with experimental results with a prediction error of 3.21% and 2.17%, respectively, whilst TS values obtained through MLR and SVM showed a decent agreement with an error of 6.86% and 12.65%. That emphasizes that these models are able to be trained and involved in assuming the tensile strength of natural fibers composite materials. Furthermore, luffa/biopoxy at 0.3 V_f revealed the highest tensile strength values throughout all the considered ML approaches. Most suitable machine learning approach for predicting tensile strength of natural fibers composites is ANFIS as it showed least prediction error “2.17%”.

Chapter 5

CONCLUSION

Natural Fibers Composites (NFC) became prevalent in polymers science field, as these materials have a range of advantages such as: environmental friendly, high strength to weight, lightweight, low density, abundance in nature, and negligible cost. Thus, research in natural fibers area, like Jute, Hemp, Bamboo, Kenaf, Sisal, and Coir, have emerged in a wide spectrum in science and engineering disciplines.

This research presents an investigation on the mechanical properties of luffa and palm NFCs in epoxy, ecopoxy “biopoxy 36”, PP and HDPE matrices. Two representative volume element models, unidirectional and chopped, as well as Rule of Mixture, Halpin-Tsai, Chamis, and Nielsen analytical approaches, were involved and compared in order to validate the most convenient simulation method for the considered NFCs. FEA RVE models were conducted using materials designer ANSYS. Throughout the aforementioned numerical and analytical models, RVE chopped model was considered for analyzing the orthotropic properties of palm and luffa NFCs, thereby, the output of RVE chopped was assigned into a 120 x 20 x 5 mm beam as for ASTM D3039, and loaded under tensile load till failure. Moreover, experimental tensile test was conducted for testing the tensile properties of the considered NFCs as well as validating the simulation results. Thus, different machine learning techniques were implemented in order to identify the design space, i.e., Artificial Neural Network, Multiple Linear Regression, Adaptive Neuro-Fuzzy Inference System, and Support

Vector Machine. Effect of increasing fiber content in the matrix was taken into account by considering several fibers' volume fractions, from 0.1 to 0.5 in model validation and from 0.1 to 0.3 V_f for the simulation, experiment and machine learning models.

In model validation, increasing fiber volume fraction increased the longitudinal moduli of palm and luffa natural fibers composites. Palm NFCs revealed higher E_1 than luffa NFCs, whereas peak longitudinal modulus was exhibited by palm in ecopoxy matrix with 0.5 fibers volume fraction. Although RVE UD results were slightly greater than the findings of analytical models, yet they showed a significant agreement. RVE chopped E_1 of palm/HDPE was in accordance with the experimental results reported in literature. However, RVE UD displayed a drastic agreement with rule of mixture in predicting E_2 of palm and luffa reinforced thermosets, whereas it agreed with Chamis in the prediction of palm and luffa in PP and HDPE, yet the values obtained from Chamis model were higher than those of other analytical models. Meanwhile, Halpin-Tsai model revealed the lowest transverse moduli. Palm/ecopoxy at 0.5 V_f exhibited the peak transverse modulus of 3923 MPa. While regarding the shear moduli of the considered NFCs, increasing the fibers volume fraction led to an increment in G_{23} . Shear moduli findings obtained through Halpin-Tsai model were the least and that of Chamis were the greatest, which was a similar behavior to E_2 . Thus, RVE UD exhibited good agreement with rule of mixture in the prediction of shear modulus. Highest shear modulus was 1575 MPa, attained in Ecopoxy with 0.5 palm fibers. In terms of poisson's ratio, increasing fiber volume fraction led to a reduction in ν_{12} of epoxy, ecopoxy, HDPE and PP, yet Poisson's ratios of luffa NFCs was higher than that of palm NFCs. A good agreement was shown between the RVE UD and analytical ν_{12} results. However, RVE chopped model revealed different trends in properties compared to the applied models.

Regarding the experimental tensile test, NFCs with BioPoxy matrix showed the greatest tensile strength values and lowest strain, whereas NFCs with epoxy matrix displayed least tensile strengths in this research with highest strain values. Furthermore, NFCs with PP matrix exhibited significant tensile strength values ranging between 18 and 25 MPa. TS of NFCs with HDPE matrix ranged from 10 to 17 MPa. Peak tensile strength was observed in luffa/biopoxy at 0.3 with a value of 35.5 MPa. Increasing the fibers' volume fraction from 0.1 to 0.2 of natural fibers' reinforced BioPoxy increased TS then decreased at 0.3. Reinforcing BioPoxy with luffa fibers showed better properties compared to Date palm fibers. Growing the content of palm as well as luffa fibers' up to 0.3 increased the tensile strength of epoxy. Peak TS in natural fibers' reinforced epoxy was 4.34 MPa in Palm/Epoxy at 0.3. While addition of luffa and palm fibers decreased the tensile strength of HDPE and PP matrices, however, palm revealed higher TS values in PP (25.23 MPa at 0.1) and in HDPE (16.97 MPa at 0.1). Based on the revealed results, Palm/BioPoxy can be utilized for industrial applications, luffa/biopoxy can be used for producing aircraft components, luffa/epoxy and palm/epoxy can be involved in appliances' coating, while luffa/PP and palm/PP have the ability to emerge in automotive parts' production. It is worthy to mention that simulation results significantly agreed with the tensile test findings, where these FEA results followed the exact same trends observed in the experimental findings, as well as majority of the TS values were in accordance. Furthermore, in terms of machine learning application, predicted tensile strengths through ANN, and ANFIS drastically agreed with the experimental outcome, having a prediction error of 3.21% and 2.17%. Whereas tensile strength predicted using MLR and SVM displayed an acceptable agreement with a prediction error of 6.86% and 12.65%. Which therefore evidences the capability of these machine learning models

of being trained and utilized for predicting TS of natural fibers composites. Moreover, throughout all the considered ML approaches, highest tensile strength values were revealed in luffa/biopoly at 0.3 V_f . ANFIS can be considered as a suitable machine learning approach for predicting tensile strength of natural fibers composites as it exhibited lowest prediction error.

5.1 Research Limitations and Future Recommendations

After conducting this research, main limitations were observed to be as follows:

- 1) Unavailability of composite materials' machining equipment like water jet, which could contribute in following different samples' preparation procedure. In other words, if a water jet machine was available, the samples could be prepared by hand layup technique in wide mold, and compressed in the mold till it was cured, thereby the samples could be obtained from the plate by cutting them into the specimen's dimensions provided in the ASTM standard. Thus, this technique provides better surface finish as well as less voids in NFC.
- 2) Unavailability of a small injection molding machine for preparing the NFC samples that includes thermoplastic matrices, which was able to save time, provide good surface finish.
- 3) Due to the current situation (COVID 19) many restrictions were applied on laboratories' schedules, yet only tensile test was able to be conducted, otherwise further properties could be investigated, such as mechanical, acoustic, dielectric, and so on.

Therefore, future recommendations include:

- 1) Test the flexural, impact, compression, hardness, acoustic, dielectric, and chemical characteristics of palm/biopoxy, palm/epoxy, palm/PP, palm/HDPE, luffa/biopoxy, luffa/epoxy, luffa/PP, and luffa/HDPE.
- 2) Follow other samples' preparation methods to the considered natural fibers composites.
- 3) Investigate the performance of a hybrid NFC made from palm and luffa fibers in biopoxy, epoxy, PP, and HDPE.

REFERENCES

- [1] Yusuf, S., N. Islam, H. Ali, W. Akram, & A. Siddique (2020). *Impact Strength of Natural Fiber Reinforced Composites: Taguchi Method*. Advances in Materials Science. 20(2), p. 54-70.
- [2] Yuan, Y., K. Zhao, Y. Zhao, S. Sahmani, & B. Safaei (2020). *Couple stress-based nonlinear buckling analysis of hydrostatic pressurized functionally graded composite conical microshells*. Mechanics of Materials. 148, p. 103507.
- [3] Yuan, Y., K. Zhao, Y. Han, S. Sahmani, & B. Safaei (2020). *Nonlinear oscillations of composite conical microshells with in-plane heterogeneity based upon a couple stress-based shell model*. Thin-Walled Structures. 154, p. 106857.
- [4] Mitra, B. (2014). *Environment friendly composite materials: biocomposites and green composites*. Defence Science Journal. 64(3), p. 244.
- [5] Safaei, B. (2020). *The effect of embedding a porous core on the free vibration behavior of laminated composite plates*. Steel and Composite Structures. 35(5), p. 659-670.
- [6] Rajkumar, D.R., K. Santhy, & K.P. Padmanaban (2020). *Influence of Mechanical Properties on Modal Analysis of Natural Fiber Reinforced Laminated Composite Trapezoidal Plates*. Journal of Natural Fibers, p. 1-17.

- [7] Navaneethakrishnan, G., T. Karthikeyan, S. Saravanan, V. Selvam, N. Parkunam, G. Sathishkumar, & S. Jayakrishnan (2020). *Structural analysis of natural fiber reinforced polymer matrix composite*. Materials Today: Proceedings. 21, p. 7-9.
- [8] Javanbakht, Z., W. Hall, A.S. Virk, J. Summerscales, & A. Öchsner (2020). *Finite element analysis of natural fiber composites using a self-updating model*. Journal of Composite Materials. 54(23), p. 3275-3286.
- [9] Fan, F., B. Lei, S. Sahmani, & B. Safaei (2020). *On the surface elastic-based shear buckling characteristics of functionally graded composite skew nanoplates*. Thin-Walled Structures. 154, p. 106841.
- [10] Huzaifah, M., S. Sapuan, Z. Leman, M. Ishak, & M. Maleque (2017). *A review of sugar palm (Arenga pinnata): application, fibre characterisation and composites*. Multidiscipline Modeling in Materials and Structures. 13, p. 678-698.
- [11] Behdinin, K., R. Moradi-Dastjerdi, B. Safaei, Z. Qin, F. Chu, & D. Hui (2020). *Graphene and CNT impact on heat transfer response of nanocomposite cylinders*. Nanotechnology Reviews. 9(1), p. 41-52.
- [12] Mazzanti, V., R. Pariente, A. Bonanno, O. Ruiz de Ballesteros, F. Mollica, & G. Filippone (2019). *Reinforcing mechanisms of natural fibers in green composites: Role of fibers morphology in a PLA/hemp model system*. Composites Science and Technology. 180, p. 51-59.

- [13] Sanjay, M.R., P. Madhu, M. Jawaid, P. SenthamaraiKannan, S. Senthil, & S. Pradeep (2018). *Characterization and properties of natural fiber polymer composites: A comprehensive review*. Journal of Cleaner Production. 172, p. 566-581.
- [14] Davoodi, M., S. Sapuan, D. Ahmad, A. Aidy, A. Khalina, & M. Jonoobi (2012). *Effect of polybutylene terephthalate (PBT) on impact property improvement of hybrid kenaf/glass epoxy composite*. Materials Letters. 67(1), p. 5-7.
- [15] Alhijazi, M., Q. Zeeshan, B. Safaei, M. Asmael, & Z. Qin (2020). *Recent Developments in Palm Fibers Composites: A Review*. Journal of Polymers and the Environment.
- [16] Ishak, M., Z. Leman, S. Sapuan, M. Rahman, & U. Anwar (2013). *Chemical composition and FT-IR spectra of sugar palm (Arenga pinnata) fibers obtained from different heights*. Journal of Natural Fibers. 10(2), p. 83-97.
- [17] Moghaddam, M.K. & S.M. Mortazavi (2016). *Physical and chemical properties of natural fibers extracted from typha australis leaves*. Journal of Natural Fibers. 13(3), p. 353-361.
- [18] Saravanakumar, S., A. Kumaravel, T. Nagarajan, & I.G. Moorthy (2014). *Investigation of physico-chemical properties of alkali-treated Prosopis juliflora fibers*. International Journal of Polymer Analysis and Characterization. 19(4), p. 309-317.

- [19] Vignesh, V., A. Balaji, & M. Karthikeyan (2016). *Extraction and characterization of new cellulosic fibers from Indian mallow stem: An exploratory investigation*. International Journal of Polymer Analysis and Characterization. 21(6), p. 504-512.
- [20] Safri, S.N.A., M.T.H. Sultan, M. Jawaid, & K. Jayakrishna (2018). *Impact behaviour of hybrid composites for structural applications: A review*. Composites Part B: Engineering. 133, p. 112-121.
- [21] Safaei, B., A. Fattahi, & F. Chu (2018). *Finite element study on elastic transition in platelet reinforced composites*. Microsystem Technologies. 24(6), p. 2663-2671.
- [22] Lau, K.-t., P.-y. Hung, M.-H. Zhu, & D. Hui (2018). *Properties of natural fibre composites for structural engineering applications*. Composites Part B: Engineering. 136, p. 222-233.
- [23] Elanchezhian, C., B.V. Ramnath, G. Ramakrishnan, M. Rajendrakumar, V. Naveenkumar, & M.K. Saravanakumar (2018). *Review on mechanical properties of natural fiber composites*. Materials Today: Proceedings. 5(1), p. 1785-1790.
- [24] Dhanola, A., A.S. Bisht, A. Kumar, & A. Kumar (2018). *Influence of natural fillers on physico-mechanical properties of luffa cylindrica/ polyester composites*. Materials Today: Proceedings. 5(9), p. 17021-17029.
- [25] Bisen, H.B., C.K. Hirwani, R.K. Satankar, S.K. Panda, K. Mehar, & B. Patel (2018). *Numerical Study of Frequency and Deflection Responses of Natural Fiber*

- (*Luffa*) Reinforced Polymer Composite and Experimental Validation. Journal of Natural Fibers. 17(4), p. 505-519.
- [26] Kiruthika, A.V. (2017). *A review on physico-mechanical properties of bast fibre reinforced polymer composites*. Journal of Building Engineering. 9, p. 91-99.
- [27] Chen, Y., N. Su, K. Zhang, S. Zhu, L. Zhao, F. Fang, L. Ren, & Y. Guo (2017). *In-Depth Analysis of the Structure and Properties of Two Varieties of Natural Luffa Sponge Fibers*. Materials (Basel). 10(5), p. 479.
- [28] Chandramohan, D.& A.J. Presin Kumar (2017). *Experimental data on the properties of natural fiber particle reinforced polymer composite material*. Data Brief. 13, p. 460-468.
- [29] Jauhari, N., R. Mishra, & H. Thakur (2015). *Natural fibre reinforced composite laminates—a review*. Materials Today: Proceedings. 2(4-5), p. 2868-2877.
- [30] Yan, L., N. Chouw, & K. Jayaraman (2014). *Flax fibre and its composites – A review*. Composites Part B: Engineering. 56, p. 296-317.
- [31] Węclawski, B.T., M. Fan, & D. Hui (2014). *Compressive behaviour of natural fibre composite*. Composites Part B: Engineering. 67, p. 183-191.
- [32] Sathishkumar, T.P., P. Navaneethakrishnan, S. Shankar, R. Rajasekar, & N. Rajini (2013). *Characterization of natural fiber and composites – A review*. Journal of Reinforced Plastics and Composites. 32(19), p. 1457-1476.

- [33] Nguong, C., S. Lee, & D. Sujan (2013). *A review on natural fibre reinforced polymer composites*. Proceedings of world academy of science, engineering and technology. 7(1), p. 52-59.
- [34] Koronis, G., A. Silva, & M. Fontul (2013). *Green composites: A review of adequate materials for automotive applications*. Composites Part B: Engineering. 44(1), p. 120-127.
- [35] Rohan, T., B. Tushar, & G. Mahesha. *Review of natural fiber composites*. in *IOP Conference Series: Materials Science and Engineering*. 2018. IOP Publishing.
- [36] Lucintel (2015). *Growth Opportunities in the Global Natural Fiber Composites Market*.
- [37] Kozłowski, R. & M. Władyka-Przybylak, *Uses of natural fiber reinforced plastics*, in *Natural fibers, plastics and composites*. 2004, Springer. p. 249-274.
- [38] Lee, B.-H., H.-J. Kim, & W.-R. Yu (2009). *Fabrication of long and discontinuous natural fiber reinforced polypropylene biocomposites and their mechanical properties*. Fibers and Polymers. 10(1), p. 83-90.
- [39] Cao, Y. & Y.-q. Wu (2008). *Evaluation of statistical strength of bamboo fiber and mechanical properties of fiber reinforced green composites*. Journal of Central South University of Technology. 15(1), p. 564-567.

- [40] Li, X., L.G. Tabil, & S. Panigrahi (2007). *Chemical treatments of natural fiber for use in natural fiber-reinforced composites: a review*. Journal of Polymers and the Environment. 15(1), p. 25-33.
- [41] Mohanty, A., M.A. Khan, S. Sahoo, & G. Hinrichsen (2000). *Effect of chemical modification on the performance of biodegradable jute yarn-Biopol® composites*. Journal of Materials Science. 35(10), p. 2589-2595.
- [42] Mehta, G., A.K. Mohanty, K. Thayer, M. Misra, & L.T. Drzal (2005). *Novel biocomposites sheet molding compounds for low cost housing panel applications*. Journal of Polymers and the Environment. 13(2), p. 169-175.
- [43] Ho, M.-p., H. Wang, J.-H. Lee, C.-k. Ho, K.-t. Lau, J. Leng, & D. Hui (2012). *Critical factors on manufacturing processes of natural fibre composites*. Composites Part B: Engineering. 43(8), p. 3549-3562.
- [44] Jeyapragash, R., V. Srinivasan, & S. Sathiyamurthy (2020). *Mechanical properties of natural fiber/particulate reinforced epoxy composites – A review of the literature*. Materials Today: Proceedings. 22, p. 1223-1227.
- [45] Alshammari, B.A., M.D. Alotaibi, O.Y. Alothman, M.R. Sanjay, L.K. Kian, Z. Almutairi, & M. Jawaaid (2019). *A New Study on Characterization and Properties of Natural Fibers Obtained from Olive Tree (Olea europaea L.) Residues*. Journal of Polymers and the Environment. 27(11), p. 2334-2340.

- [46] Raju, A.& M. Shanmugaraja (2020). *Recent researches in fiber reinforced composite materials: A review*. Materials Today: Proceedings.
- [47] Karthi, N., K. Kumaresan, S. Sathish, S. Gokulkumar, L. Prabhu, & N. Vigneshkumar (2020). *An overview: Natural fiber reinforced hybrid composites, chemical treatments and application areas*. Materials Today: Proceedings.
- [48] Moge, J., B. Seibert, & W. Smits (1991). *Multipurpose palms: the sugar palm (Arenga pinnata (Wurmb) Merr.)*. Agroforestry systems. 13(2), p. 111-129.
- [49] Orwa, C., A. Mutua, R. Kindt, R. Jamnadass, & A. Simons, *Agroforestry Database: a tree reference and selection guide. Version 4*. 2009: ICRAF Science Domain 3 (tree domestication, diversity and delivery).
- [50] Huzaifah, M.R.M., S.M. Sapuan, Z. Leman, M.R. Ishak, & M.A. Maleque (2017). *A review of sugar palm (Arenga pinnata): application, fibre characterisation and composites*. Multidiscipline Modeling in Materials and Structures. 13(4), p. 678-698.
- [51] Bachtiar, D., S.M. Sapuan, & M.M. Hamdan (2009). *The Influence of Alkaline Surface Fibre Treatment on the Impact Properties of Sugar Palm Fibre-Reinforced Epoxy Composites*. Polymer-Plastics Technology and Engineering. 48(4), p. 379-383.

- [52] Dakheel, A. (2003). *Date palm and biosaline agriculture in the United Arab Emirates*. The date palm from traditional resource to green wealth. Emirates Centre for Strategic Studies and Research, Abu Dhabi, p. 199-211.
- [53] Al-Oqla, F.M., O.Y. Alothman, M. Jawaaid, S.M. Sapuan, & M.H. Es-Saheb, *Processing and Properties of Date Palm Fibers and Its Composites*, in *Biomass and Bioenergy*. 2014, Springer. p. 1-25.
- [54] Alshammari, B.A., N. Saba, M.D. Alotaibi, M.F. Alotibi, M. Jawaaid, & O.Y. Alothman (2019). *Evaluation of Mechanical, Physical, and Morphological Properties of Epoxy Composites Reinforced with Different Date Palm Fillers*. *Materials* (Basel). 12(13), p. 2145.
- [55] Bonner, F.T.& R.P. Karrfalt (2008). *The woody plant seed manual*. Agric. Handbook No. 727. Washington, DC. US Department of Agriculture, Forest Service. 1223 p. 727.
- [56] Graefe, S., D. Dufour, M. van Zonneveld, F. Rodriguez, & A. Gonzalez (2012). *Peach palm (Bactris gasipaes) in tropical Latin America: implications for biodiversity conservation, natural resource management and human nutrition*. *Biodiversity and Conservation*. 22(2), p. 269-300.
- [57] Sahari, J., S. Sapuan, E. Zainudin, & M. Maleque (2012). *A new approach to use Arenga pinnata as sustainable biopolymer: Effects of plasticizers on physical properties*. *Procedia Chemistry*. 4, p. 254-259.

- [58] Khalil, H.S.A., M.S. Alwani, & A.K.M. Omar (2007). *Chemical composition, anatomy, lignin distribution, and cell wall structure of Malaysian plant waste fibers*. BioResources. 1(2), p. 220-232.
- [59] Ahmad, Z., H.M. Saman, & P. Tahir (2010). *Oil Palm Trunk Fiber as a Bio-Waste Resource for Concrete Reinforcement*. International Journal of Mechanical and Materials Engineering. 5(2), p. 199-207.
- [60] Mohanty, A., M.a. Misra, & G. Hinrichsen (2000). *Biofibres, biodegradable polymers and biocomposites: An overview*. Macromolecular Materials and Engineering. 276(1), p. 1-24.
- [61] Jino, R., R. Pugazhenth, K.G. Ashok, T. Ilango, & P.R.K. Chakravarthy (2017). *Enhancement of Mechanical Properties of Luffa Fiber/Epoxy Composite Using B4C*. Journal of Advanced Microscopy Research. 12(2), p. 89-91.
- [62] Ekici, B., A. Kentli, & H. Küçük (2012). *Improving Sound Absorption Property of Polyurethane Foams by Adding Tea-Leaf Fibers*. Archives of Acoustics. 37(4), p. 515-520.
- [63] Shen, J., Y. Min Xie, X. Huang, S. Zhou, & D. Ruan (2012). *Mechanical properties of luffa sponge*. J Mech Behav Biomed Mater. 15, p. 141-52.
- [64] Chen, Q., Q. Shi, S.N. Gorb, & Z. Li (2014). *A multiscale study on the structural and mechanical properties of the luffa sponge from Luffa cylindrica plant*. J Biomech. 47(6), p. 1332-9.

- [65] Sinnott, E.W.& R. Bloch (1943). *Development of the fibrous net in the fruit of various races of Luffa cylindrica*. Botanical Gazette. 105(1), p. 90-99.
- [66] Sabarinathan, P., K. Rajkumar, & A. Gnanavelbabu (2016). *Investigation of mechanical properties of Luffa cylindrical and flax reinforced hybrid polymer composite*. J Adv Eng Res. 3(2), p. 124-127.
- [67] Saw, S.K., R. Purwar, S. Nandy, J. Ghose, & G. Sarkhel (2013). *Fabrication, characterization, and evaluation of luffa cylindrica fiber reinforced epoxy composites*. BioResources. 8(4), p. 4805-4826.
- [68] Mohanta, N.& S.K. Acharya (2016). *Fiber surface treatment: Its effect on structural, thermal, and mechanical properties of Luffa cylindrica fiber and its composite*. Journal of Composite Materials. 50(22), p. 3117-3131.
- [69] Porterfield, W. (1955). *Loofah—the sponge gourd*. Economic Botany. 9(3), p. 211-223.
- [70] Mohammed, L., M.N. Ansari, G. Pua, M. Jawaid, & M.S. Islam (2015). *A review on natural fiber reinforced polymer composite and its applications*. International Journal of Polymer Science. 2015.
- [71] Bongarde, U.& V. Shinde (2014). *Review on natural fiber reinforcement polymer composites*. International Journal of Engineering Science and Innovative Technology. 3(2), p. 431-436.

- [72] Sen, T.& H.J. Reddy (2011). *Various industrial applications of hemp, kinaf, flax and ramie natural fibres*. International Journal of Innovation, Management and Technology. 2(3), p. 192.
- [73] Ticoalu, A., T. Aravinthan, & F. Cardona. *A review of current development in natural fiber composites for structural and infrastructure applications*. in *Proceedings of the southern region engineering conference (SREC 2010)*. 2010. Engineers Australia.
- [74] Mwaikambo, L. (2006). *Review of the history, properties and application of plant fibres*. African Journal of Science and Technology. 7(2), p. 121.
- [75] Suddell, B. *Industrial fibres: recent and current developments*. in *Proceedings of the symposium on natural fibres*. 2008. FAO and CFC Rome.
- [76] Mohanty, A. (2005). *Mohanty AK, Misra M and Drzal LT, editors. Natural Fibers*. Biopolymers and Biocomposites.
- [77] Bos, H.L., *The potential of flax fibres as reinforcement for composite materials*. 2004: Technische Universiteit Eindhoven Eindhoven.
- [78] Pickering, K., *Properties and performance of natural-fibre composites*. 2008: Elsevier.
- [79] Midani, M., *Date Palm fibre composites: A novel and sustainable material for the aerospace industry*. Vol. 54. 2017. 45-47.

- [80] Shinoj, S., R. Visvanathan, S. Panigrahi, & M. Kochubabu (2011). *Oil palm fiber (OPF) and its composites: A review*. Industrial Crops and Products. 33(1), p. 7-22.
- [81] Khalid, M., C.T. Ratnam, T.G. Chuah, S. Ali, & T.S.Y. Choong (2008). *Comparative study of polypropylene composites reinforced with oil palm empty fruit bunch fiber and oil palm derived cellulose*. Materials & Design. 29(1), p. 173-178.
- [82] Mylsamy, K.& I. Rajendran (2011). *Influence of fibre length on the wear behaviour of chopped agave americana fibre reinforced epoxy composites*. Tribology Letters. 44(1), p. 75.
- [83] Yousif, B.& N. El-Tayeb (2008). *Adhesive wear performance of T-OPRP and UT-OPRP composites*. Tribology Letters. 32(3), p. 199-208.
- [84] Hashmi, S., U. Dwivedi, & N. Chand (2006). *Friction and sliding wear of UHMWPE modified cotton fibre reinforced polyester composites*. Tribology Letters. 21(2), p. 79-87.
- [85] Misri, S., Z. Leman, S.M. Sapuan, & M.R. Ishak (2010). *Mechanical properties and fabrication of small boat using woven glass/sugar palm fibres reinforced unsaturated polyester hybrid composite*. IOP Conference Series: Materials Science and Engineering. 11, p. 012015.
- [86] Benmansour, N., B. Agoudjil, A. Gherabli, A. Kareche, & A. Boudenne (2014). *Thermal and mechanical performance of natural mortar reinforced with date palm*

- fibers for use as insulating materials in building*. Energy and Buildings. 81, p. 98-104.
- [87] Tahri, I., I. Ziegler-Devin, J. Ruelle, C. Segovia, & N. Brosse (2016). *Extraction and Characterization of Fibers from Palm Tree*. BioResources. 11(3), p. 7016-7025.
- [88] Alawar, A., A.M. Hamed, & K. Al-Kaabi (2009). *Characterization of treated date palm tree fiber as composite reinforcement*. Composites Part B: Engineering. 40(7), p. 601-606.
- [89] Ilyas, R.A., S.M. Sapuan, M.R. Ishak, & E.S. Zainudin (2018). *Development and characterization of sugar palm nanocrystalline cellulose reinforced sugar palm starch bionanocomposites*. Carbohydrate Polymers. 202, p. 186-202.
- [90] Agrebi, F., N. Ghorbel, B. Rashid, A. Kallel, & M. Jawaid (2018). *Influence of treatments on the dielectric properties of sugar palm fiber reinforced phenolic composites*. Journal of Molecular Liquids. 263, p. 342-348.
- [91] Leman, Z., S.M. Sapuan, M. Azwan, M.M.H.M. Ahmad, & M.A. Maleque (2008). *The Effect of Environmental Treatments on Fiber Surface Properties and Tensile Strength of Sugar Palm Fiber-Reinforced Epoxy Composites*. Polymer-Plastics Technology and Engineering. 47(6), p. 606-612.

- [92] Mohammed, A.A., D. Bachtiar, M.R.M. Rejab, & J.P. Siregar (2018). *Effect of microwave treatment on tensile properties of sugar palm fibre reinforced thermoplastic polyurethane composites*. Defence Technology. 14(4), p. 287-290.
- [93] Yousif, B.F.& N.S.M. El-Tayeb (2008). *High-stress three-body abrasive wear of treated and untreated oil palm fibre-reinforced polyester composites*. Proceedings of the Institution of Mechanical Engineers, Part J: Journal of Engineering Tribology. 222(5), p. 637-646.
- [94] Chaiwong, W., N. Samoh, T. Eksomtramage, & K. Kaewtatip (2019). *Surface-treated oil palm empty fruit bunch fiber improved tensile strength and water resistance of wheat gluten-based bioplastic*. Composites Part B: Engineering. 176, p. 107331.
- [95] Hermawan, D., C.M. Hazwan, F.A.T. Owolabi, D.A. Gopakumar, M. Hasan, S. Rizal, N.A. Sri Aprilla, A.R. Mohamed, & H.P.S.A. Khalil (2019). *Oil palm microfiber-reinforced handsheet-molded thermoplastic green composites for sustainable packaging applications*. Progress in Rubber, Plastics and Recycling Technology. 35(4), p. 173-187.
- [96] Jawaaid, M., H.P.S.A. Khalil, A.A. Bakar, & P.N. Khanam (2011). *Chemical resistance, void content and tensile properties of oil palm/jute fibre reinforced polymer hybrid composites*. Materials & Design. 32(2), p. 1014-1019.

- [97] Suradi, S.S., R.M. Yunus, & M.D.H. Beg (2010). *Oil palm bio-fiber-reinforced polypropylene composites: effects of alkali fiber treatment and coupling agents*. Journal of Composite Materials. 45(18), p. 1853-1861.
- [98] Norul Izani, M.A., M.T. Paridah, U.M.K. Anwar, M.Y. Mohd Nor, & P.S. H'ng (2013). *Effects of fiber treatment on morphology, tensile and thermogravimetric analysis of oil palm empty fruit bunches fibers*. Composites Part B: Engineering. 45(1), p. 1251-1257.
- [99] Karina, M., H. Onggo, A.H.D. Abdullah, & A. Syampurwadi (2008). *Effect of Oil Palm Empty Fruit Bunch Fiber on the Physical and Mechanical Properties of Fiber Glass Reinforced Polyester Resin*. Journal of Biological Sciences. 8(1), p. 101-106.
- [100] Anggawan, A.D.& N. Mohamad, *Effect of different fibre treatment of oil palm fibre reinforced polyester composite*, in *13th International Engineering Research Conference*. 2020.
- [101] Raut, A.N.& C.P. Gomez (2020). *Utilization of Glass Powder and Oil Palm Fibers to Develop Thermally Efficient Blocks*. Arabian Journal for Science and Engineering. 45(5), p. 3959-3972.
- [102] Ishak, M.R., S.M. Sapuan, Z. Leman, M.Z. Rahman, U.M. Anwar, & J.P. Siregar (2013). *Sugar palm (Arenga pinnata): Its fibres, polymers and composites*. Carbohydrate Polymers. 91(2), p. 699-710.

- [103] Nurazzi, N., K. Khalina, & S. Sapuan (2019). *Mechanical properties of sugar palm yarn/woven glass fiber reinforced unsaturated polyester composites: effect of fiber loadings and alkaline treatment*. Polimery. 64(10), p. 665-675.
- [104] Radzi, A.M., S.M. Sapuan, M. Jawaid, & M.R. Mansor (2019). *Effect of Alkaline Treatment on Mechanical, Physical and Thermal Properties of Roselle/Sugar Palm Fiber Reinforced Thermoplastic Polyurethane Hybrid Composites*. Fibers and Polymers. 20(4), p. 847-855.
- [105] Bachtiar, D., S.M. Sapuan, & M.M. Hamdan (2008). *The effect of alkaline treatment on tensile properties of sugar palm fibre reinforced epoxy composites*. Materials & Design. 29(7), p. 1285-1290.
- [106] Bachtiar, D., S. Sapuan, & M. Hamdan (2010). *Flexural properties of alkaline treated sugar palm fibre reinforced epoxy composites*. International Journal of Automotive and Mechanical Engineering. 1(1), p. 79-90.
- [107] Nurazzi, N.M., A. Khalina, S.M. Sapuan, R.A. Ilyas, S.A. Rafiqah, & Z.M. Hanafiee (2020). *Thermal properties of treated sugar palm yarn/glass fiber reinforced unsaturated polyester hybrid composites*. Journal of Materials Research and Technology. 9(2), p. 1606-1618.
- [108] Mukhtar, I.i., Z. Leman, E.S. Zainudin, & M.R. Ishak (2020). *Effectiveness of Alkali and Sodium Bicarbonate Treatments on Sugar Palm Fiber: Mechanical, Thermal, and Chemical Investigations*. Journal of Natural Fibers. 17(6), p. 877-889.

- [109] Devaraju, A.& P. Murali (2020). *Experimental investigation of mechanical and tribological properties of palm fiber composite with Al₂O₃ ceramic particles*. Materials Today: Proceedings. 22, p. 1161-1166.
- [110] Sadik, T., N. Sivaram, & P. Senthil (2017). *Evaluation of mechanical properties of date palm fronds polymer composites*. Int. J. ChemTech Res. 10, p. 558-564.
- [111] Mulinari, D.R., A.J. Marina, & G.S. Lopes (2015). *Mechanical Properties of the Palm Fibers Reinforced HDPE Composites*. World Academy of Science, Engineering and Technology, International Journal of Chemical, Molecular, Nuclear, Materials and Metallurgical Engineering. 9(7), p. 903-906.
- [112] Ibrahim, H., M. Farag, H. Megahed, & S. Mehanny (2014). *Characteristics of starch-based biodegradable composites reinforced with date palm and flax fibers*. Carbohydrate Polymers. 101, p. 11-9.
- [113] Mahdavi, S., H. Kermanian, & A. Varshoei (2010). *Comparison of mechanical properties of date palm fiber-polyethylene composite*. BioResources. 5(4), p. 2391-2403.
- [114] Saravanan, P.& A. Devaraju (2018). *Improving mechanical properties of palm sheath composites using sodium hydroxide [naoh] treatment*. Materials Today: Proceedings. 5(6), p. 14355-14361.

- [115] Shalwan, A.& B.F. Yousif (2014). *Influence of date palm fibre and graphite filler on mechanical and wear characteristics of epoxy composites*. Materials & Design. 59, p. 264-273.
- [116] Dehghani, A., S. Madadi Ardekani, M.A. Al-Maadeed, A. Hassan, & M.U. Wahit (2013). *Mechanical and thermal properties of date palm leaf fiber reinforced recycled poly (ethylene terephthalate) composites*. Materials & Design (1980-2015). 52, p. 841-848.
- [117] Alsaeed, T., B.F. Yousif, & H. Ku (2013). *The potential of using date palm fibres as reinforcement for polymeric composites*. Materials & Design. 43, p. 177-184.
- [118] Abdal-hay, A., N.P.G. Suardana, D.Y. Jung, K.-S. Choi, & J.K. Lim (2012). *Effect of diameters and alkali treatment on the tensile properties of date palm fiber reinforced epoxy composites*. International Journal of Precision Engineering and Manufacturing. 13(7), p. 1199-1206.
- [119] Elseify, L.A., M. Midani, A.H. Hassanin, T. Hamouda, & R. Khiari (2020). *Long textile fibres from the midrib of date palm: Physiochemical, morphological, and mechanical properties*. Industrial Crops and Products. 151, p. 112466.
- [120] Delzendehrooy, F., M.R. Ayatollahi, A. Akhavan-Safar, & L.F.M. da Silva (2020). *Strength improvement of adhesively bonded single lap joints with date palm fibers: Effect of type, size, treatment method and density of fibers*. Composites Part B: Engineering. 188, p. 107874.

- [121] Khakpour, H., M.R. Ayatollahi, A. Akhavan-Safar, & L.F.M. da Silva (2020). *Mechanical properties of structural adhesives enhanced with natural date palm tree fibers: Effects of length, density and fiber type*. Composite Structures. 237, p. 111950.
- [122] Chaari, R., M. Khlif, H. Mallek, C. Bradai, C. Lacoste, H. Belguith, H. Tounsi, & P. Dony (2020). *Enzymatic treatments effect on the poly (butylene succinate)/date palm fibers properties for bio-composite applications*. Industrial Crops and Products. 148, p. 112270.
- [123] Santos, A.S., M.Z. Farina, P.T. Pezzin, & D.A.K. Silva (2008). *The Application of Peach Palm Fibers as an Alternative to Fiber Reinforced Polyester Composites*. Journal of Reinforced Plastics and Composites. 27(16-17), p. 1805-1816.
- [124] Bendahou, A., H. Kaddami, H. Sautereau, M. Raihane, F. Erchiqui, & A. Dufresne (2008). *Short Palm Tree Fibers Polyolefin Composites: Effect of Filler Content and Coupling Agent on Physical Properties*. Macromolecular Materials and Engineering. 293(2), p. 140-148.
- [125] Senthilraja, R., R. Sarala, A.G. Antony, & Seshadhri (2020). *Effect of acetylation technique on mechanical behavior and durability of palm fibre vinyl-ester composites*. Materials Today: Proceedings. 21, p. 634-637.
- [126] Jawaid, M., H.P.S. Abdul Khalil, A. Hassan, R. Dungani, & A. Hadiyane (2013). *Effect of jute fibre loading on tensile and dynamic mechanical properties of oil palm epoxy composites*. Composites Part B: Engineering. 45(1), p. 619-624.

- [127] Jawaid, M., H.P.S. Abdul Khalil, & A. Abu Bakar (2010). *Mechanical performance of oil palm empty fruit bunches/jute fibres reinforced epoxy hybrid composites*. Materials Science and Engineering: A. 527(29-30), p. 7944-7949.
- [128] Leman, Z., S.M. Sapuan, A.M. Saifol, M.A. Maleque, & M.M.H.M. Ahmad (2008). *Moisture absorption behavior of sugar palm fiber reinforced epoxy composites*. Materials & Design. 29(8), p. 1666-1670.
- [129] Atiqah, A., M. Jawaid, S.M. Sapuan, & M.R. Ishak (2018). *Dynamic mechanical properties of sugar palm/glass fiber reinforced thermoplastic polyurethane hybrid composites*. Polymer Composites. 40(4), p. 1329-1334.
- [130] Wu, C.-S., H.-T. Liao, & Y.-X. Cai (2017). *Characterisation, biodegradability and application of palm fibre-reinforced polyhydroxyalkanoate composites*. Polymer Degradation and Stability. 140, p. 55-63.
- [131] Huzaifah, M., S. Sapuan, Z. Leman, & M. Ishak (2019). *Comparative study of physical, mechanical, and thermal properties on sugar palm fiber (Arenga pinnata (Wurmb) Merr.) reinforced Vinyl Ester composites obtained from different geographical locations*. BioResources. 14(1), p. 619-637.
- [132] Al-Kaabi, K., A. Al-Khanbashi, & A. Hammami, *Natural Fiber Reinforced Composites From Date Palm Fibers*, in *11th European conference on composite materials*. Greece: Rhodes. 2004.

- [133] Kakou, C.A., F.Z. Arrakhiz, A. Trokourey, R. Bouhfid, A. Qaiss, & D. Rodrigue (2014). *Influence of coupling agent content on the properties of high density polyethylene composites reinforced with oil palm fibers*. Materials & Design. 63, p. 641-649.
- [134] Lah, N.C.& N.M. Ismail (2019). *Empty Fruit Bunch (EFB) Fibers as Reinforcement in Polypropylene*. Journal of Modern Manufacturing Systems and Technology. 2, p. 84-92.
- [135] Munawar, N.S.Z.M.N., M.R. Ishak, R.M. Shahroze, M. Jawaidd, & M.Y.M. Zuhri (2019). *An Investigation of the Morphological and Tensile Properties of Vacuum Resin Impregnated Sugar Palm Fibers with Various Thermosetting Resins*. BioResources. 14(3), p. 5212-5223.
- [136] Nurazzi, N.M., A. Khalina, M. Chandrasekar, H.A. Aisyah, S.A. Rafiqah, R.A. Ilyas, & Z.M. Hanafiee (2020). *Effect of fiber orientation and fiber loading on the mechanical and thermal properties of sugar palm yarn fiber reinforced unsaturated polyester resin composites*. Polimery. 65(02), p. 115-124.
- [137] de Farias, M.A., M.Z. Farina, A.P.T. Pezzin, & D.A.K. Silva (2009). *Unsaturated polyester composites reinforced with fiber and powder of peach palm: Mechanical characterization and water absorption profile*. Materials Science and Engineering: C. 29(2), p. 510-513.
- [138] Jawaidd, M., H.P.S. Abdul Khalil, P. Noorunnisa Khanam, & A. Abu Bakar (2011). *Hybrid Composites Made from Oil Palm Empty Fruit Bunches/Jute Fibres*:

Water Absorption, Thickness Swelling and Density Behaviours. Journal of Polymers and the Environment. 19(1), p. 106-109.

[139] Hanan, F., M. Jawaid, & P. Md Tahir (2020). *Mechanical performance of oil palm/kenaf fiber-reinforced epoxy-based bilayer hybrid composites*. Journal of Natural Fibers. 17(2), p. 155-167.

[140] Gheith, M.H., M.A. Aziz, W. Ghori, N. Saba, M. Asim, M. Jawaid, & O.Y. Alothman (2019). *Flexural, thermal and dynamic mechanical properties of date palm fibres reinforced epoxy composites*. Journal of Materials Research and Technology. 8(1), p. 853-860.

[141] Saba, N., O.Y. Alothman, Z. Almutairi, M. Jawaid, & W. Ghori (2019). *Date palm reinforced epoxy composites: tensile, impact and morphological properties*. Journal of Materials Research and Technology. 8(5), p. 3959-3969.

[142] Mahdi, E., D. Ochoa, A. Vaziri, & E. Eltai (2019). *Energy absorption capability of date palm leaf fiber reinforced epoxy composites rectangular tubes*. Composite Structures. 224, p. 111004.

[143] Masri, T., H. Ounis, L. Sedira, A. Kaci, & A. Benchabane (2018). *Characterization of new composite material based on date palm leaflets and expanded polystyrene wastes*. Construction and Building Materials. 164, p. 410-418.

- [144] AlMaadeed, M.A., R. Kahraman, P. Noorunnisa Khanam, & N. Madi (2012). *Date palm wood flour/glass fibre reinforced hybrid composites of recycled polypropylene: Mechanical and thermal properties*. Materials & Design. 42, p. 289-294.
- [145] Sh Al-Otaibi, M., O.Y. Alothman, M.M. Alrashed, A. Anis, J. Naveen, & M. Jawaaid (2020). *Characterization of Date Palm Fiber-Reinforced Different Polypropylene Matrices*. Polymers (Basel). 12(3), p. 597.
- [146] Rihayat, T., S. Salim, N. Audina, N.S.P. Khan, Zaimahwati, M. Sami, M. Yunus, Z. Salisah, P.N. Alam, Saifuddin, & I. Yusuf (2018). *Composite material making from empty fruit bunches of palm oil (EFB) and Ijuk (Arengapinnata) using plastic bottle waste as adhesives*. IOP Conference Series: Materials Science and Engineering. 334, p. 012083.
- [147] Momoh, E.O. & A.I. Osofero (2019). *Behaviour of oil palm broom fibres (OPBF) reinforced concrete*. Construction and Building Materials. 221, p. 745-761.
- [148] Chennouf, N., B. Agoudjil, T. Alioua, A. Boudenne, & K. Benzarti (2019). *Experimental investigation on hygrothermal performance of a bio-based wall made of cement mortar filled with date palm fibers*. Energy and Buildings. 202, p. 109413.
- [149] Baali, B., Z.E.A. Rahmouni, & M. Rokbi (2019). *Flexural characterization of polymer concrete comprising waste marble and date palm fibers*. Technical Sciences. 2(22), p. 169-182.

- [150] Aljalawi, N.M.F. (2019). *Effect of sustainable palm fiber on high strength concrete properties*. IOP Conference Series: Materials Science and Engineering. 518, p. 022004.
- [151] Nordin, N.A., N.M.M. Abd Rahman, & A. Hassan (2019). *Thermal and mechanical properties of injection moulded heat-treated oil palm empty fruit bunch fibre-reinforced high-density polyethylene composites*. *Plastics, Rubber and Composites*. 48(9), p. 410-421.
- [152] Maou, S., A. Meghezzi, N. Nebbache, & Y. Meftah (2019). *Mechanical, morphological, and thermal properties of poly(vinyl chloride)/low-density polyethylene composites filled with date palm leaf fiber*. *Journal of Vinyl and Additive Technology*. 25(s2), p. E88-E93.
- [153] Asim, M., M. Jawaid, A. Khan, A.M. Asiri, & M.A. Malik (2020). *Effects of Date Palm fibres loading on mechanical, and thermal properties of Date Palm reinforced phenolic composites*. *Journal of Materials Research and Technology*. 9(3), p. 3614-3621.
- [154] Afzaluddin, A., M. Jawaid, M.S. Salit, & M.R. Ishak (2019). *Physical and mechanical properties of sugar palm/glass fiber reinforced thermoplastic polyurethane hybrid composites*. *Journal of Materials Research and Technology*. 8(1), p. 950-959.

- [155] Atiqah, A., M. Jawaid, S.M. Sapuan, M.R. Ishak, & O.Y. Alothman (2018). *Thermal properties of sugar palm/glass fiber reinforced thermoplastic polyurethane hybrid composites*. Composite Structures. 202, p. 954-958.
- [156] Ibrahim, M.I.J., S.M. Sapuan, E.S. Zainudin, & M.Y.M. Zuhri (2020). *Preparation and characterization of cornhusk/sugar palm fiber reinforced Cornstarch-based hybrid composites*. Journal of Materials Research and Technology. 9(1), p. 200-211.
- [157] Ali, M.E.& A. Alabdulkarem (2017). *On thermal characteristics and microstructure of a new insulation material extracted from date palm trees surface fibers*. Construction and Building Materials. 138, p. 276-284.
- [158] Sahari, J., S.M. Sapuan, E.S. Zainudin, & M.A. Maleque (2013). *Mechanical and thermal properties of environmentally friendly composites derived from sugar palm tree*. Materials & Design. 49, p. 285-289.
- [159] Alaaeddin, M.H., S.M. Sapuan, M.Y.M. Zuhri, E.S. Zainudin, & F.M. Al- Oqla (2019). *Physical and mechanical properties of polyvinylidene fluoride - Short sugar palm fiber nanocomposites*. Journal of Cleaner Production. 235, p. 473-482.
- [160] Taban, E., A. Khavanin, A.J. Jafari, M. Faridan, & A.K. Tabrizi (2019). *Experimental and mathematical survey of sound absorption performance of date palm fibers*. Heliyon. 5(6), p. e01977.

- [161] Taban, E., A. Khavanin, M. Faridan, S.E. Samaei, K. Samimi, & R. Rashidi (2019). *Comparison of acoustic absorption characteristics of coir and date palm fibers: experimental and analytical study of green composites*. International Journal of Environmental Science and Technology. 17(1), p. 39-48.
- [162] Kharrat, F., M. Khlif, L. Hilliou, M. Haboussi, J.A. Covas, H. Nouri, & C. Bradai (2020). *Minimally processed date palm (Phoenix dactylifera L.) leaves as natural fillers and processing aids in poly(lactic acid) composites designed for the extrusion film blowing of thin packages*. Industrial Crops and Products. 154, p. 112637.
- [163] Bellatrache, Y., L. Ziyani, A. Dony, M. Taki, & S. Haddadi (2020). *Effects of the addition of date palm fibers on the physical, rheological and thermal properties of bitumen*. Construction and Building Materials. 239, p. 117808.
- [164] Raghavendra, S.& G.N. Lokesh, *Evaluation of mechanical properties in date palm fronds polymer composites*, in *AIP Conference Proceedings*. 2019, AIP Publishing LLC. p. 020021.
- [165] Bezazi, A., S. Amroune, F. Scarpa, A. Dufresne, & A. Imad (2020). *Investigation of the date palm fiber for green composites reinforcement: Quasi-static and fatigue characterization of the fiber*. Industrial Crops and Products. 146, p. 112135.
- [166] Mohammad, M., N.I.R. Nik Syukri, & M.Z. Nuawi (2019). *Sound Properties Investigation of Date Palm Fiber*. Journal of Physics: Conference Series. 1150, p. 012003.

- [167] Ray, D., B.K. Sarkar, A. Rana, & N.R. Bose (2001). *Effect of alkali treated jute fibres on composite properties*. Bulletin of Materials Science. 24(2), p. 129-135.
- [168] Jino, R., M. Sriraman, B. Arthika, & K. Ashok (2018). *Studies on mechanical properties of luffa acutangula/lignite fly ash reinforced composites*. International Journal of Engineering & Technology. 7(2.21), p. 251-254.
- [169] Chen, Y., N. Su, K. Zhang, S. Zhu, Z. Zhu, W. Qin, Y. Yang, Y. Shi, S. Fan, Z. Wang, & Y. Guo (2018). *Effect of fiber surface treatment on structure, moisture absorption and mechanical properties of luffa sponge fiber bundles*. Industrial Crops and Products. 123, p. 341-352.
- [170] Thangaraju, R.& A. Aravindakumar (2016). *Experimental study on the characteristics of surface treated luffa fiber composites*. Journal of Chemical and Pharmaceutical Sciences. 9, p. 646-651.
- [171] Parida, C., S.K. Dash, & S.C. Das (2015). *Effect of Fiber Treatment and Fiber Loading on Mechanical Properties of Luffa-Resorcinol Composites*. Indian Journal of Materials Science. 2015, p. 1-6.
- [172] Parida, C., S.K. Dash, & P. Chatterjee (2015). *Mechanical properties of injection molded poly (lactic) Acid—Luffa fiber composites*. Soft Nanoscience Letters. 5(04), p. 65.

- [173] Anbukarasi, K.& S. Kalaiselvam (2015). *Study of effect of fibre volume and dimension on mechanical, thermal, and water absorption behaviour of luffa reinforced epoxy composites*. Materials & Design (1980-2015). 66, p. 321-330.
- [174] Tanobe, V., T. Flores-Sahagun, S. Amico, G. Muniz, & K. Satyanarayana (2014). *Sponge Gourd (Luffa Cylindrica) Reinforced Polyester Composites: Preparation and Properties*. Defence Science Journal. 64(3), p. 273-280.
- [175] Srinivasan, C., S. Sathish, & K. Vignesh (2014). *Mechanical properties of chemically treated Luffa Aegyptiaca fiber reinforced epoxy matrix composites*. Int. J. Sci. Res. Manage. 2, p. 1515-1524.
- [176] Panneerdhass, R., A. Gnanavelbabu, & K. Rajkumar (2014). *Mechanical Properties of Luffa Fiber and Ground nut Reinforced Epoxy Polymer Hybrid Composites*. Procedia Engineering. 97, p. 2042-2051.
- [177] Panneerdhass, R., R. Baskaran, K. Rajkumar, & A. Gnanavelbabu (2014). *Mechanical Properties of Chopped Randomly Oriented Epoxy - Luffa Fiber Reinforced Polymer Composite*. Applied Mechanics and Materials. 591, p. 103-107.
- [178] Botaro, V.R., K.M. Novack, & É.J. Siqueira (2012). *Dynamic mechanical behavior of vinylester matrix composites reinforced by Luffa cylindrica modified fibers*. Journal of Applied Polymer Science. 124(3), p. 1967-1975.

- [179] Ghali, L.H., M. Aloui, M. Zidi, H.B. Daly, S. Msahli, & F. Sakli (2011). *Effect of chemical modification of luffa cylindrica fibers on the mechanical and hygrothermal behaviours of polyester/luffa composites*. BioResources. 6(4), p. 3836-3849.
- [180] Ghali, L., S. Msahli, M. Zidi, & F. Sakli (2011). *Effects of Fiber Weight Ratio, Structure and Fiber Modification onto Flexural Properties of Luffa-Polyester Composites*. Advances in Materials Physics and Chemistry. 01(03), p. 78-85.
- [181] Ghali, L., S. Msahli, M. Zidi, & F. Sakli (2009). *Effect of pre-treatment of Luffa fibres on the structural properties*. Materials Letters. 63(1), p. 61-63.
- [182] Demir, H., U. Atikler, D. Balköse, & F. Tihminlioğlu (2006). *The effect of fiber surface treatments on the tensile and water sorption properties of polypropylene–luffa fiber composites*. Composites Part A: Applied Science and Manufacturing. 37(3), p. 447-456.
- [183] Tanobe, V.O.A., T.H.D. Sydenstricker, M. Munaro, & S.C. Amico (2005). *A comprehensive characterization of chemically treated Brazilian sponge-gourds (Luffa cylindrica)*. Polymer Testing. 24(4), p. 474-482.
- [184] Boynard, C., S. Monteiro, & J. d'Almeida (2003). *Aspects of alkali treatment of sponge gourd (Luffa cylindrica) fibers on the flexural properties of polyester matrix composites*. Journal of Applied Polymer Science. 87(12), p. 1927-1932.

- [185] Kalusuraman, G., I. Siva, Y. Munde, C.P. Selvan, S.A. Kumar, & S.C. Amico (2020). *Dynamic-mechanical properties as a function of luffa fibre content and adhesion in a polyester composite*. Polymer Testing. 87, p. 106538.
- [186] Dharmalingam, S., O. Meenakshisundaram, & V. Kugarajah (2020). *Effect of Degree of Silanization of Luffa on the properties of Luffa-Epoxy Composites*. Colloids and Surfaces A: Physicochemical and Engineering Aspects. 603, p. 125273.
- [187] Ashok, K., K. Kalaichelvan, & A. Damodaran (2020). *Effect of Nano Fillers on Mechanical Properties of Luffa Fiber Epoxy Composites*. Journal of Natural Fibers, p. 1-18.
- [188] Mohana Krishnudu, D., D. Sreeramulu, P.V. Reddy, & P. Rajendra Prasad (2020). *Influence of Filler on Mechanical and Di-electric Properties of Coir and Luffa Cylindrica Fiber Reinforced Epoxy Hybrid Composites*. Journal of Natural Fibers. 17, p. 1-10.
- [189] Chakrabarti, D., M.S. Islam, K. Jubair, & M.R.H. Sarker (2020). *Effect of Chemical Treatment on the Mechanical Properties of Luffa Fiber Reinforced Epoxy Composite*. Journal of Engineering Advancements. 1(1), p. 37-42.
- [190] Yang, X., X. Wang, Y. Zhao, L. Xu, T. Wang, & X. Zhang (2018). *Preparation of recyclable BiOI/luffa fiber composite and its highly efficient visible light photocatalytic properties*. Journal of Cleaner Production. 200, p. 945-953.

- [191] Shen, J., Y.M. Xie, X. Huang, S. Zhou, & D. Ruan (2013). *Behaviour of luffa sponge material under dynamic loading*. International Journal of Impact Engineering. 57, p. 17-26.
- [192] Parida, C., S.C. Das, & S.K. Dash (2012). *Mechanical Analysis of Bio Nanocomposite Prepared from Luffa cylindrica*. Procedia Chemistry. 4, p. 53-59.
- [193] Pires, C., L.A.d.C. Motta, R.A.d.R. Ferreira, C.d.O. Caixeta, & H. Savastano (2020). *Thermomechanical and Thermo-hydro-mechanical Treatments of Luffa Cylindrical Fibers*. Journal of Natural Fibers. 17, p. 1-13.
- [194] Kakar, A., E. Jayamani, K.H. Soon, & M.K.B. Bakri (2018). *Study of dielectric properties of luffa-poly lactide quadratic splint composites: The effect of cyclic absorption and desorption of water*. Journal of Vinyl and Additive Technology. 24(4), p. 388-394.
- [195] Al-Mobarak, T., M. Mina, & M. Gafur (2020). *Improvement in mechanical properties of sponge-gourd fibers through different chemical treatment as demonstrated by utilization of the Weibull distribution model*. Journal of Natural Fibers. 17(4), p. 573-588.
- [196] Yin, S., H. Wang, J. Li, R.O. Ritchie, & J. Xu (2019). *Light but tough bio-inherited materials: Luffa sponge based nickel-plated composites*. Journal of the mechanical behavior of biomedical materials. 94, p. 10-18.

- [197] Guo, Y., L. Wang, Y. Chen, P. Luo, & T. Chen (2019). *Properties of luffa fiber reinforced phbv biodegradable composites*. *Polymers*. 11(11), p. 1765.
- [198] Sivakandhan, C., R. Balaji, G.B. Loganathan, D. Madan, & G. Murali (2020). *Investigation of mechanical behaviour on sponge/ridge gourd (Luffa aegyptiaca) natural fiber using epoxy and polyester resin*. *Materials Today: Proceedings*. 22, p. 705-714.
- [199] Kalusuraman, G., S.T. Kumaran, I. Siva, & S.A. Kumar (2020). *Cutting performance of luffa cylindrica fiber–reinforced composite by abrasive water jet*. *Journal of Testing and Evaluation*. 48(5), p. 20180330.
- [200] Daniel-Mkpume, C., C. Ugochukwu, E. Okonkwo, O. Fayomi, & S. Obiorah (2019). *Effect of Luffa cylindrica fiber and particulate on the mechanical properties of epoxy*. *The International Journal of Advanced Manufacturing Technology*. 102(9-12), p. 3439-3444.
- [201] Koruk, H.& G. Genc (2015). *Investigation of the acoustic properties of bio luffa fiber and composite materials*. *Materials Letters*. 157, p. 166-168.
- [202] Mohanta, N.& S. Acharya (2013). *Tensile, flexural and interlaminar shear properties of Luffa cylindrica fibre reinforced epoxy composites*. *Int. J. Macromol. Sci*. 3, p. 6-10.
- [203] Genc, G.& H. Körük (2016). *Investigation of the vibro-acoustic behaviors of luffa bio composites and assessment of their use for practical applications*. In

Proceedings of the 23rd International Congress on Sound and Vibration 2016, ICSV 2016, Athens, Greece, 10–14 July, p. pp. 1-8.

[204] Mohanta, N.& S.K. Acharya (2015). *Mechanical and tribological performance of Luffa cylindrica fibre-reinforced epoxy composite*. BioResources. 10(4), p. 8364-8377.

[205] Mohanta, N.& S.K. Acharya (2015). *Investigation of mechanical properties of luffa cylindrica fibre reinforced epoxy hybrid composite*. International Journal of Engineering, Science and Technology. 7(1).

[206] Genc, G., A. Sarikas, U. Kesen, & S. Aydin (2020). *Luffa/Epoxy composites: Electrical properties for PCB application*. IEEE Transactions on Components, Packaging and Manufacturing Technology. 10(6), p. 933-940.

[207] Saygili, Y., G. Genc, K.Y. Sanliturk, & H. Koruk (2020). *Investigation of the acoustic and mechanical properties of homogenous and hybrid jute and luffa bio composites*. Journal of Natural Fibers, p. 1-9.

[208] Boynard, C.A.& J.R.M. D'Almeida (2000). *Morphological Characterization and Mechanical Behavior of Sponge Gourd (Luffa Cylindrica)–Polyester Composite Materials*. Polymer-Plastics Technology and Engineering. 39(3), p. 489-499.

- [209] Boynard, C.& J. d'Almeida (1999). *Water absorption by sponge gourd (luffa cylindrica)-polyester composite materials*. Journal of Materials Science Letters. 18(21), p. 1789-1791.
- [210] NagarajaGanesh, B.& R. Muralikannan (2016). *Extraction and characterization of lignocellulosic fibers from Luffa cylindrica fruit*. International Journal of Polymer Analysis and Characterization. 21(3), p. 259-266.
- [211] Akgül, M., S. Korkut, O. Çamlıbel, & Ü. Ayata (2013). *Some chemical properties of luffa and its suitability for medium density fiberboard (MDF) production*. BioResources. 8(2), p. 1709-1717.
- [212] Escocio, V.A., L.L.Y. Visconte, A.d.P. Cavalcante, A.M.S. Furtado, & E.B.A.V. Pacheco (2015). *Study of mechanical and morphological properties of bio-based polyethylene (HDPE) and sponge-gourds (Luffa-cylindrica) agroresidue composites*. p. 060012.
- [213] Jamaluddin, J., A. Firouzi, M. Islam, & A. Yahaya (2020). *Effects of luffa and glass fibers in polyurethane-based ternary sandwich composites for building materials*. SN Applied Sciences. 2(7), p. 1-10.
- [214] Alshaaer, M., S.A. Mallouh, J.a. Al-Kafawein, Y. Al-Faiyz, T. Fahmy, A. Kallel, & F. Rocha (2017). *Fabrication, microstructural and mechanical characterization of Luffa Cylindrical Fibre - Reinforced geopolymer composite*. Applied Clay Science. 143, p. 125-133.

- [215] Kaewtatip, K. & J. Thongmee (2012). *Studies on the structure and properties of thermoplastic starch/luffa fiber composites*. Materials & Design. 40, p. 314-318.
- [216] Chen, Y., F. Yuan, Y. Guo, D. Hu, Z. Zhu, K. Zhang, & S. Zhu (2018). *A novel mattress filling material comprising of luffa fibers and EVA resin*. Industrial Crops and Products. 124, p. 213-215.
- [217] Quadri, A.I. & O. Alabi (2020). *Assessment of Sponge Gourd (Luffa Aegyptical) Fiber as a Polymer Reinforcement in Concrete*. Journal of civil Engineering and Materials Application. 4(2), p. 125-132.
- [218] Jeyapragash, R., V. Srinivasan, & S. Sathiyamurthy (2020). *Mechanical properties of natural fiber/particulate reinforced epoxy composites—A review of the literature*. Materials Today: Proceedings. 22, p. 1223-1227.
- [219] Wang, X., J. Shen, Z.H. Zuo, X. Huang, S. Zhou, & Y.M. Xie (2015). *Numerical investigation of compressive behaviour of luffa-filled tubes*. Composites Part B: Engineering. 73, p. 149-157.
- [220] Ashok, K., K. Kalaichelvan, V. Elango, A. Damodaran, B. Gopinath, & M. Raju (2020). *Mechanical and morphological properties of luffa/carbon fiber reinforced hybrid composites*. Materials Today: Proceedings.
- [221] Mani, P., G. Dellibabu, K. Anilbasha, & K. Anbukarsi (2014). *Tensile and flexural properties of Luffa fiber reinforced composite material*. International Journal of Engineering Research and Technology. 3, p. 1882-1885.

- [222] Paglicawan, M.A., M.S. Cabillon, R.P. Cerbito, & E.O. Santos (2005). *Loofah fiber as reinforcement material for composite*. Philippine Journal of Science. 134(2), p. 113.
- [223] Gopinath, A., M.S. Kumar, & A. Elayaperumal (2014). *Experimental Investigations on Mechanical Properties Of Jute Fiber Reinforced Composites with Polyester and Epoxy Resin Matrices*. Procedia Engineering. 97, p. 2052-2063.
- [224] Goutianos, S., T. Peijs, B. Nystrom, & M. Skrifvars (2006). *Development of flax fibre based textile reinforcements for composite applications*. Applied Composite Materials. 13(4), p. 199-215.
- [225] Kumar, A.M.& B.S.K. Reddy (2015). *Modeling and Analysis of Mono Composite Leaf Spring under the Dynamic load condition using FEA for LCV*. International Journal of Science and Research (IJSR). 4(6), p. 2135-2141.
- [226] Mejri, M., L. Toubal, J.C. Cuillière, & V. François (2017). *Fatigue life and residual strength of a short- natural-fiber-reinforced plastic vs Nylon*. Composites Part B: Engineering. 110, p. 429-441.
- [227] Yang, X., S. Sahmani, & B. Safaei (2020). *Postbuckling analysis of hydrostatic pressurized FGM micro sized shells including strain gradient and stress-driven nonlocal effects*. Engineering with Computers, p. 1-16.

- [228] Sahmani, S.& B. Safaei (2020). *Influence of homogenization models on size-dependent nonlinear bending and postbuckling of bi-directional functionally graded micro/nano-beams*. Applied Mathematical Modelling. 82, p. 336-358.
- [229] Safaei, B., F.H. Khoda, & A. Fattahi (2019). *Non-classical plate model for single-layered graphene sheet for axial buckling*. Adv Nano Res. 7, p. 265-275.
- [230] Peng, G., C.-C. Wu, C.-C. Diao, & C.-F. Yang (2018). *Investigation of the composites of epoxy and micro-scale BaTi4O9 ceramic powder as the substrate of microwave communication circuit*. Microsystem Technologies. 24(1), p. 343-349.
- [231] Spainhour, L.K.& W.J. Rasdorf (1997). *Development of an information model for composites design data*. Engineering with Computers. 13(1), p. 48-64.
- [232] Rasdorf, W.J., L.K. Spainhour, E.M. Patton, & B.P. Burns (1993). *A design environment for laminated fiber-reinforced thick composite materials*. Engineering with Computers. 9(1), p. 36-48.
- [233] Karthi, N., K. Kumaresan, S. Sathish, S. Gokulkumar, L. Prabhu, & N. Vigneshkumar (2020). *An overview: Natural fiber reinforced hybrid composites, chemical treatments and application areas*. Materials Today: Proceedings. 27, p. 2828-2834.
- [234] Kebir, H.& R. Ayad (2014). *A specific finite element procedure for the analysis of elastic behaviour of short fibre reinforced composites. The Projected Fibre approach*. Composite Structures. 118, p. 580-588.

- [235] Adeniyi, A.G., A.S. Adeoye, J.O. Ighalo, & D.V. Onifade (2020). *FEA of effective elastic properties of banana fiber-reinforced polystyrene composite*. Mechanics of Advanced Materials and Structures, p. 1-9.
- [236] Shinde, S.S., A. Salve, & S. Kulkarni (2017). *Theoretical modeling of mechanical properties of woven jute fiber reinforced polyurethane composites*. Materials Today: Proceedings. 4(2), p. 1683-1690.
- [237] Koh, R.& B. Madsen (2018). *Strength failure criteria analysis for a flax fibre reinforced composite*. Mechanics of Materials. 124, p. 26-32.
- [238] Srinivasan, S.& L. Raajarajan (2017). *Wear rate and surface coating optimization of coconut coir-based polymer using fuzzy logic*. Sādhanā. 42(3), p. 281-290.
- [239] Mamtaz, H., M. Hosseini Fouladi, M.Z. Nuawi, S. Narayana Namasivayam, M. Ghassem, & M. Al-Atabi (2017). *Acoustic absorption of fibro-granular composite with cylindrical grains*. Applied Acoustics. 126, p. 58-67.
- [240] Mahboob, Z., Y. Chemisky, F. Meraghni, & H. Bougherara (2017). *Mesoscale modelling of tensile response and damage evolution in natural fibre reinforced laminates*. Composites Part B: Engineering. 119, p. 168-183.
- [241] Facca, A.G., M.T. Kortschot, & N. Yan (2006). *Predicting the elastic modulus of natural fibre reinforced thermoplastics*. Composites Part A: Applied Science and Manufacturing. 37(10), p. 1660-1671.

- [242] Chen, Y., L. Xin, Y. Liu, Z. Guo, L. Dong, & Z. Zhong (2019). *A viscoelastic model for particle-reinforced composites in finite deformations*. Applied Mathematical Modelling. 72, p. 499-512.
- [243] Rahman, M.Z. (2017). *Mechanical Performance of Natural/Natural Fiber Reinforced Hybrid Composite Materials Using Finite Element Method Based Micromechanics and Experiments*.
- [244] Jiang, W.G., R.Z. Zhong, Q.H. Qin, & Y.G. Tong (2014). *Homogenized finite element analysis on effective elastoplastic mechanical behaviors of composite with imperfect interfaces*. Int J Mol Sci. 15(12), p. 23389-407.
- [245] Prasad, V., A. Joy, G. Venkatachalam, S. Narayanan, & S. Rajakumar (2014). *Finite Element Analysis of Jute and Banana Fibre Reinforced Hybrid Polymer Matrix Composite and Optimization of Design Parameters Using ANOVA Technique*. Procedia Engineering. 97, p. 1116-1125.
- [246] Xiong, X., L. Hua, M. Miao, S.Z. Shen, X. Li, X. Wan, & W. Guo (2018). *Multi-scale constitutive modeling of natural fiber fabric reinforced composites*. Composites Part A: Applied Science and Manufacturing. 115, p. 383-396.
- [247] Blanchard, J., U. Mutlu, A. Sobey, & J. Blake (2019). *Modelling the different mechanical response and increased stresses exhibited by structures made from natural fibre composites*. Composite Structures. 215, p. 402-410.

- [248] Wang, W., A. Lowe, S. Davey, N. Akhavan Zanjani, & S. Kalyanasundaram (2015). *Establishing a new Forming Limit Curve for a flax fibre reinforced polypropylene composite through stretch forming experiments*. Composites Part A: Applied Science and Manufacturing. 77, p. 114-123.
- [249] Scarponi, C. (2015). *Hemp fiber composites for the design of a Naca cowling for ultra-light aviation*. Composites Part B: Engineering. 81, p. 53-63.
- [250] Sowmya, C., V. Ramesh, & D. Karibasavaraja (2018). *An Experimental Investigation of New Hybrid Composite Material using Hemp and Jute Fibres and Its Mechanical Properties through Finite Element Method*". Materials Today: Proceedings. 5(5), p. 13309-13320.
- [251] Ahmad, F.& P.K. Bajpai (2018). *Evaluation of stiffness in a cellulose fiber reinforced epoxy laminates for structural applications: Experimental and finite element analysis*. Defence Technology. 14(4), p. 278-286.
- [252] Campilho, R.D.S.G., D.C. Moura, D.J.S. Gonçalves, J.F.M.G. da Silva, M.D. Banea, & L.F.M. da Silva (2013). *Fracture toughness determination of adhesive and co-cured joints in natural fibre composites*. Composites Part B: Engineering. 50, p. 120-126.
- [253] Javanbakht, Z., W. Hall, A.S. Virk, J. Summerscales, & A. Öchsner (2020). *Finite element analysis of natural fiber composites using a self-updating model*. Journal of Composite Materials.

- [254] José da Silva, L., T. Hallak Panzera, A. Luis Christoforo, L. Miguel Pereira Dur, & F. Antonio Rocco Lahr (2012). *Numerical and Experimental Analyses of Biocomposites Reinforced with Natural Fibres*. International Journal of Materials Engineering. 2(4), p. 43-49.
- [255] Kumar, L.J., D. Praveen, R. Thara, & G. Irfan *Experimental & Finite element analysis of sisal fibre reinforced composites*. International Journal of Recent trends in Engineering & Research. 2(07), p. 155-160.
- [256] Gonzalez-Murillo, C.& M.P. Ansell (2010). *Co-cured in-line joints for natural fibre composites*. Composites Science and Technology. 70(3), p. 442-449.
- [257] Bajpai, P.K., I. Singh, & J. Madaan (2012). *Joining of natural fiber reinforced composites using microwave energy: Experimental and finite element study*. Materials & Design. 35, p. 596-602.
- [258] Potluri, R., V. Diwakar, K. Venkatesh, & B. Srinivasa Reddy (2018). *Analytical Model Application for Prediction of Mechanical Properties of Natural Fiber Reinforced Composites*. Materials Today: Proceedings. 5(2), p. 5809-5818.
- [259] Joffre, T., A. Miettinen, E.L.G. Wernersson, P. Isaksson, & E.K. Gamstedt (2014). *Effects of defects on the tensile strength of short-fibre composite materials*. Mechanics of Materials. 75, p. 125-134.
- [260] Escalante-Solis, M.A., A. Valadez-Gonzalez, & P.J. Herrera-Franco (2015). *A note on the effect of the fiber curvature on the micromechanical behavior of*

natural fiber reinforced thermoplastic composites. Express Polymer Letters. 9(12), p. 1119-1132.

[261] Mohamadzadeh, M., A. Rostampour Haftkhani, G. Ebrahimi, & H. Yoshihara (2012). *Numerical and experimental failure analysis of screwed single shear joints in wood plastic composite*. Materials & Design. 35, p. 404-413.

[262] Kern, W.T., W. Kim, A. Argento, E.C. Lee, & D.F. Mielewski (2016). *Finite element analysis and microscopy of natural fiber composites containing microcellular voids*. Materials & Design. 106, p. 285-294.

[263] Zhong, Y., U. Kureemun, L.Q.N. Tran, & H.P. Lee (2017). *Natural plant fiber composites-constituent properties and challenges in numerical modeling and simulations*. International Journal of Applied Mechanics. 9(04), p. 1750045.

[264] Petrone, G.& V. Meruane (2017). *Mechanical properties updating of a non-uniform natural fibre composite panel by means of a parallel genetic algorithm*. Composites Part A: Applied Science and Manufacturing. 94, p. 226-233.

[265] Davoodi, M.M., S.M. Sapuan, D. Ahmad, A. Aidy, A. Khalina, & M. Jonoobi (2011). *Concept selection of car bumper beam with developed hybrid bio-composite material*. Materials & Design. 32(10), p. 4857-4865.

[266] Glouia, Y., Y. Chaabouni, A. El Oudiani, I. Maatoug, & S. Msahli (2019). *Finite element analysis of mechanical response of cellulosic fiber-reinforced composites*.

The International Journal of Advanced Manufacturing Technology. 103(9-12), p. 4671-4680.

[267] Dragonetti, R., M. Napolitano, L. Boccarusso, & M. Durante (2020). *A study on the sound transmission loss of a new lightweight hemp/bio-epoxy sandwich structure*. Applied Acoustics. 167.

[268] Pattnaik, P., A. Sharma, M. Choudhary, V. Singh, P. Agarwal, & V. Kukshal (2020). *Role of machine learning in the field of Fiber reinforced polymer composites: A preliminary discussion*. Materials Today: Proceedings.

[269] Antil, S.K., P. Antil, S. Singh, A. Kumar, & C.I. Pruncu (2020). *Artificial neural network and response surface methodology based analysis on solid particle Erosion behavior of polymer matrix composites*. Materials. 13(6), p. 1381.

[270] Pati, P.R. (2019). *Prediction and wear performance of red brick dust filled glass–epoxy composites using neural networks*. International Journal of Plastics Technology. 23(2), p. 253-260.

[271] Baseer, A.A., D. Ravi Shankar, & M.M. Hussain (2020). *Interfacial And Tensile Properties Of Hybrid Frp Composites Using Dnn Structure With Optimization Model*. Surface Review and Letters. 27(02), p. 1950099.

[272] Atuanya, C.U., C.C. Nwobi-Okoye, & O.D. Onukwuli (2014). *Predicting the mechanical properties of date palm wood fibre-recycled low density polyethylene*

composite using artificial neural network. International Journal of Mechanical and Materials Engineering. 9(1), p. 1-20.

[273] Daghigh, V., T.E. Lacy Jr, H. Daghigh, G. Gu, K.T. Baghaei, M.F. Horstemeyer, & C.U. Pittman Jr (2020). *Heat deflection temperatures of bio-nano-composites using experiments and machine learning predictions*. Materials Today Communications. 22, p. 100789.

[274] Daghigh, V., T.E. Lacy Jr, H. Daghigh, G. Gu, K.T. Baghaei, M.F. Horstemeyer, & C.U. Pittman Jr (2020). *Machine learning predictions on fracture toughness of multiscale bio-nano-composites*. Journal of Reinforced Plastics and Composites. 39(15-16), p. 587-598.

[275] Garg, A., S. Bordoloi, S. Mondal, J.-J. Ni, & S. Sreedeeep (2020). *Investigation of mechanical factor of soil reinforced with four types of fibers: An integrated experimental and extreme learning machine approach*. Journal of Natural Fibers. 17(5), p. 650-664.

[276] Wang, Z., F. Chegdani, N. Yalamarti, B. Takabi, B. Tai, M. El Mansori, & S. Bukkapatnam (2020). *Acoustic emission characterization of natural fiber reinforced plastic composite machining using a random forest machine learning model*. Journal of Manufacturing Science and Engineering. 142(3).

[277] Alhijazi, M., Q. Zeeshan, Z. Qin, B. Safaei, & M. Asmael (2020). *Finite element analysis of natural fibers composites: A review*. Nanotechnology Reviews. 9(1), p. 853-875.

- [278] Khalevitsky, Y.V.& A.V. Konovalov (2019). *A gravitational approach to modeling the representative volume geometry of particle-reinforced metal matrix composites*. Engineering with Computers. 35(3), p. 1037-1044.
- [279] Biswas, K., J. Bandyopadhyay, & D. De (2019). *A computational study on the quantum transport properties of silicene–graphene nano-composites*. Microsystem Technologies. 25(5), p. 1881-1899.
- [280] Schlabach, S., R. Ochs, T. Hanemann, & D.V. Szabó (2011). *Nanoparticles in polymer-matrix composites*. Microsystem Technologies. 17(2), p. 183-193.
- [281] Hemmat Esfe, M., S. Esfandeh, & M. Bahiraei (2020). *A two-phase simulation for investigating natural convection characteristics of nanofluid inside a perturbed enclosure filled with porous medium*. Engineering with Computers.
- [282] Alhijazi, M., Q. Zeeshan, B. Safaei, M. Asmael, & Z. Qin (2020). *Recent Developments in Palm Fibers Composites: A Review*. Journal of Polymers and the Environment. 28(12), p. 3029-3054.
- [283] Alemi Parvin, S., N.A. Ahmed, & A.M. Fattahi (2020). *Numerical prediction of elastic properties for carbon nanotubes reinforced composites using a multi-scale method*. Engineering with Computers.
- [284] Swati, R.F., L.H. Wen, H. Elahi, A.A. Khan, & S. Shad (2019). *Extended finite element method (XFEM) analysis of fiber reinforced composites for prediction of*

micro-crack propagation and delaminations in progressive damage: a review.
Microsystem Technologies. 25(3), p. 747-763.

[285] Zhong, B., C. Li, & P. Li (2020). *Modeling and vibration analysis of sectional-laminated cylindrical thin shells with arbitrary boundary conditions.* Applied Acoustics. 162, p. 107184.

[286] Qin, B., R. Zhong, T. Wang, Q. Wang, Y. Xu, & Z. Hu (2020). *A unified Fourier series solution for vibration analysis of FG-CNTRC cylindrical, conical shells and annular plates with arbitrary boundary conditions.* Composite Structures. 232, p. 111549.

[287] Liu, T., A. Wang, Q. Wang, & B. Qin (2020). *Wave based method for free vibration characteristics of functionally graded cylindrical shells with arbitrary boundary conditions.* Thin-Walled Structures. 148, p. 106580.

[288] Safaei, B., R. Moradi-Dastjerdi, K. Behdinan, Z. Qin, & F. Chu (2019). *Thermoelastic behavior of sandwich plates with porous polymeric core and CNT clusters/polymer nanocomposite layers.* Composite Structures. 226, p. 111209.

[289] Gao, W., Z. Qin, & F. Chu (2020). *Wave propagation in functionally graded porous plates reinforced with graphene platelets.* Aerospace Science and Technology. 102, p. 105860.

- [290] Moradi-Dastjerdi, R.& K. Behdinan (2019). *Thermoelastic static and vibrational behaviors of nanocomposite thick cylinders reinforced with graphene*. Steel and Composite Structures. 31(5), p. 529-539.
- [291] Li, C., P. Li, B. Zhong, & B. Wen (2019). *Geometrically nonlinear vibration of laminated composite cylindrical thin shells with non-continuous elastic boundary conditions*. Nonlinear Dynamics. 95(3), p. 1903-1921.
- [292] Qin, Z., Z. Yang, J. Zu, & F. Chu (2018). *Free vibration analysis of rotating cylindrical shells coupled with moderately thick annular plates*. International Journal of Mechanical Sciences. 142, p. 127-139.
- [293] Yu, W. *An introduction to micromechanics*. in *Applied Mechanics and Materials*. 2016. Trans Tech Publ.
- [294] Naveen, J., M. Jawaid, A. Vasanathanathan, & M. Chandrasekar (2019). *Finite element analysis of natural fiber-reinforced polymer composites*. p. 153-170.
- [295] Abu Seman, S.A.H., R. Ahmad, & H. Md Akil (2019). *Experimental and numerical investigations of kenaf natural fiber reinforced composite subjected to impact loading*. Polymer Composites. 40(3), p. 909-915.
- [296] Bazli, M., H. Ashrafi, A. Jafari, X.L. Zhao, R.K.S. Raman, & Y. Bai (2019). *Effect of Fibers Configuration and Thickness on Tensile Behavior of GFRP Laminates Exposed to Harsh Environment*. Polymers (Basel). 11(9).

- [297] Dong, C. (2019). *Mechanical properties of natural fibre-reinforced hybrid composites*. Journal of Reinforced Plastics and Composites. 38(19-20), p. 910-922.
- [298] Hu, D., L. Dang, C. Zhang, & Z. Zhang (2019). *Mechanical Behaviors of Flax Fiber-Reinforced Composites at Different Strain Rates and Rate-Dependent Constitutive Model*. Materials (Basel). 12(6).
- [299] Su, J., L. Zheng, & Z. Deng (2019). *Study on acoustic properties at normal incidence of three-multilayer composite made of glass wool, glue and polyurethane foam*. Applied Acoustics. 156, p. 319-326.
- [300] Balan, M.C., T. Alioua, B. Agoudjil, A. Boudenne, F. Bode, C. Croitoru, A. Dogeanu, A. Georgescu, C. Georgescu, I. Nastase, & M. Sandu (2019). *Numerical modelling and experimental study of heat and moisture properties of a wall based on date palm fibers concrete*. E3S Web of Conferences. 85.
- [301] Chen, X., M.-H. Fu, & L.-L. Hu (2019). *A simple equivalent method for orthogonal assembling three-dimensional composite structures elastic parameters*. Smart Materials and Structures. 28(8).
- [302] Ma, P., L. Jin, & L. Wu (2018). *Experimental and numerical comparisons of ballistic impact behaviors between 3D angle-interlock woven fabric and its reinforced composite*. Journal of Industrial Textiles. 48(6), p. 1044-1058.

- [303] Qin, J.-L., W.-G. Qiao, D.-G. Lin, S. Zhang, & J.-Y. Wang (2019). *Mechanical Properties and Numerical Analyses of Basalt Fiber Crumb Rubber Mortars in Soft Rock Roadways*. *Advances in Civil Engineering*. 2019, p. 1-13.
- [304] Sun, X., Z. Gao, P. Cao, & C. Zhou (2019). *Mechanical properties tests and multiscale numerical simulations for basalt fiber reinforced concrete*. *Construction and Building Materials*. 202, p. 58-72.
- [305] Ye, C., J. Ren, Y. Wang, W. Zhang, C. Qian, J. Han, C. Zhang, K. Jin, M.J. Buehler, D.L. Kaplan, & S. Ling (2019). *Design and Fabrication of Silk Templated Electronic Yarns and Applications in Multifunctional Textiles*. *Matter*. 1(5), p. 1411-1425.
- [306] Hao, X., H. Zhou, B. Mu, L. Chen, Q. Guo, X. Yi, L. Sun, Q. Wang, & R. Ou (2020). *Effects of fiber geometry and orientation distribution on the anisotropy of mechanical properties, creep behavior, and thermal expansion of natural fiber/HDPE composites*. *Composites Part B: Engineering*. 185.
- [307] Lv, M., L. Wang, J. Liu, F. Kong, A. Ling, T. Wang, & Q. Wang (2019). *Surface energy, hardness, and tribological properties of carbon-fiber/polytetrafluoroethylene composites modified by proton irradiation*. *Tribology International*. 132, p. 237-243.
- [308] Lima, P.R.L., J.A.O. Barros, D.J. Santos, C.M. Fontes, J.M.F. Lima, & R. Toledo Filho (2017). *Experimental and numerical analysis of short sisal fiber-*

- cement composites produced with recycled matrix*. European Journal of Environmental and Civil Engineering. 23(1), p. 70-84.
- [309] Potluri, R. (2017). *Mechanical Properties of Pineapple Leaf Fiber Reinforced Epoxy Infused with Silicon Carbide Micro Particles*. Journal of Natural Fibers. 16(1), p. 137-151.
- [310] Sun, X., Z. Gao, P. Cao, C. Zhou, Y. Ling, X. Wang, Y. Zhao, & M. Diao (2019). *Fracture performance and numerical simulation of basalt fiber concrete using three-point bending test on notched beam*. Construction and Building Materials. 225, p. 788-800.
- [311] Meyghani, B., M. Awang, S.S. Emamian, M. Nor, M. Khalid, & S.R. Pedapati (2017). *A comparison of different finite element methods in the thermal analysis of Friction Stir Welding (FSW)*. Metals. 7(10), p. 450.
- [312] Fragassa, C., F. Vannucchi de Camargo, A. Pavlovic, & G. Minak (2019). *Explicit numerical modeling assessment of basalt reinforced composites for low-velocity impact*. Composites Part B: Engineering. 163, p. 522-535.
- [313] ANSYS, I., *ANSYS mechanical APDL Element Reference*. Vol. 15.0. 2013: ANSYS, Inc.
- [314] Dufour, P. (2003). *Picking an element type for structural analysis*. Belcan Engineering Group, p. 5.

- [315] Mohamedou, M., K. Zulueta, C.N. Chung, H. Rappel, L. Beex, L. Adam, A. Arriaga, Z. Major, L. Wu, & L. Noels (2019). *Bayesian identification of Mean-Field Homogenization model parameters and uncertain matrix behavior in non-aligned short fiber composites*. Composite Structures. 220, p. 64-80.
- [316] Modniks, J.& J. Andersons (2010). *Modeling elastic properties of short flax fiber-reinforced composites by orientation averaging*. Computational Materials Science. 50(2), p. 595-599.
- [317] Worthy III, J.L. (2013). *Design Tool for Simulation of Nanocomposite Material Properties*.
- [318] Djebloun, Y., M. Hecini, T. Djoudi, & B. Guerira (2019). *Experimental determination of elastic modulus of elasticity and Poisson's coefficient of date palm tree fiber*. Journal of Natural Fibers. 16(3), p. 357-367.
- [319] Mulinari, D.R., A.J. Marina, & G.S. Lopes (2015). *Mechanical properties of the palm fibers reinforced HDPE composites*. International Journal of Chemical and Molecular Engineering. 9(7), p. 903-906.
- [320] AlMaadeed, M.A., R. Kahraman, P.N. Khanam, & N. Madi (2012). *Date palm wood flour/glass fibre reinforced hybrid composites of recycled polypropylene: Mechanical and thermal properties*. Materials & Design. 42, p. 289-294.
- [321] Afddl, J.H.& J. Kardos (1976). *The Halpin-Tsai equations: a review*. Polymer Engineering & Science. 16(5), p. 344-352.

- [322] Sudheer, M., K. Pradyoth, & S. Somayaji (2015). *Analytical and numerical validation of epoxy/glass structural composites for elastic models*. Am. J. Mater. Sci. 5, p. 162-168.
- [323] Chamis, C.C. (1989). *Mechanics of composite materials: past, present, and future*. Journal of Composites, Technology and Research. 11(1), p. 3-14.
- [324] Madhu, P., M. Sanjay, P. Senthamarai Kannan, S. Pradeep, S. Saravanakumar, & B. Yogesha (2018). *A review on synthesis and characterization of commercially available natural fibers: Part-I*. Journal of Natural Fibers.
- [325] Tam, D.K.Y., S. Ruan, P. Gao, & T. Yu, *10 - High-performance ballistic protection using polymer nanocomposites*, in *Advances in Military Textiles and Personal Equipment*, E. Sparks, Editor. 2012, Woodhead Publishing. p. 213-237.
- [326] Hanan, F., M. Jawaaid, M.T. Paridah, & J. Naveen (2020). *Characterization of Hybrid Oil Palm Empty Fruit Bunch/Woven Kenaf Fabric-Reinforced Epoxy Composites*. Polymers. 12(9), p. 2052.
- [327] Al-Oqla, F.M., M.S. Salit, M.R. Ishak, & N.A. Aziz (2015). *Selecting natural fibers for bio-based materials with conflicting criteria*. American Journal of Applied Sciences. 12(1), p. 64.
- [328] Cavazzuti, M., *Optimization methods: from theory to design scientific and technological aspects in mechanics*. 2012: Springer Science & Business Media.

- [329] Bouktif, S., A. Fiaz, A. Ouni, & M.A. Serhani (2018). *Optimal deep learning lstm model for electric load forecasting using feature selection and genetic algorithm: Comparison with machine learning approaches*. *Energies*. 11(7), p. 1636.
- [330] Wuest, T., D. Weimer, C. Irgens, & K.-D. Thoben (2016). *Machine learning in manufacturing: advantages, challenges, and applications*. *Production & Manufacturing Research*. 4(1), p. 23-45.
- [331] Barton, R.R.& M. Meckesheimer (2006). *Chapter 18 Metamodel-Based Simulation Optimization*. 13, p. 535-574.
- [332] Box, G.E.& K.B. Wilson (1951). *On the experimental attainment of optimum conditions*. *Journal of the Royal Statistical Society: Series B (Methodological)*. 13(1), p. 1-38.
- [333] Box, G.E. (1954). *The exploration and exploitation of response surfaces: some general considerations and examples*. *Biometrics*. 10(1), p. 16-60.
- [334] Mittal, V., R. Saini, & S. Sinha (2016). *Natural fiber-mediated epoxy composites—a review*. *Composites Part B: Engineering*. 99, p. 425-435.
- [335] Alothman, O.Y., M.M. Alrashed, A. Anis, J. Naveen, & M. Jawaid (2020). *Characterization of date palm fiber-reinforced different polypropylene matrices*. *Polymers*. 12(3), p. 597.

[336] Chokshi, S., P. Gohil, & D. Patel (2020). *Experimental investigations of bamboo, cotton and viscose rayon fiber reinforced Unidirectional composites*. Materials Today: Proceedings. 28, p. 498-503.

[337] Balasubramanian, K., N. Rajeswari, & K. Vaidheeswaran (2020). *Analysis of mechanical properties of natural fibre composites by experimental with FEA*. Materials Today: Proceedings. 28, p. 1149-1153.